SPATIOTEMPORAL BRAIN DYNAMICS OF INHIBITORY CONTROL IN ADOLESCENTS AND YOUNG ADULTS

by

Kai Hwang

B.S., National Chung Cheng University, 2004

M.A., San Diego State University, 2007

Submitted to the Graduate Faculty of

the Kenneth P. Dietrich School of Arts and Sciences

in partial fulfillment

of the requirements for the degree of

Doctor of Philosophy

University of Pittsburgh

2012

UNIVERSITY OF PITTSBURGH

THE DIETRICH SCHOOL OF ARTS AND SCIENCES

This dissertation was presented

by

Kai Hwang

It was defended on

November 26, 2012

and approved by

Raymond Cho, Assistant Professor, Psychiatry & Psychology

Julie Fiez, Professor, Psychology & Neuroscience

Mark Wheeler, Associate Professor, Psychology

Dissertation Advisor: Beatriz Luna, Professor, Psychiatry & Psychology

SPATIOTEMPORAL BRAIN DYNAMICS OF INHIBITORY CONTROL IN ADOLESCENTS AND YOUNG ADULTS

Kai Hwang, PhD

University of Pittsburgh, 2012

Inhibitory control, the ability to inhibit impulsive responses in favor of voluntary responses, remains immature during adolescence. Although this behavior has been well documented, the cognitive and neural processes associated with immature inhibitory control during adolescence are still not well understood. To address this question, we collected Magnetoencephalography (MEG) data from 17 adolescents (age 14-16) and 20 adult participants (age 20-30), where participants performed the antisaccade (AS) and control prosaccade (PS) tasks. Leveraging MEG's high temporal resolution, our goal was to delineate developmental changes in local neural oscillations and inter-regional neural synchronization associated with preparatory inhibitory control. Participants were shown a preparatory cue (a red "x" for AS or a green "x" for PS) for 1500 ms, followed by a peripheral target where participants were instructed to make a saccade toward (PS) or away (AS) from the target. Neural activity estimates from *a priori* brain regions were then extracted for oscillatory power and phase synchrony analyses. We found that compared to adults, adolescents showed decreased alpha-band power in the oculomotor regions in preparation to inhibit an upcoming reflexive saccade, suggesting immaturities in functional inhibition of task-inappropriate activity. Furthermore, adolescents showed weaker beta-band power in prefrontal cognitive control regions, which could reflect less robust top-down biasing of sensory and motor processes. Lastly, we found that adolescents showed decreased levels of phase synchrony between frontal and parietal regions, possibly reflecting immaturities in

coordinating distributed cortical activities. Our results suggest that immaturities in functional inhibition, top-down control, and inter-regional synchrony collectively contribute to immature inhibitory control during adolescence.

TABLE OF CONTENTS

LIST OF FIGURES

PREFACE

First of all, I would like to thank my mentor, Dr. Beatriz Luna. I am especially indebted to her advising, insight, vision, and her ability to integrate divergent findings.

I would like to extend my thanks to all present and past members of the LNCD. Thanks to Andrew Lynn, Barbara Fritz, Catherine Wright, Emily Mente, Missy Resutko, Raj Chahal, Laryssa Richards for helping with testings and recruitments, thanks to Amanda Wright, Natalie Nawarawong and Soma Chatterji for spending countless hours with me at the MEG center, and thanks to Mel Wilds for her extraordinary lab managing skills. Particular thanks go out to Dr. Aarthi Padmanabhan, Dr. Sarah Ordaz, Dr. Michael Hallquist, Will Foran, Dr. Katerina Velanova, and David Montez for providing advice, encouragement, and laughter.

The UPMC MEG center has provided indispensable support to make this research possible. Thanks to Dr. Avniel Ghuman for his analyses insight, and thanks to Anna Haridis, Erika Laing, and TJ Amdurs for their technical support.

Finally, I dedicate this work to my family, who has always supported me in who I am:

To my parents and my sister, for never doubting me, and for your enduring love.

To my wife Queena, for your generous patience, understanding, sacrifice, and encouragement.

1.0 INTRODUCTION

In our daily lives, successful goal-directed behaviors often require inhibiting task-irrelevant, reflexive, or impulsive behaviors. *Inhibitory control* allows us to act flexibly in service of behavioral goals, while suppressing contextually inappropriate or reflexive responses that may be compelling but less optimal. Increases in risk-taking behavior during adolescence, such as reckless driving, unprotected sex, and substance abuse (Spear, 2000; Steinberg et al., 2008), may reflect immaturities in inhibitory control (Luna, Garver, Urban, Lazar, & Sweeney, 2004). In addition, impaired inhibitory control is a prominent clinical syndrome across major psychological disorders (Sweeney, Levy, & Harris, 2002; Sweeney, Takarae, Macmillan, Luna, & Minshew, 2004) that frequently emerge during adolescence (Cicchetti & Rogosch, 1999, 2002; Cicchetti & Toth, 1998; Resnick et al., 1997). The goal of this dissertation is to improve our understanding of the neural mechanisms underlying the development of inhibitory control during adolescence, which could be of considerable theoretical and translational significance.

We will first review what is known about the development of inhibitory control and its neural bases (Chapter 2). We will argue that from functional mapping studies we know much more about which segregated brain regions contribute to inhibitory control, but less about how the spectral and temporal neurodynamics within these functional regions develop. Furthermore, how these functionally specialized but anatomically distributed regions interact and how inter-regional communication develops is less understood. Robust evidence suggests that different

oscillatory neurodynamics reflect distinct circuit level physiological processes underlying higher cognitive functions (Donner & Siegel, 2011; Kopell, Kramer, Malerba, & Whittington, 2010; Wang, 2010), and that flexible coupling between distributed brain regions could be achieved through the synchronization of neural oscillations (Fries, 2005; Siegel, Donner, & Engel, 2012; Varela, Lachaux, Rodriguez, & Martinerie, 2001). Despite these important advances, our current knowledge of how oscillatory neurodynamics develop to support inhibitory control from adolescence to adulthood is limited, largely because of methodological limitations.

The main thrust behind this dissertation is to fill this critical gap. Based on known structural neurodevelopment during adolescence (Chapter 4), we hypothesized that the development of inhibitory control is associated with developmental changes in the expression and synchronization of neural oscillations in task-related regions. To test these hypotheses, we collected MEG data from adolescent (aged 14-16) and adult participants (aged 20-30) while they performed an oculomotor inhibitory control task. We found that compared to adults, adolescents showed decreased alpha-band power in the oculomotor regions in preparation to inhibit an upcoming reflexive saccade, which may suggest immaturities in functional inhibition of task-inappropriate activity. Adolescents also showed weaker beta-band power in the prefrontal cognitive control regions, which could reflect less robust top-down biasing of sensory and motor processes. Finally, we found that adolescents showed decreased levels of phase synchrony between frontal and parietal regions, reflecting immaturities in long-distance cortical communication.

2.0 THE DEVELOPMENT OF INHIBITORY CONTROL

2.1 THE OCULOMOTOR PARADIGM OF INHIBITORY CONTROL

Inhibitory control is defined as the ability to inhibit an automatic, habitual, reflexive, or prepotent behavior in favor of a voluntary, goal-directed behavior (Luna, Padmanabhan, & O'Hearn, 2010). Several paradigms have been developed for studying the neurobiology and psychology of inhibitory control, including the AS task, the stop signal task, and the Go/NoGo task (Aron, 2011). All these paradigms have consistently demonstrate developmental improvements in inhibitory control capacity from childhood through adulthood (Bedard et al., 2002; Luna, et al., 2004; Williams, Ponesse, Schachar, Logan, & Tannock, 1999).

Although all these paradigms require participants to suppress a naturally prepotent or overlearned response, in the current dissertation we utilized the oculomotor paradigm (Hallett, 1978) to probe the development of inhibitory control because it has several important advantages. First, the neural system associated with saccadic responses has been well delineated using both invasive electrophysiology recordings (e.g., Everling, Dorris, Klein, & Munoz, 1999; Everling & Munoz, 2000; Zhang & Barash, 2000), non-invasive neuroimaging techniques (e.g., Connolly, Goodale, Menon, & Munoz, 2002; Curtis, Cole, Rao, & D'Esposito, 2005; DeSouza, Menon, & Everling, 2003; Luna et al., 1998), and neuropsychological testings of patients with brain lesions (e.g., Hodgson et al., 2007; Pierrot-Deseilligny et al., 2003; Pierrot-Deseilligny,

Rivaud, Gaymard, & Agid, 1991). These studies have characterized the oculomotor system's neurochemistry, neuroanatomy, and neurophysiology, providing a strong foundation to inform developmental neuroimaging studies. Second, the stimulus input and response output are in the same domain, and this simplicity limits the potential confound of task comprehension and multisensory integration. Finally, and of crucial importance, this paradigm is sensitive to adolescent development (Luna, et al., 2004; Luna et al., 2001; Ordaz, Davis, & Luna, 2010; Velanova, Wheeler, & Luna, 2008, 2009), and has been widely used to study cognitive deficits in patients with neurological and psychiatric disorders (Sweeney, et al., 2002; Sweeney, et al., 2004).

The oculomotor paradigm of inhibitory control (Figure 1) consists of two tasks: the AS task and the control PS task. The AS task requires participants to suppress a prepotent saccadic response to a peripheral stimulus that appears in an unpredictable location and instead make a goal-directed eye movement response to the mirror location of the stimulus. The AS task is typically presented in conjunction with trials or blocks of PS trials, where subjects are instructed to gaze at the peripheral stimulus, and it is used to control for basic oculomotor processes. Each task consists of a *preparatory period* followed by a *response period*. During the preparatory period, participants are asked to fixate on an instructional cue on the center of the screen. A red "X" instructs participants to make an AS when the target appears, whereas a green "X" instructs the participants to make a prosaccade PS towards the target. After a certain amount of delay, the cue disappears from the screen, signaling the beginning of the response period, and a yellow flash target appears on a peripheral location within the visual field. Crucial to this task is that the location where the target will appear is not known during the preparatory period, allowing *preparatory signals* to be separated from *response signals*. Preparatory signals are involved in

anticipatory cognitive control processes (Braver, 2012), whereby goal-relevant information is maintained and used to prepare sensory and motor systems to inhibit an anticipating response tendency (Aron, 2011), whereas response signals are related to the actual execution of motor response (Brown, Vilis, & Everling, 2007).

The AS task induces more errors than the reflexive PS task (Munoz & Everling, 2004); an AS error is characterized by a reflexive saccade generated toward the target, and is treated as an indication of inhibitory control failure. The latency (reaction time) to initiate an AS is longer than a PS, and could be contributed to the extra requirement of inverting the stimulus location vector into the saccade direction vector for AS (termed *vector inversion*). For the PS task the stimulus location vector is congruent with the saccade vector and can be automatically or reflexively executed (Munoz & Everling, 2004).

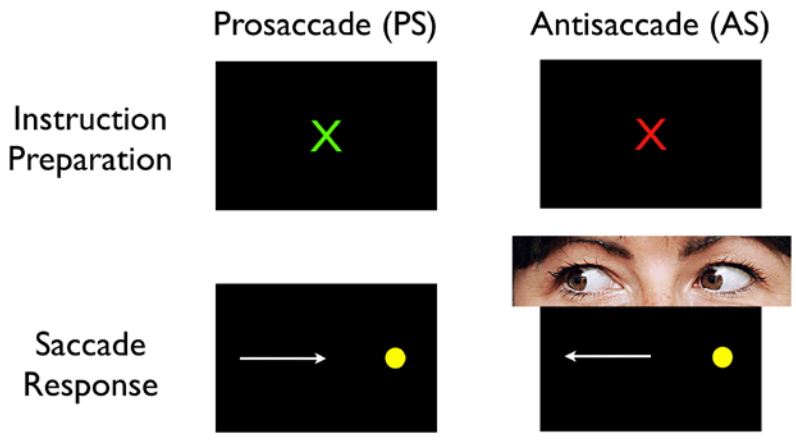

Figure 1. The oculomotor paradigm of inhibitory control.

2.1.1 Preparatory Inhibitory Control Processes

Non-human primate studies indicate that the preparatory period is crucial for AS task performance (Everling & Johnston, 2011; Munoz & Everling, 2004). Specifically, neural activities during the preparatory period in oculomotor regions such as the frontal eyefield (FEF), the supplementary eyefield (SEF), and the superior colliculus (SC) predict correct vs. incorrect AS task performance (Everling, et al., 1999; Everling, Dorris, & Munoz, 1998; Everling & Munoz, 2000; Schlag-Rey, Amador, Sanchez, & Schlag, 1997). In addition, longer preparatory time correlates with fewer AS errors and faster reaction time (Barton, Greenzang, Hefter, Edelman, & Manoach, 2006; Connolly, et al., 2002; Ordaz, et al., 2010). These findings suggest that preparatory physiological and psychological processes have pivotal impact on inhibitory control. The preparatory neural signals likely reflect two cognitive processes (Brown, et al., 2007):

1. The instructional cue is first converted into a task-rule ("red means look away from the dot" and "green means look towards the dot"). The encoded task-rule should be actively maintained in working memory throughout the preparatory period. We will refer to this process as *task-rule maintenance*.

2. The encoded task-rule should bias task-relevant sensory and motor processes (Miller & Cohen, 2001) in preparation for the upcoming saccade target. For example, the AS task requires participants to first suppress the prepotent saccade towards the peripheral stimulus, instead generate a goal-directed saccade toward the opposite direction. This could be achieved by inhibiting the saccade-generation mechanism to prevent the oculomotor system from triggering a saccade upon seeing the target (Everling, et al., 1999; Everling & Munoz, 2000), while preparing both the visuospatial and oculomotor systems to compute the vector inversion. We will refer to

this process as *top-down signaling*, which *control signals* are sent to task-relevant regions for task-specific preparations.

It has been suggested that the AS task can be regarded as an arbitrary stimulus-response (SR) mapping task (Munoz & Everling, 2004) because the stimulus and response vectors are incompatible. To prepare to execute an AS, top-down signaling is needed to inhibit the more automatic and prepotent congruent SR mapping (a PS), while preparing sensory and motor resources to execute the arbitrary SR mapping for a correct AS response. The PS task allows the more automatic congruent SR mapping to be executed, lessening the need for top-down signaling. Because PS responses are automatic and prepotent, participants will not need to actively maintain task instructions during the preparatory period for PS, but just respond reflexively to the visual target. To summarize, differences in preparatory neural activities between AS and PS should reflect differences in top-down signaling and task-rule maintenance.

2.2 BEHAVIORAL STUDIES

Behavioral studies indicate that the capacity for inhibitory control is present in infants (Amso & Johnson, 2005; Diamond, 1989), who can successfully inhibit motor responses on some trials. Nevertheless, the consistency continues to improve over the course of development (Fischer, Biscaldi, & Gezeck, 1997; Klein & Foerster, 2001; Luna, et al., 2004; Munoz, Broughton, Goldring, & Armstrong, 1998). The development of AS task performance (percentage of error trials) is best fitted by an inverse function (Luna et al., 2004), indicating that error rates decreases with age as the capacity for inhibitory control continues to develop. The behavioral improvement is more rapid (steeper slope) from childhood to adolescence, and accuracy increases (fewer error

trials) whereas reaction time decreases from childhood through adolescence (Fischer, et al., 1997; Klein & Foerster, 2001; Luna, et al., 2004; Munoz, et al., 1998). Critically, the performance asymptotes in early adulthood, indicating inhibitory control remains immature during adolescence (Luna, et al., 2004).

Although contextual factors such as reward anticipation could improve performance, adolescents still showed higher AS error rates (Geier & Luna, 2012). Adolescents' immature performance could not be explained by slower processing speed; even when the preparatory time was increased up to six seconds, adolescents still made more errors than adults (Ordaz, et al., 2010). Considered together, these studies suggest that there are critical immaturities in the neurocognitive processes being engaged in preparation to inhibit reflexive saccades.

2.3 NEURAL SYSTEMS OF INHIBITORY CONTROL

An extensive body of literature of human neuroimaging, human neuropsychology, and primate electrophysiology studies has identified several distributed brain regions associated with inhibitory control processes. These regions include the dorsal anterior cingulate cortex (ACC), the ventral lateral prefrontal cortex (VLPFC), the dorsal lateral prefrontal cortex (DLPFC), and the posterior parietal cortex (for in-depth reviews, see Aron, 2011; Aron, Robbins, & Poldrack, 2004; Luna & Sweeney, 2004). The antisaccade task also recruits a set of regions that are associated with the initiation and suppression of saccadic eye movements, including the FEF, the SEF, the intraparietal sulcus (IPS), the basal ganglia (BG), the SC, the thalamus, and the cerebellum (for in-depth reviews, see Curtis, 2011; Munoz & Everling, 2004).

2.3.1 Preparatory Neural Activities Associated with Inhibitory Control

Single-neuron recordings in non-human primates showed differential neural activities between AS and PS. Saccade neurons in the monkey FEF and SC showed higher firing rates during the preparatory period of the PS task, compared to the AS task; in contrast, fixation neurons in the FEF and SC exhibited higher firing rates for the AS task compared to the PS task (Everling, et al., 1999; Everling & Munoz, 2000). Furthermore, Everling and Munoz (1998, 1999, 2000) found that firing rates of saccade neurons during the preparatory period could be used to predict success vs. failure in inhibiting the upcoming reflexive saccade. Specifically, trials with higher saccade-related activity during the preparatory period show a higher probability of inhibition failure. These findings were extended into a mechanistic model predicting the success vs. failure in inhibiting reflexive saccades (Munoz & Everling, 2004). The model proposes that during the preparatory period, there is a competition between fixation and saccade mechanisms. To successfully inhibit a reflexive PS, pretarget activity in saccade-generating neurons has to be dampened. In an accumulator model, the suppression of saccade-related activation will prevent the stochastically fluctuating saccade-related activity from reaching a critical triggering threshold (Curtis, 2011; Hanes & Schall, 1996), ensuring that no reflexive saccades will be prematurely triggered upon seeing the visual target, and fixation can be maintained. If pretarget saccade-related activity is not sufficiently suppressed, its activation can reach the triggering threshold, and a reflexive saccade will be triggered toward the visual target, resulting in inhibition failure. The lateral PFC has been hypothesized to be involved in top-down signaling processes required for generating preparatory signal necessary to inhibit saccade-related activity in the FEF and the SC (Brown, et al., 2007; DeSouza, et al., 2003).

Functional magnetic resonance imaging (fMRI) studies found that the DLPFC, the SEF, the ACC, the FEF, and the IPS showed significantly higher preparatory activations for AS, when compared to PS (Brown, et al., 2007; Connolly, et al., 2002; Curtis, et al., 2005; DeSouza, et al., 2003). Given that the eye movement response is the same for AS and PS trials, increased activity in these brain regions reflects the engagement of preparatory inhibitory control. For example, the DLPFC has been suggested to be involved in task-rule encoding and task goal maintenance (Cole, Bagic, Kass, & Schneider, 2010; Sakai, 2008), and the VLPFC is involved in inhibiting motor-related activities for stopping actions (Aron, Fletcher, Bullmore, Sahakian, & Robbins, 2003; Aron, et al., 2004; Rubia, Smith, Brammer, & Taylor, 2003). The lateral frontal and parietal regions could also be involved in working memory maintenance (Curtis & D'Esposito, 2003a; Pesaran, Pezaris, Sahani, Mitra, & Andersen, 2002).

The above model appears to be contradictory to human fMRI studies, results which greater activation has been repeatedly observed in the human FEF for the AS task (e.g., Brown, et al., 2007; Connolly, et al., 2002; Curtis & D'Esposito, 2003b). However, fMRI cannot measure fixation and saccade neurons separately, and the increase in blood oxygenation level dependent (BOLD) activity might reflect increased activities of fixation neurons. Furthermore, it has been shown that BOLD response is more highly correlated with local field potentials (LFP) than spiking outputs (Logothetis, Paulsen, Augath, Trinath, & Oeltermann, 2001), and thus may better reflect the input to an area. Because fMRI cannot easily distinguish excitatory vs. inhibitory postsynaptic potentials (Logothetis, 2008), higher BOLD activity might reflect an elevated level of inhibition, or increased top-down biasing input, or both (Curtis, 2011).

2.4 THE DEVELOPMENT OF NEURAL SYSTEMS ASSOCIATED WITH INHIBITORY CONTROL

Developmental fMRI studies indicate that children, adolescents, and adult recruit a similar set of distributed brain regions for inhibitory control (Luna, Padmanabhan, et al., 2010). However, the magnitude of activation within each region varies across development (Bunge, Dudukovic, Thomason, Vaidya, & Gabrieli, 2002; Casey et al., 1997; Durston et al., 2002; Rubia, Smith, Taylor, & Brammer, 2007; Rubia et al., 2006; Tamm, Menon, & Reiss, 2002). Particular interests has been placed on the PFC, given its putative role in top-down control of goal-directed behavior (Miller & Cohen, 2001). Developmental differences in the magnitudes of activations in the VLPFC and the DLPFC have been reported in some studies, suggesting that improvement in inhibitory control is supported by maturing PFC function (Bunge, et al., 2002; Rubia, et al., 2007; Rubia, et al., 2006). However, the direction of developmental differences (adults greater than adolescents or vice versa) has not been consistent across studies, and researchers typically interpreted age-related increases in activation as an index of increased cognitive control function, and a age-related decreases as increased effort (Luna, Velanova, & Geier, 2010; Tamm, et al., 2002). Note that results from several early studies were confounded by task performance discrepancy between age groups, making it difficult to interpret differences across age as being related to either changes in brain function or differences in performance.

In our own studies using the AS task (Velanova, et al., 2008, 2009), we equated performance across age groups by separating the *transient*, trial-locked evoked responses between correct and incorrect trials, and performed group comparisons for correct and incorrect trials separately. For correct trials, we found no developmental differences in the magnitudes of activity between adolescents (age 13-17 years) and adults (age 18 years or older) in either

oculomotor or prefrontal cognitive control regions such as the DLPFC (Velanova, et al., 2008). Three possible explanations could account for the lack of developmental effect. First, localized brain functions could be matured and stabilized by adolescence, and developmental improvements from adolescence to adulthood could be better explained by changes in connectivity supporting the coordination of global brain functions. For example, the effectiveness of PFC sending task-control signals to the oculomotor cortices could show a more protracted development. As described in Chapter 4, white matter connectivity is still immature in adolescence. Second, it is known that there are vast and complex neurodynamics that cannot be adequately measured by fMRI (Cohen, 2011). For example, it has been shown that oscillatory neurodynamics undergo significant changes during adolescence (Uhlhaas et al., 2009), yet both cognitive and neurodynamics typically evolve at a much faster timescale than fMRI's sampling rate. Because BOLD measures hemodynamic changes to infer neuronal activity summated across slow and fast neural oscillations, it is possible that the BOLD is not sensitive to subtle developmental changes in neural electrophysiology. Lastly, because we could not separate the preparatory signal and the response signal in those studies, it is possible that adolescents could have immaturities in preparatory inhibitory control processes that we were unable to detect. These possibilities motivated this dissertation.

2.5 THE DEVELOPMENT OF BRAIN CONNECTIVITY AND INHIBITORY CONTROL

The distributed nature of neural systems suggests that a full understanding of the neural bases of inhibitory control necessitates research examining both how activity within brain regions

changes with development, and also how brain connectivity develops supporting interaction between functional regions. Using Granger causality analysis (GCA; Roebroeck, Formisano, & Goebel, 2005), we examined developmental differences in effective connectivity between regions supporting AS and PS task performance (Hwang, Velanova, & Luna, 2010). Children (8–12 years of age), adolescents (13–17 years of age), and adults (18–27 years of age) performed blocks of AS trials and blocks of PS trials. Since the basic perceptual motor processes are equivalent between the AS task and the PS task, contrasting the strength of connections during the AS and the PS task block allowed us to identify connections associated with top-down signaling processes. We found that children demonstrated strong effective connectivity within the oculomotor network (FEF and IPS) and within the parietal cortex, but few top-down effective connections from the VLPFC and the DLPFC to sensory and motor regions. From adolescence to adulthood, connectivity from the right VLPFC to the thalamus, from the ACC to the right DLPFC, from the right DLPFC to the thalamus, the IPS, and the FEF continued to strengthen. These results suggest that children may rely on visuospatial processing to compensate for limitations in prefrontal functions resulting in relatively poor inhibitory control. In contrast, by adolescence, top-down connectivity is available but limited, and the strength of top-down connectivity from the PFC to down-stream oculomotor regions continues to develop from adolescence into adulthood, possibly supporting behavioral improvements in inhibitory control.

These results provide initial evidence suggesting that strengthening of connectivity supports developmental improvements in inhibitory control from adolescence to adulthood. The next step is to probe the possible mechanisms that may contribute to these changes. However, fMRI has limited temporal resolution in tracking neurodynamics. For example, the strength of connectivity had to be estimated using block time-series that consisted of series of AS or PS

trials. As such, it was not possible to separate preparatory signals from motor related signals, and it remains an open question whether or not the age-related strengthening in top-down connectivity we observed reflects enhanced top-down inhibition of preparatory saccade-related activity. Similarly, we were unable to separate correct trials from error trials within each block, and differences in performance between age groups could have biased our results. Together, these limitations make it difficult to draw inferences regarding the underlying neurocognitive processes associated with immature inhibitory control during adolescence. To overcome these limitations, we need a neuroimaging technique that can more faithfully measure that fast-changing dynamics of neural electrophysiology.

3.0 OSCILLATORY NEURODYNAMICS

Oscillations are ubiquitous in neural systems—the time-varying voltages of neural currents unambiguously show rhythmicity (Buzsaki, 2006). Furthermore, cognitive, perceptual, and motor tasks are known to induce and modulate neural oscillations (Donner & Siegel, 2011; Siegel, et al., 2012; Wang, 2010). In this chapter, we will discuss how neural circuits generate distinct rhythmic neural activities—defined as brain rhythms. One theme that will be emphasized throughout is that different brain rhythms are associated with different physiology, thus reflecting different circuit-level biophysical processes that together may support different components of higher order cognitive functions.

By definition, oscillations occur when the recorded neural signal shows periodic activity within a well-defined time window (Figure 2). Time-domain neural signals can be transformed into the frequency-domain by time-frequency decomposition techniques (Jensen & Hesse, 2010), whereby the *power* and *phase* of oscillation are available as separate measures. The strength of neural oscillation can be determined by examining the amplitude. Amplitude is defined as the distance from zero to the maximum absolute value of the sinusoidal curve; taking the square of the amplitude converts amplitude into *oscillatory power*. A strong oscillation has larger deflections within each cycle, resulting in greater power comparing to a weaker oscillation (Figure 2A). The phase of an oscillating signal is defined as the initial angle of the sinusoidal function at its origin. With two oscillating signals, the correlation can be measured with *phase*

synchrony. If the phase relationship between the two signals is stable across time, these two time-varying signals are *synchronized* (Figure 2B). If the phase relationship is randomized, signals are *desynchronized* (Figure 2C). Modeling studies suggest that phase synchrony improves the effectiveness of communication between signals (Buehlmann & Deco, 2010; Canolty et al., 2010; Kopell, Ermentrout, Whittington, & Traub, 2000), and is widely used as a measure of functional connectivity (Lachaux, Rodriguez, Martinerie, & Varela, 1999).

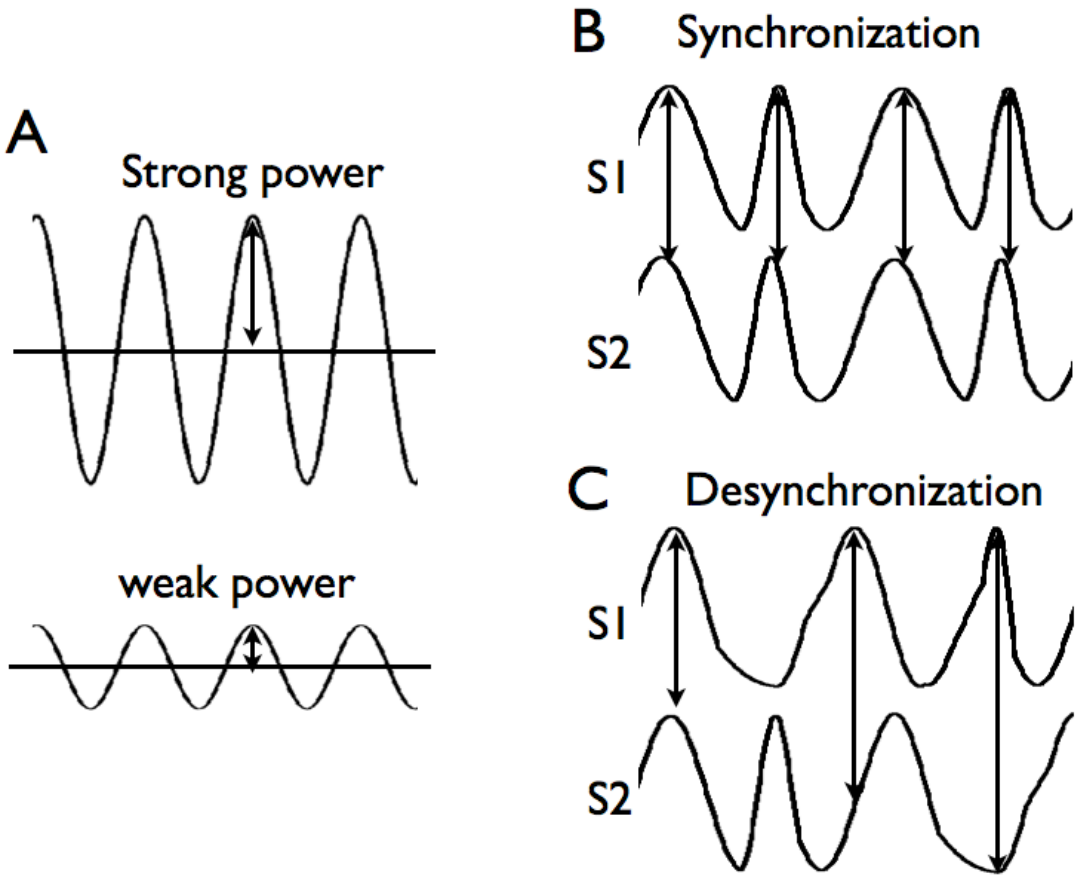

Figure 2. Oscillatory power and synchronization.
A. A strong oscillation will show larger deflections within each cycle. B. The phase relationship between the S1 and S2 is stable across time; therefore these two time-varying signals are synchronized. C. The phase relationship between S1 and S2 is inconsistent across time, therefore these two signals are desynchronized.

3.1 NEURAL OSCILLATIONS

Neural ensembles, groups of neurons forming microcircuits, are known to express intrinsic and task-related rhythmic activities across a broad range of frequencies that reflect the simultaneous oscillations of extracellular potentials (Wang, 2010). Several biophysical properties of neural circuits, such as the excitatory-inhibitory interaction, the temporal structure of synaptic inputs, and the electric and chemical properties of neurons, together determine the frequency of oscillation (Jones et al., 2009; Kopell, et al., 2010; Roopun et al., 2010; Siegel, et al., 2012; Vierling-Claassen, Cardin, Moore, & Jones, 2010; Whittington, Kopell, & Traub, 2010). Therefore, distinct brain rhythms at different frequency bands (alpha-band: 8–14 Hz; beta-band: 15–29 Hz; gamma-band: >30 Hz; Buzsaki and Draguhn, 2004) are associated with different physiology (Buzsaki & Draguhn, 2004; Kopell, et al., 2010), and may be treated as indices of different microcircuit activities (Donner & Siegel, 2011; Siegel, et al., 2012).

Using non-invasive neuroimaging techniques with high temporal resolution such as MEG, electroengephalography (EEG), or invasive electrophysiology methods that measure local field potentials (LFP), one can record electrophysiology signals from a brain region and analyze their embedded information regarding oscillatory neurodynamics. Higher-level cognitive functions are mediated by different lower-level neural interactive processes among microcircuits that encode information, maintain information, output signals, boost or inhibit representation. The spectral content of a functional brain region may be process-dependent, depending on how a specific cognitive act is mediated by local microcircuit processes (Donner & Siegel, 2011). Note

that oscillatory activities reflect summated rhythmic potentials of groups of neurons, and are different from spike-rate measures that reflect spiking outputs of a single neuron.

3.1.1 Circuit Mechanisms of Neural Oscillations

To understand how circuits generate rhythms, it is useful to first discuss a canonical microcircuit model built on features of anatomy that are shared across brain regions (Douglas & Martin, 2004; Kaas, 2010). The primate neocortex has been found to be organized by large numbers of microcolumns and microcircuits (Mountcastle, 1997). Primate neocortical column can be specified as a vertical structure that consists of six layers of neurons; there are three superficial layers (1-3) and three deep layers (4-6). In each column, microcircuits are formed by excitatory and inhibitory neurons. Excitatory pyramidal neurons can be crudely divided into the superficial pyramidal cells and the deep pyramidal cells, each are recurrently connected with a wide variety of GABAergic inhibitory neurons. Thalamic inputs primarily (but not exclusively) terminate at layer 4, while other cortical and subcortical inputs primarily (but not exclusively) terminate at the superficial layers. Pyramidal neurons in layer 5/6 send outputs of the microcolumn to the BG, the thalamus, or other cortical regions.

Short-distance, within microcircuit communication tends to occur at the gamma-band (> 30 Hz). Studies found that gamma-band oscillation is generated by interactions between local excitatory pyramidal cells and fast-spiking GABAergic inhibitory interneurons (Cardin et al., 2009; Sohal, Zhang, Yizhar, & Deisseroth, 2009). In contrast, slower beta- (15-29 Hz) and alpha-band (8-14 Hz) rhythms likely involve inhibitory neurons with longer time constants, such as the low-threshold spiking interneurons (Jones, et al., 2009; Moore, Carlen, Knoblich, & Cardin, 2010; Vierling-Claassen, et al., 2010). Slower rhythms are typically more strongly expressed in

deep laminar layers (Buffalo, Fries, Landman, Buschman, & Desimone, 2011; Roopun, et al., 2010), suggesting that alpha and beta rhythms could reflect thalamic-cortical, cortical-thalamic-cortical, or cortical-cortical interactions (Bollimunta, Mo, Schroeder, & Ding, 2011; Jones, et al., 2009). Furthermore, different brain rhythms can be generated simultaneously in the same brain region, collectively reflecting different microcircuit level computation and integration functions that support cognition and behavior.

3.2 COMMUNICATION THROUGH NEURAL SYNCHRONIZATION

The communication through coherence hypothesis proposes that synchronization between distant oscillating neurons could act as a general neuronal communication mechanism (Fries, 2005; Varela, et al., 2001). As mentioned in Chapter 3.1, neural activity is known to show periodic oscillations, and such periodicity has been suggested to reflect rhythmic modulations in neuronal excitability (Burchell, Faulkner, & Whittington, 1998; Haider & McCormick, 2009; Lakatos et al., 2005). Rhythmic fluctuation of the excitability of a group of neurons makes its sensitivity to synaptic input predictable (Canolty, et al., 2010; Fries, 2005). In other words, the window for *optimal communication* becomes temporally predictable. For effective communication, transmitting and receiving neurons should have a consistent phase relationship, allowing neural spike-trains to consistently arrive at the phase when the targeted neuron is excitable. If spikes arrive at random phases, transmission can miss the optimal window for communication, rendering it ineffective. Therefore, different groups of neurons can communicate with each other more effectively when their activity patterns are well-synched—defined as *neural synchrony*, or *phase synchrony* (Figure 3).

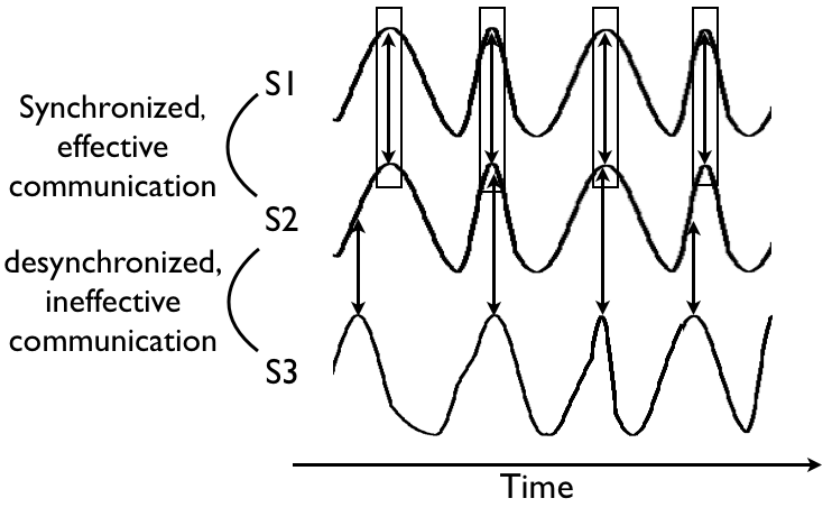

Figure 3. Phase synchronization as an index of neural synchrony.
Neural activities from S1, S2, and S3 show rhythmic oscillation across time. S1 and S2 are phase synchronized. In contrast, S2 and S3 are not synchronized. Phase synchronization allows effective information transfer between S1 and S2 (indicated by arrows) during optimal windows of communication (indicated by the boxes circling the peak of oscillation). In contrast, communication between S3 and S2 will be ineffective.

Communication between neurons could be established by reciprocally opening the optimal window for communication through entrainment of neural oscillations into the same frequency band (Canolty, et al., 2010; Lakatos, Karmos, Mehta, Ulbert, & Schroeder, 2008); whereas communication could be lessened through asynchronous oscillation (Akam & Kullmann, 2010). Such selective communication mechanism could be critical for top-down biasing and biased-competition. For example, neural synchrony could be strengthened between neurons encoding for the to-be-selected perceptual/motor information and neurons encoding for higher-order cognitive variables (Womelsdorf & Fries, 2007).

To summarize, neural synchrony at different frequencies is thought to support communication across different spatial scales. Short-distance synchronization tends to occur at higher frequencies (gamma-band), whereas long-distance communication is associated with the slower beta- or alpha-band frequencies (Kopell, et al., 2000; von Stein & Sarnthein, 2000). This hypothesis is consistent with rhythms' putative circuit mechanisms: Gamma-band neural synchrony is generated by local interactions between excitatory and fast-spiking inhibitory neurons (Cardin, et al., 2009), whereas alpha-band and beta-band activities involve cortical-cortical or cortical-subcortical interactions (Donner & Siegel, 2011; Jones, et al., 2009; Saalmann, Pinsk, Wang, Li, & Kastner, 2012; Siegel, et al., 2012). As such, frequency information could potentially provide a window into investigating potential circuit mechanisms supporting inhibitory control, and provide insights regarding developmental differences in neural mechanisms that support inhibitory control.

3.3 OSCILLATORY NEURODYNAMICS AND INHIBITORY CONTROL

Although few studies have directly examined the relationship between oscillatory neurodynamics and AS task performance, studies have characterized the time-frequency structure of neural oscillations associated with working memory and selective attention, both are closely related to the processes we hypothesized to be engaged during the preparatory period. Below we briefly review relevant findings.

3.3.1 Gamma Rhythm and Working Memory Maintenance

We hypothesized that to successfully perform the AS task, participants should actively maintain task-rule in working memory throughout the preparatory period. It has been suggested that sustained gamma-band activity (> 30 Hz) reflects active information maintenance in neural circuits through recurrent excitatory-inhibitory interactions (Jensen, Kaiser, & Lachaux, 2007). In support of this hypothesis, several human and nonhuman primate studies have found increased gamma-band power in the frontal and parietal cortices during the delay period of working memory tasks (Howard et al., 2003; Pesaran, et al., 2002; Roux, Wibral, Mohr, Singer, & Uhlhaas, 2012). Increased gamma-band power has been found in the lateral intraparietal sulcus (LIP) in macaque monkeys during a memory-guided saccade task, task which eye movements have to be made to a remembered location (Pesaran et al., 2002). Using a spatial-working memory task, a human MEG study also found increased gamma-band power in the DLPFC as well as the IPS during the delay period (Roux, et al., 2012). Furthermore, using the Steinberg working memory task, an intracranial electroencephalography (iEEG) study found that gamma-band power was positively correlated with working memory load (Howard, et al., 2003), and these positive correlations were predominantly found in electrodes placed over the lateral PFC. Together these results suggest that increases in gamma-band power might reflect local brain region actively maintaining information on-line.

3.3.2 Beta Rhythm and Top-Down Signaling

We hypothesized that for the AS task, the maintained task-rule should be converted to control signals and communicated to the oculomotor system to decrease the probability of making

reflexive saccades. The physiological origin of the beta rhythm (15-29 Hz) suggests it may reflect cortico-cortical communication and top-down signaling. In one *in vitro* study that recorded field potentials from slices obtained from rat's parietal cortices, beta rhythms were generated by glutamatergic excitation in the deep layers of cortical columns (Roopun, et al., 2010). Because excitatory pyramidal neurons in layer 5/6 send outputs of cortical columns to subcortical structures or other cortical areas or both (Douglas & Martin, 2004), beta-band activities expressed in higher-order association cortices could reflect top-down signaling that transmits control signals to influence down-stream sensory and motor processes.

Further, one computational modeling study showed the genesis of the beta rhythm in the primary somatosensory circuit could be accurately modeled by two inputs into laminar circuits; one thalamic *feedforward* input to the granular layer (layer 4) followed by a delayed *feedback* input into the superficial layers of cortical columns (Jones, et al., 2009). This is in contrast to the alpha rhythm, which could be modeled by the thalamic-cortical feedforward input. Feedback projections into the superficial layers are thought to be originated from either non-specific thalamic nuclei that have extensive connections throughout the cortex (Sherman & Guillery, 2011), or from other cortical columns (Douglas & Martin, 2004). This result suggests that local beta-band activity could be generated by recurrent cortical-subcortical-cortical loops (Alexander, DeLong, & Strick, 1986), when outputs originated from deep layers of a cortical column induce feedbacks from non-specific thalamic nuclei or other cortical columns back into the superficial layers. In a broader context, synchronous beta activity could also reflect global integrative functions (Donner & Siegel, 2011) that involve cortical-cortical or cortical-subcortical-cortical interactive processes.

In support of these hypotheses, increased beta-band activity has been found to be implicated in top-down control of goal-directed behaviors (Buschman, Denovellis, Diogo, Bullock, & Miller, in press; Buschman & Miller, 2007; Gross et al., 2006; Hipp, Engel, & Siegel, 2011; Saalmann, Pigarev, & Vidyasagar, 2007; Swann et al., 2009). An iEEG study reported increased beta-band power in the right VLPFC when patients successfully inhibited a motor response in the stop-signal task (Swann, et al., 2009). This increased beta-band power could reflect the right VLPFC outputting control-signals to inhibit down-stream motor circuitries. A similar finding has also been reported in a recent monkey electrophysiology study (Buschman, et al., in press). In this study, monkeys were trained to acquire and execute two different arbitrary SR mapping rules, and distributed neural ensembles within the PFC were found to encode each rule. Critically, when monkeys were executing a specific rule, beta-band neural synchrony increased among PFC neural ensembles that were previously found to encode the selected rule, whereas alpha-band neural synchrony increased among neural ensembles that coded the competing rule. This result further suggests that beta-band activity could also be involved in executing arbitrary SR mapping rules for goal-directed behaviors.

In a nonhuman primate study comparing top-down (memory search) and bottom-up (pop-out) sensory processing, neural synchrony between the PFC and the IPS has been found to strengthen in the beta frequency range during top-down attention selection (Buschman & Miller, 2007). Consistent with this finding, a human MEG study also found increased beta-band synchrony between frontal and parietal regions in anticipation of an incoming visual stimuli (Gross, et al., 2006). Furthermore, beta-band neural synchrony between the frontal and sensory cortices (occipital and temporal) increased when participants combined visual and auditory stimuli into a coherent percept (Hipp, et al., 2011). Collectively these results suggest beta-band

neural synchrony may reflect cortical-cortical communication, and increases in local beta-band oscillatory power may reflect top-down signaling from higher-order cortices; we hypothesized that preparatory inhibitory control will engage both processes.

3.3.3 Alpha Rhythm and Functional Inhibition

Studies suggest that correct AS task performance requires pretarget saccade-related activity to be sufficiently suppressed (Everling, et al., 1999; Everling & Munoz, 2000). What is the neural signal that might reflect this inhibition process? It has been suggested that functional inhibition is associated with increases in alpha-band power (8-14 Hz; Jensen & Mazaheri, 2010; Klimesch, Sauseng, & Hanslmayr, 2007). In support of this hypothesis, studies found that when participants directed attention to one hemifield, alpha-band power decreased in the contralateral hemisphere but increased in the ipsilateral hemisphere (Handel, Haarmeier, & Jensen, 2011; Thut, Nietzel, Brandt, & Pascual-Leone, 2006; Worden, Foxe, Wang, & Simpson, 2000). These findings suggest that increases in alpha-band power might reflect disengagement of task-irrelevant regions. In addition, if increased alpha-band power also reflects active inhibition of neuronal processes, it should also influence behavioral performance and neuronal firing. In support, it has been found that alpha-band power expressed in the somatosensory cortex was negatively correlated with the detection rate of tactile stimuli (Jones et al., 2010), and increased alpha power in the visual cortex negatively correlated the discrimination of near-threshold visual stimuli (van Dijk, Schoffelen, Oostenveld, & Jensen, 2008). Furthermore, a study that recorded neural activity from the monkey premotor cortex found that neural spike-rate was negatively correlated with alpha-band power—when alpha-band power was high, neurons fired less frequently (Haegens, Nacher, Luna, Romo, & Jensen, 2011).

The physiological mechanism of the alpha rhythm is currently not well understood, and different hypotheses have been proposed. Because thalamic neuronal populations are known to show intrinsic alpha-band activity (Hughes & Crunelli, 2005), most models agree that alpha-band activity reflect some forms of cortico-thalamic interactions (Bollimunta, et al., 2011; Jones, et al., 2009), yet still no firm explanation exist. If increased alpha-band power is an index of cortical inhibition, it should involve inhibitory neurons that can sustain inhibition to pyramidal neurons to reduce spiking outputs. It has been found that one type of low-threshold spiking interneurons, the somatostatin (SOM) expressing neurons, reduce burst firing in excitatory neurons by providing tonic inhibition to pyramidal neurons' distal dendrites (Gentet et al., 2012). Computer simulations of microcircuits suggests that activation of SOM inhibitory neurons could amplify low frequency oscillation (Vierling-Claassen, et al., 2010). Furthermore, SOM neurons receive inputs from the thalamus (Tan, Hu, Huang, & Agmon, 2008), consistent with existing models suggesting that alpha rhythm involves thalamic-cortical interactions (Bollimunta, et al., 2011; Jones, et al., 2009). Together these studies suggest that during the preparatory period, alpha-band power will increase in oculomotor regions, reflecting active functional inhibition of saccade-related activity.

4.0 DEVELOPMENTAL OF OSCILLATORY NEURODYNAMICS

In Chapter 3, we discussed how neural circuits could generate oscillatory neurodynamics, and its involvement in preparatory inhibitory control processes. In this chapter, we will review studies describing structural neurodevelopment during adolescence, and discuss how brain maturation might affect neural oscillation and neural synchrony. Several related issues had been previously discussed in Hwang & Luna (2012).

4.1 BRAIN MATURATION DURING ADOLESCENCE

4.1.1 Synaptic Pruning and Myelination

The brain continues to show important morphological changes during adolescence. Neocortical gray matter shows continued thinning into adulthood, especially in the PFC and the temporal cortex (Gogtay et al., 2004). The pruning of synapses is believed to be a primary contributor to gray matter thinning, and continued synaptic pruning has been found during adolescence (Rakic, Bourgeois, Eckenhoff, Zecevic, & Goldman-Rakic, 1986). Histological studies found that the reduction in synapses in the middle frontal gyrus reached adult levels at a later age (16 years), when compared to age 7 in the visual cortex (Huttenlocher, 1979; Huttenlocher, de Courten,

Garey, & Van der Loos, 1982), and at age 10 in Heschls's gyrus in the temporal cortex (Huttenlocher & Dabholkar, 1997).

Concurrent with gray matter maturation, white matter connections also show protracted development during adolescence. Distant brain regions are interconnected by bundles of axon fibers that support communication between gray matter regions. During development, glial cells form myelin sheets that wrap around these axon fibers, enhancing the speed and efficiency of neuronal transmission. Histological findings indicate that myelination begins during the second trimester of pregnancy and continues into adult life (Yakovlev, Lecours, & Minkowski, 1967). Myelination reaches adult levels in the sensory regions first, followed by the motor regions, and association regions continue to myelinate through adolescence (Yakovlev, et al., 1967).

4.1.2 Structural Connectivity

Diffusion tensor imaging (DTI) measures the coherence of water diffusion in the brain parenchyma; in white matter tracts, because the direction of diffusion is more confined, greater coherence of water diffusion reflects increased integrity of white matter tracts. Fractional anisotropy (FA) measures the diffusion along the length of axons of the white matter, and radial diffusivity (RD) measures the width and depth of diffusion. Both measures are routinely used to characterize the integrity of white matter tracts in developmental DTI studies.

Several DTI studies found that FA values increased with age in major white matter tracts that provide cortical-cortical and cortical-subcortical connections. These tracts included the internal capsule, the superior longitudinal fasciculus, and the corpus callosum (Asato, Terwilliger, Woo, & Luna, 2010; Ashtari et al., 2007; Barnea-Goraly et al., 2005; Schmithorst, Wilke, Dardzinski, & Holland, 2002). In our own DTI study, we found continued maturational

changes in major white matter tracts from adolescence to adulthood (Asato, et al., 2010). For that study, we recruited 36 children (8–12 years of age), 45 adolescents (13–17 years of age), 33 adults (18–28 years of age), and examined age-related changes in RD. RD has been found to be a more faithful measure of histological changes in myelination and dysmyelination; decreases in RD value was suggested to be associated with increases in myelination (Song et al., 2002; Song et al., 2005). Specifically, the uncinate fasciculus, a frontal portion of the superior longitudinal fasciculus, frontal portions of the anterior thalamic radiations, the genu of the internal capsule, a frontal-parietal portion of the corona radiata, and the posterior portion of the corpus callosum had not reached adult levels in adolescence. Among these white matter tracts, the superior longitudinal fasciculus connects the PFC with the parietal cortex, and the thalamic radiata encapsulates thalamic-cortical projections. Immaturities in these white matter tracts could be related our previous effective connectivity study (Hwang, et al., 2010), suggesting that both functional and structural brain connectivity between frontal-cortical and frontal-subcortical regions continues to develop into adulthood.

Myelination increases the speed of neuronal transmission (Stufflebeam et al., 2008), potentially enhancing the precision of inter-regional synchronization. Specifically, immaturities in association tracts and thalamic radiata could be particularly relevant to the expression and synchronization of alpha and beta rhythms. As discussed previously, the physiological mechanisms that generate alpha and beta rhythms could involve cortical-cortical and subcortical-cortical interactions (Jones, et al., 2009). If association tracts and projection tracts are immature during adolescence, this immaturity could affect both the expression of alpha and beta oscillations, as well as the synchrony between oscillations.

4.1.3 Inhibitory Neurons

As discussed in the previous chapter, the expression of oscillatory neurodynamics is intimately linked to the excitatory/inhibitory interactions of microcircuits. Critically, different types of inhibitory interneurons and gamma-aminobutryic acid (GABA) functioning are pivotal in modulating the frequencies of neural oscillations (Moore, et al., 2010). Thus, cellular developmental changes in inhibitory neurons could influence the synchrony and power of neural oscillations, and inturn influence behavior.

Using primate models, studies suggest fast-spiking interneurons' functions remains immature during adolescence (Lewis & Melchitzky, 2012). For example, the density of axon terminals in fast-spiking parvalbumin (PV) GABA inhibitory neuron increases continuously into adulthood in the PFC (Erickson & Lewis, 2002), and the expression of messenger ribonucleic acid (mRNAs) encoding postsynaptic GABA receptors subunits also have a protracted developmental trajectory through adolescence (Hashimoto et al., 2009). PV GABA neurons innervate the axon initial segment (axon hillock) of pyramidal cells, regulating their firing output; therefore immaturities in layer 5 fast-spiking GABA interneurons could potentially affect prefrontal cortex's top-down signaling to subcortical and cortical regions.

Low-threshold spiking inhibitory neurons, such as the SOM neuron that targets the dendritic branch of pyramidal cells, has been hypothesized to be involved in the genesis of the alpha rhythm (Vierling-Claassen, et al., 2010). While low-threshold spiking interneurons' developmental trajectories and its function over adolescence remain poorly understood, it has been found that in human postmortem DLPFC samples, the expression level of mRNA encoding for SOM showed continuously change into early adulthood (Fung et al., 2010). This result suggests that the density of SOM neurons and the level of SOM peptide expression continue to

change during adolescence. Collectively, cellular changes in PV GABA interneurons and SOM interneurons could change the strength and kinetics of GABA neurotransmission, altering excitatory/inhibitory interactions in microcircuits, ultimately affecting the expression and synchrony of neural oscillations.

4.2 THE DEVELOPMENT OF NEURAL OSCILLATION

Both the amplitude of neural oscillations and the strength of neural synchrony have been found to change throughout development. A set of resting-state EEG studies that recruited a large cohort of participants ranging in age from 2 months to 26 years have revealed continuous changes in the synchrony of spontaneous neural activity from infancy to adolescence (Thatcher, North, & Biver, 2008; Thatcher, Walker, & Giudice, 1987); specifically beta-band neural synchrony between anterior-poster pairs of electrodes increased with age in an exponential manner from 2 months to 26 years of age (Thatcher et al., 1987). Another resting-state EEG study has also found that alpha- and beta-band power increased from age 6 to 24 (Dustman, Shearer, & Emmerson, 1999). Similarly, using an auditory oddball task, it was found that synchrony between long-distance electrode pairs in the 0–12 Hz frequency range was weaker in young children (9-13 years), compared to young adults (18-25 years; Muller, Gruber, Klimesch, & Lindenberger, 2009).

To date the most comprehensive study on the development of neural synchrony was carried out by Uhlhaas and colleagues (2009). In this study, 68 6- to 21-year-olds were studied with EEG while subjects performed a Mooney face perception task. Mooney faces are black and white pictures of faces with minimal identify information, and are known to induce strong

synchronization of oscillatory activity in the beta- and gamma-band (Rodriguez et al., 1999). Adults showed strong gamma-band power over parietal electrodes and long-range neural synchrony in the theta- and beta-band between distant electrodes. Developmentally, oscillation power in the gamma-band increased until early adolescence (12–14 years) but dropped during late adolescence (15–17 years) and increased again in early adulthood. The same nonlinear developmental pattern was also observed for beta- and theta-band synchrony between all electrodes. This finding highlights late adolescence as a critical developmental period when neural oscillations undergo critical changes.

The EEG studies discussed above only analyzed sensor signals, and results could be confounded by signal mixing—signals measured in one sensor reflect signals summated across multiple different anatomical structures (S. Palva & Palva, 2012). Without identifying anatomical sources, it is difficult to make effective interpretation on how regional-specific oscillatory neurodynamics could contribute to cognitive development. Furthermore, volume conduction could inflate synchrony estimates in the sensor space (Schoffelen & Gross, 2009). Nevertheless, when taken together, these EEG studies suggest that both the amplitude of neural oscillations and the strength of neural synchrony continue to develop during adolescence. Specifically, beta-neural synchrony, alpha-band power, and gamma-band power continue to develop during adolescence. In turn, these developmental changes in oscillatory neurodynamics could contribute to developmental improvements in inhibitory control.

4.3 MOTIVATION

We have reviewed studies that found maturational changes in brain morphology, histology, structural connectivity, inhibitory neurons, and neural synchrony. Together these studies provide evidence for a protracted development of oscillatory neurodynamics, specifically alpha, beta, and gamma rhythms. Maturational changes in the expression of neural oscillations in distributed cortical regions, as well as the inter-regional synchrony of oscillations, could further affect inhibitory control processes. Given that the biophysical mechanisms of neural oscillations are still being intensively investigated, studying developmental changes of oscillatory neural activity has the potential linking system-level descriptions of brain activity to circuit-level biophysical processes. Our results will have the potential to provide insights into the physiological basis of aberrant development that can lead to disturbances in behavior and emergence of major psychopathology during adolescence.

5.0 HYPOTHESES AND METHODS

The primary aim of this dissertation was to delineate developmental changes in oscillatory neurodynamics associated with preparatory inhibitory control from adolescence to adulthood. We addressed this aim using oculomotor tasks with high temporal resolution MEG, where participants performed the AS and the PS tasks. MEG was used because of its superior temporal resolution and reasonable spatial resolution, making it an optimal tool for tracking fast-changing cortical neurodynamics occurring in parallel of cognitive dynamics. As discussed above, the AS task has been found to be sensitive to detecting behavioral immaturities in inhibitory control during adolescence (Luna, et al., 2004), and the PS task is an important control for age-related differences in basic perceptual and oculomotor processing. We focused on the preparatory signal, given its importance in predicting success vs. failure of AS task performance. Specifically, we had two specific aims:

1. To investigate oscillatory neurodynamics associated with preparatory inhibitory control processes.

2. To investigate the development of oscillatory neurodynamics associated with inhibitory control from adolescence to adulthood.

5.1 PARADIGM

Each trial began with a 1.5 seconds cue fixation (Figure 4). For AS trials, a red "x" instruction cue instructed participants to look at the mirror location of an upcoming peripheral target, whereas for PS trials a green "x" instructed participants to look at the target. The colored "x" will be referred to as the *cue* in the following sections. The cue lasted for 1.5 seconds, during which the participants maintained fixation. This stage of the task denotes the "preparatory period". A target stimulus was then presented after the extinction of the cue. The target stimulus was a solid yellow circle presented on the horizontal meridian at one of four unpredictable eccentricities (±6.3° and ±10.6° from center fixation) for 1.5 seconds, and participants had to either look at the yellow dot for PS, or look at the opposite direction of the dot for AS. The peripherally presented yellow dot will be referred to as the *target* here on. Ninety percent of the targets were presented at the far location (±10.6°), and only the far trials were included for analyses to control for saccade amplitude. A 1.2 to 1.6 seconds jittered white fixation "x" was presented between trials.

We presented AS and PS trials in blocks. This was chosen to minimize task-switching effects, as mixing AS with PS had been shown to alter both behavioral performance and neural activity significantly (Akaishi, Morishima, Rajeswaren, Aoki, & Sakai, 2010; Lee, Hamalainen, Dyckman, Barton, & Manoach, 2010). A three seconds text instruction was presented at the beginning of each task block to signal the beginning of task blocks. Each block lasted 30 seconds with five trials, and a five seconds short rest period was inserted between blocks. The order of task blocks was counter-balanced across participants, and 210 AS trials and 210 PS trials were distributed across eight MEG runs (six minutes each).

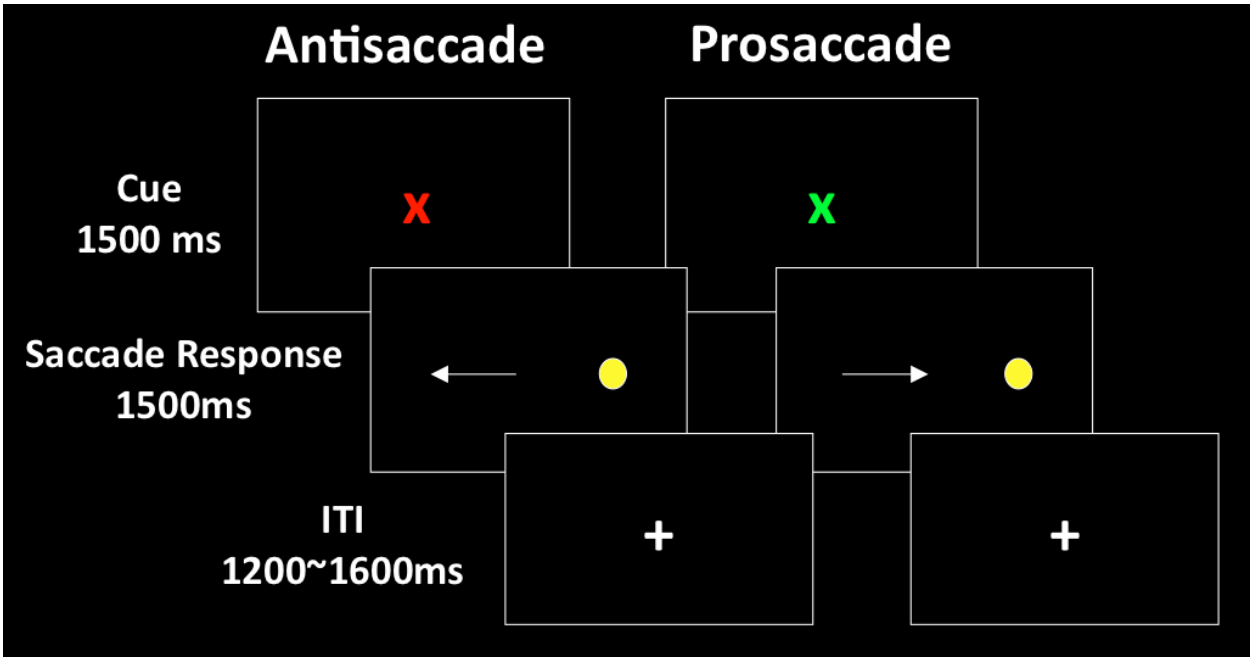

Figure 4. Task diagram.
Arrow indicates correct saccade direction.

5.2 HYPOTHESES

5.2.1 Aim 1: To Investigate Oscillatory Neurodynamics Associated with Inhibitory Control Processes during the Preparatory Period

Studies discussed above strongly suggest that oscillatory neurodynamics may be related to different preparatory inhibitory control processes.

1. We hypothesized that task-rule maintenance would be associated with increases in gamma-band power in the PFC and the IPS. We hypothesized that because the PS task is a

reflexive task that requires less cognitive resources, the PS task could engage less working memory processes, resulting in weaker gamma power when compared to the AS task.

2. We hypothesized that for the AS task, the encoded task-rule would be converted to top-down control signals and bias the oculomotor system to decrease the probability of making a reflexive saccade (Brown, et al., 2007; Everling & Munoz, 2000; Munoz & Everling, 2004). We further hypothesized that beta-band power would increase in the PFC, reflecting top-down signaling through projection and association pathways to down-stream subcortical and oculomotor regions. Furthermore, beta-band neural synchrony between the PFC and oculomotor regions would increase. For the PS task, given that there is no need to inhibit reflexive saccades, the need for top-down signaling would be lessened, resulting in weaker beta-band power and beta-band neural synchrony compared to the PS task.

3. We hypothesized that alpha-band power would increase in the FEF for the AS task when compared to the PS task, reflecting functional inhibition of saccade-related activities.

5.2.2 Aim 2: To Investigate the Development of Oscillatory Neurodynamics Associated with Inhibitory Control from Adolescence to Adulthood

To date, how oscillatory neurodynamics develop to support inhibitory control during adolescence has not yet been directly examined. Studies of neurodevelopment provide compelling evidence that microcircuitries and major white matter tracts continue to develop during adolescence, potentially affecting the expression and synchronization of alpha, beta, and gamma oscillations. Initial EEG studies also showed changes in both the power and synchrony of neural oscillations. Based on these findings, we proposed sets of developmental hypotheses.

1. As previously hypothesized, task-rule maintenance would be associated with increased gamma-band power in the PFC and the IPS. Given that fast-spiking GABA interneurons remain immature during adolescence (Lewis & Melchitzky, 2012), we hypothesized that adolescents would show weaker gamma-band power in fronto-parietal cortices.

2. We hypothesized that top-down signaling processes would be associated with increases in beta-band power in the PFC, as well as increases in beta neural synchrony between the PFC and oculomotor regions. Given subcortical-cortical projection and cortical-cortical association tracts' hypothesized involvement in beta rhythm (Jones et al., 2009), and their known immaturities in adolescents (Asato, et al., 2010), we hypothesized that adolescents would show weaker beta-band oscillatory power in the PFC, reflecting immaturities in top-down signaling processes, as well as weaker long-range beta neural synchrony, indicating ineffective cortical-cortical communication.

3. We hypothesized that during the preparatory period, saccade-related activities would be functionally inhibited, indicated by increases in alpha power in oculomotor regions. Due to known immaturities in thalamic-cortical projection tracts during adolescence (Asato et al., 2010) and their hypothesized involvement in alpha rhythm (Bollimunta, et al., 2011; Jones, et al., 2009), we hypothesized that alpha-band power would be decreased in adolescents, indicating immature functional inhibition.

5.3 METHODS

5.3.1 Participants

Twenty-six adults (12 male; aged 19 to 30) and 22 adolescents (11 male; aged 14 to 16) participated in the study in accordance with University of Pittsburgh Institutional Review Board guidelines. Participants and their first-degree relatives had no history of psychiatric disorders. Two adults were excluded from analyses because of excessive blinking. Data from four adults and four adolescents were excluded because of excessive artifacts that could not be removed during post-processing. One adolescent was excluded because of history of psychiatric disorder that was revealed after participation. After exclusions, we reported data from 20 adults (10 male) aged 20 to 30 (M = 26.11 years, SD = 3.41) and 17 adolescents, (8 male) aged 14 to 16 (M = 15.74 years, SD = 0.94). IQs were not significantly different between adults and adolescents (adults: M = 112.25, SD = 8.09; adolescents: M = 110.64, SD = 12.91; $t(35) = 0.45$, $p = 0.65$). All participants gave inform consent.

5.3.2 Data Acquisition

All MEG data were acquired using an Elekta Neuromag VectorView MEG system (Elekta Oy, Helskink, Finland) located in a three-layer magnetically shielded room. The system includes 102 identical sensor triplets, two orthogonal planar gradiometers, and one magnetometer (306 sensors in total). Subjects were seated upright with the head positioned inside the helmet containing the sensors. Visual stimuli were projected to a screen located one meter in front of the participant. Before the MEG scan began, three anatomical cardinal landmarks (nasion and two preauricular

points), 20 additional anatomical points, and four head position indicators (HPI) were digitized using a 3D-digitizer (ISOTRACK, Polhemus, Inc., Colchester, VT) to define the head coordinate system and to assist co-registration of MEG data with MRI data. MEG data were acquired continuously with a sampling rate of 1000 Hz. Head position relative to the MEG sensors was measured throughout the recording period to allow off-line head movement correction (Wehner, Hamalainen, Mody, & Ahlfors, 2008). Two electrocardiogram (ECG) electrodes were placed on each subject's chest to record cardiac signals. A ground electrode was placed behind participants' right ear, and a reference electrode was placed behind particpants' left ear.

For all participants, structural MRI data were collected at a Siemens 3T Tim Trio system scanner. Structural images were obtained using a magnetization-prepared rapid acquisition with gradient echo (MP-RAGE) sequence with the following parameters: TR = 2100ms, TI = 1050 ms, TE = 3.43ms, 8° flip angle, 256x256x192 acquisition matrices, FOV = 256 mm, and 1 mm isotropic voxels.

5.3.3 Eye Movement Data

To monitor eye movements and eye blinks during MEG scans, two bipolar electrode pairs were used to record vertical and horizontal electrooculogram (EOG) signals. Horizontal EOG electrodes were placed above and below the left eye; vertical EOG electrodes were placed laterally to each eye. At the beginning of each participant's MEG scanning session, EOG calibration data were collected to convert EOG voltages into saccade directions and amplitudes (Lee, et al., 2010; Moon et al., 2007). Calibrated EOG data were then scored offline in MATLAB (2011a, The MathWorks, Natick, MA.) using a costum program to code correctly and incorrectly performed trials. For each trial, the direction of and latency of the initial saccade were

determined. Saccades were identified as horizontal eye movements with velocities exceeding 40°/second, and the onset was defined as the time when the velocity exceeded 15% of the peak saccade velocity (Gitelman, 2002). Only trials with latencies between 110 and 800 ms were included for future analyses. The cutoff of 110 ms excluded express saccades that were not reaction to the stimulus (Fischer & Boch, 1983).

5.3.4 MEG Data Preprocessing

After acquisition, MEG sensor data were first manually inspected to reject bad or flat channels. Data were then preprocessed off-line using the temporal signal space separation (TSSS) method (Taulu & Hari, 2009; Taulu, Kajola, & Simola, 2004). TSSS reduces environmental magnetic artifacts outside the head and sensor artifacts, and performs head movement compensation by aligning sensor level data to a common reference (Nenonen et al., 2012). This head motion correction procedure also provides estimates of head motion relative to sensors coordinates every 200 ms, estimates which will be used to reject trials contaminated by motion artifacts (Wehner, et al., 2008).

5.3.4.1 Artifact Rejection

Cardiac, eye-blinks, and saccade artifacts were removed using an independent component analysis-based procedure. MEG sensor data were decomposed into 64 independent components (ICs) using EEGLAB (Delorme & Makeig, 2004) algorithms implemented in the Fieldtrip software suite (Oostenveld, Fries, Maris, & Schoffelen, 2011). The number of ICs (64) was chosen because TSSS internally reduces dimension to 64 components before re-projecting signals back to the sensor space (Taulu & Hari, 2009; Taulu, et al., 2004). To identify artifact

components, each IC was correlated with ECG and EOG data. An IC was designated as an artifact if the absolute value of the correlation was three standard deviations higher than the mean of all correlations. Across all subjects, between two and six artifact components were rejected. The “clean” ICs were then projected back to the sensor space for manual inspection. We found that for every participant, cardiac and eye-blink artifacts were successfully removed; however, this procedure failed to detect saccade-related components for most subjects, therefore artifacts introduced by eye movements were controlled for by only analyzing data prior to the onset of saccades. Note that the preparatory period was saccade free. After the removal of artifacts, sensor data were down-sampled to 250 Hz to improve calculation efficiency. Power line noise was removed using a Fourier transformation of 10 seconds long signal window that moved along the full data length, and subtracted the 60 Hz component and its harmonics.

Trials were then inspected for sensor jumps, muscle artifacts, unwanted saccades, and head movement artifacts. Trials with saccades that occurred during the preparatory period or pretrial baseline were excluded. Trials with gradiometer peak-to-peak amplitudes exceeded 3000 fT/cm or magnetometer peak-to-peak amplitudes exceeded 10 pT were also excluded (Lee, et al., 2010; Moon, et al., 2007). To mitigate the effects of head motion on data quality, we adopted a conservative approach and rejected trials with sensor displacement greater than 1 mm. The amount of head motion was estimated by calculating the frame-by-frame sensor displacement relative to the head position (Wehner, et al., 2008). Briefly, low-amplitude, high-frequency sinusoidal continuous currents (> 300 Hz) were fed to the four HPI coils positioned on the subject's head throughout the scan. The position and orientation of the head with respect to the sensor array can then be determined at 200-ms intervals, using Elekta’s MaxFilter software. If at any time during the trial the displacement of MEG sensors was greater than 1mm, the trial was

rejected from all future analyses. On average, 3.4% of trials were rejected for adults (standard deviation = 6.9%, range = 0.7% to 17%), and 4.6% of trials were rejected for adolescents (standard deviation = 3.7%, range = 1.3% to 11%).

5.3.5 Inverse Solution

The source location of neural activity cannot be determined by only analyzing MEG sensor data. To estimate source activity, we calculated the cortically constrained minimum-norm estimates (MNE; Dale & Sereno, 1993; Hamalainen & Ilmoniemi, 1994; Hamalainen, Lin, & Mosher, 2010), using the MNE software package (version 2.7.3; http://www.martinos.org/mne/) and custom MATLAB scripts. MNE is a non-parametric technique that yields distributed cortical current estimates by minimizing the norm of the estimated currents. Because the majority of MEG signal is thought to be generated by neurons structurally aligned in cortical columns at the surface of the brain, and are positioned perpendicular to the cortical surface (Hamalainen, Hari, Ilmoniemi, Knuutila, & Lounasmaa, 1993; Lopes da Silva, 2010), accuracy is improved by incorporating biophysical realistic constraints based on each participant's brain geometry (Dale & Sereno, 1993; Lin, Belliveau, Dale, & Hamalainen, 2006).

First, sensor data were bandpass filtered at 0.01 – 80 Hz. The geometry of each participant's cortical surface was reconstructed from the respective structural images using FreeSurfer (Dale, Fischl, & Sereno, 1999; Fischl, Sereno, & Dale, 1999). The solution space for the source estimation was then constrained to the gray/white matter boundary, by placing approximately ~3000 dipoles per hemisphere with 7 mm spacing. A forward solution for the constructed source space was calculated using a single compartment boundary-element model (Hamalainen & Sarvas, 1989). The noise covariance matrix was calculated from -700 to -400 ms

baseline time windows during the inter-trial-intervals (before task cues were presented) of all trials that were free of artifacts. The noise covariance matrix and the forward solution were then combined to create a linear inverse operator (Dale et al., 2000) to project MEG sensor data to the cortical surface.

5.3.6 Dynamic Statistical Parametric Maps

Although brain regions associated with AS and PS performances have been well characterized using fMRI, it is unknown if MEG has the spatial sensitivity to identify similar regions. To address this question, we calculated *dynamic statistical parametric maps* (dSPM; Dale, et al., 2000) to characterize spatiotemporal patterns of brain activity associated with AS. For each participant, preprocessed sensor data were first averaged across trials, separately for each condition. We then projected the grand-averaged sensor data into the source space by applying the inverse operator. The current estimate at each source location was divided by the estimated baseline variance (-700 to -400 ms prior to the cue presentation), resulting in an *F*-like statistics that can be visualized as dSPM (Dale et al., 2000). The dSPM values were then used to identify brain regions that were reliably activated by the task. To visualize group results, each subject's dSPM data were morphed to a common template surface from 40 adults created by the Buckner laboratory at Harvard University (Cambridge, MA). Note that dSPM patterns represent time-domain evoked responses that are phase-locked to the cue.

5.3.7 Oscillatory Analyses

To investigate neural oscillation and neural synchrony, it is necessary to obtain the instantaneous spectral power and phase information of source current estimates. It has been shown that frequency-domain oscillatory activities are not phase-locked to the stimuli (Pfurtscheller & Lopes da Silva, 1999), and will be attenuated by averaging time-domain evoked responses. Therefore it is necessary to perform time-frequency transformation on single-trial MEG data (Jensen & Hesse, 2010). For oscillatory analyses, no grand averaging was performed; instead, single-trial sensor data were projected into the source space using the linear inverse operator. Single-trial source estimates were then subjected to spectral analyses to obtain power and phase information for every trial (Lin et al., 2004). We spectrally decomposed neural currents at each source by convolving the time-domain signal with a family of complex Morelet wavelets (Lachaux, et al., 1999; Tallon-Baudry, Bertrand, Delpuech, & Permier, 1997). The Morelet wavelet was used because it is better suited for non-stationary neural signals (Jensen & Hesse, 2010), and achieves the optimal time-frequency resolution by applying a Gaussian shape tapper.

For each source location, current estimates *s* at time *t* were convolved with the wavelet *G* centering at frequency *f* to produce a time frequency representation ω:

$$\omega(t, f) = G(t, f) * s(t), \quad (1)$$

where *f* stepped from 8 to 60 Hz by one Hz increment.

The complex wavelet *G* was defined as:

$$G(t, f) = \frac{1}{\sqrt{2\pi f}} \exp\left(\frac{-t^2}{2\sigma^2}\right) \exp(i2\pi f t), \quad (2)$$

where σ was set to be 7/2 πf to achieve the optimal time-frequency resolution and to ensure the stability of wavelet transformation (Ghuman, McDaniel, & Martin, 2011; Tallon-Baudry, et al., 1997).

For each source location, the time-varying power *P* for frequency *f* was obtained with:

$$P(t, f) = |\omega(t, f)|^2, \quad (3)$$

and the phase vector ϕ was calculated using:

$$\phi(t, f) = \arctan(\omega(t, f)). \quad (4)$$

5.3.8 Frequencies of Interest

Although spectral neural activity follows 1/*f* continuum, computation models (Jones, et al., 2009; Vierling-Claassen, et al., 2010; Whittington, et al., 2010) and electrophysiology recordings (Bollimunta, et al., 2011; Cardin, et al., 2009; Haegens, et al., 2011; Roopun, et al., 2010) together strongly indicate that oscillatory neural activity can be classified into discrete rhythms, each associated with different circuit mechanisms. We defined the frequency ranges for alpha- (8-14 Hz), beta- (15-29 Hz), and gamma-band (30-60 Hz) based on previous literature and our pilot analyses whereby we observed distinct alpha- and beta-band activities (Figure 5). We did not include slower rhythms (< 8 Hz) because they required a long wavelet window to achieve the desirable frequency resolution. Having a long wavelet window will decrease temporal resolution, and makes it difficult to separate activities between task epochs (i.e., baseline vs. preparatory period vs. response period).

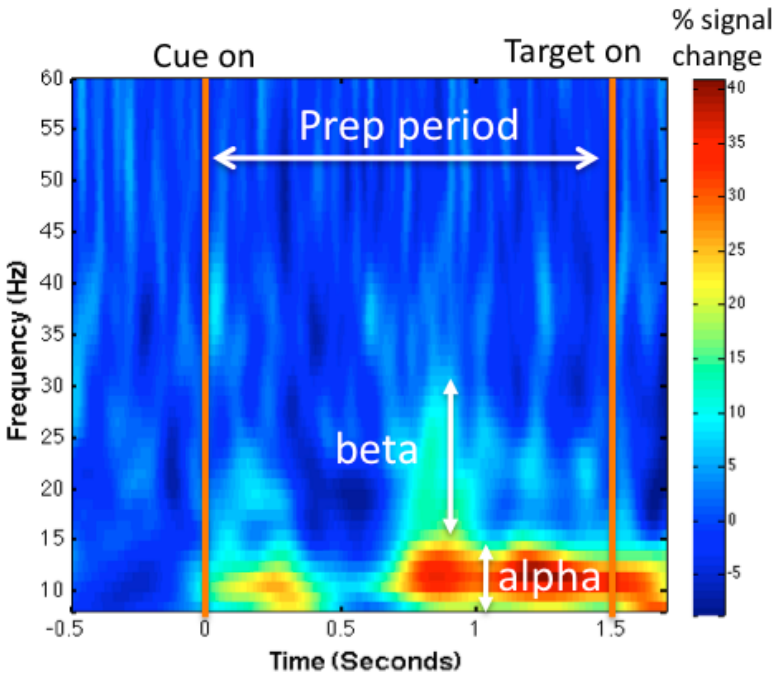

Figure 5. Prelimnary analysis of power spectrum associated with AS task performance. This is the power spectrum of all frontal ROIs (FEF, DLPFC, VLPFC), averaged across all participants. Distinct bands of alpha and beta rhythms were observed.

5.3.9 Regions of Interest

We selected regions of interest (ROIs) *a priori* based on their known involvement in inhibitory and oculomotor control, including the DLPFC, the VLPFC, the FEF, and the IPS. ROIs from both hemispheres were selected. We also included the primary visual cortex (V1) for control purposes. Because MEG is relatively insensitive to subcortical sources (Hamalainen, et al., 2010), no subcortical ROIs were included. Similarly, the ACC and the SEF were not included because we found that medial ROIs had significantly lower signal-to-noise ratio compared to lateral ROIs. Lower signal-to-noise ratio in medial ROIs could be caused by the known source

cancelation problem in MEG signal, problem which nearby sources with opposite current directions will weaken magnetic signal.

Since MEG is most sensitive to tangential sources located in the sulci (Lopes da Silva, 2010), we further restricted our ROIs within selected anatomical structures. These selected structural masks were created using FreeSurfer's automatic parcellation of sulci and gyri (Destrieux, Fischl, Dale, & Halgren, 2010) based on each participant's structural MRI. Anatomical masks used to constrain functional ROI were determined by consulting the relevant literature (Figure 6). Specifically, we defined the FEF to be located within the precentral sulcus, with distinct superior and inferior portions (sFEF and iFEF; Lee, et al., 2010; Luna, et al., 1998; Moon, et al., 2007). The VLPFC was constrained to be within the inferior frontal sulcus, the triangular and the orpercular part of the inferior frontal gyrus (Aron, et al., 2004; Levy & Wagner, 2011), and the DLPFC was defined within the middle frontal sulcus (Badre & D'Esposito, 2009; DeSouza, et al., 2003; Koval, Lomber, & Everling, 2011). The V1 was defined along the calcarine fissure. Within these anatomical masks, we functionally constrained the ROIs to dipoles that showed reliable oscillatory activity in the alpha-, beta-, and gamma-band frequencies during the preparatory period.

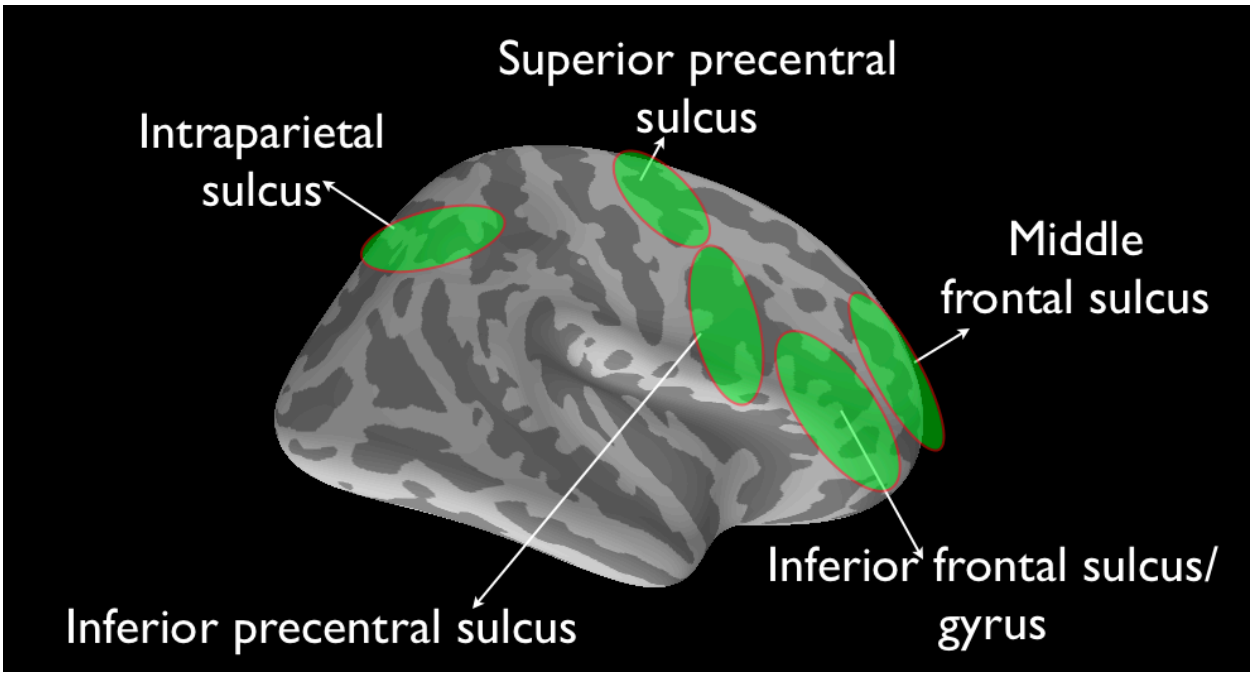

Figure 6. Anatomical structures of interest.
For illustration, anatomical structures of interest are shown on the right hemisphere. ROIs from both hemisphere were selected.

Briefly, using *Equation 3*, for every trial the time-varying power of all frequencies (8-60 Hz) was calculated for all dipole sources within each anatomical structure. Separately for each frequency, the power values were then converted to signal-to-noise estimates by subtracting it from the baseline mean and dividing by the variance of baseline power. Baseline window was defined as -700 to -400 ms prior to the cue presentation. This signal-to-noise ratio estimate is analogous to a *z*-score and can be used to identify dipoles where oscillatory activities are robust. We then took the absolute values of *z*-scores, and averaged them within the preparatory period for all trials (AS and PS), regardless of performance. This procedure is akin to deriving an omnibus test statistic for all conditions. We used absolute values to account for the possibility of having negative *z*-scores, indicating suppression in oscillatory power. Absolute *z*-scores were

then further averaged across frequencies (8-60 Hz). We then identified the dipole with the maximum averaged absolute *z*-score, and drew an ROI around the peak dipole that included 27 to 30 contiguous dipoles through an iterative spreading operation (Hamalainen, 2010). Because the MNE solution yields current estimates that are spatially smoothed (Jensen & Hesse, 2010), it is typical to include a larger number of dipoles for ROI definition, instead of selecting focal sources (Lee, et al., 2010; Moon, et al., 2007; Temereanca et al., 2012).

This ROI definition procedure includes all trials (AS and PS), performances (correct and incorrect trials), and frequencies (8-60 Hz); it is therefore unbiased and independent with regard to our hypotheses. This procedure is also age-neutral because ROIs are defined separately for each subject, and no age-related contrasts are used. Furthermore, defining ROIs in native space is advantages because MNE specifically incorporates individual's anatomical information into source estimation. This approach does not require spatial normalization, an advantage that minimizes interpolation errors and spatial smoothing of current source estimates.

5.3.10 Oscillatory Power

To analyze the power of different brain rhythms, single-trial MNE estimates were first averaged across dipoles within each ROI while aligning the sign of current fluctuations across different dipoles (Hamalainen, et al., 2010). For each trial, power time-courses were calculated using *Equation 3*. Power values were then converted to percent signal changes from baseline power. The baseline power was computed from -700 to -400 ms prior to the cue presentation. For each subject, percent signal changes in power were then averaged across trials within each condition (AS-Correct, PS-Correct, AS-Incorrect), and pooled across subjects for group analyses. Instead of treating each frequency as separate dependent measures, we averaged power time-courses

across frequencies into the three classes of rhythms that were defined *a priori* (alpha, beta, and gamma). Averaging across frequencies reduces data dimension and the number of statistical tests that have to be performed. This approach has been consistently used in the EEG/MEG literature (e.g., Hipp, et al., 2011; Siegel, Donner, Oostenveld, Fries, & Engel, 2008). Note that to control for performance, correct and incorrect trials were analyzed separately.

5.3.11 Neural Synchrony

We calculated phase locking values (PLV; Lachaux, et al., 1999) to measure the strength of neural synchrony (phase synchrony) between ROIs. First single-trial MNE estimates were first averaged across dipoles within each ROI, and phase vector was derived using *Equation 4*. Consider two ROIs *a* and *b*, PLV can then be calculated using:

$$PLV(t,f) = \frac{1}{N}\left|\sum_{n=1}^{N}\exp\{i[\phi_a(t,f) - \phi_b(t,f)]\}\right|, \quad (5)$$

where ϕ_a is the phase vector of region a, ϕ_b is the phase vector of region b, N is the number of trials, t and f are time and frequency of interest, respectively. PLV measures the trial-by-trial variance of the phase relationship between two signals at a particular frequency. Smaller trial-by-trial phase variance results in larger PLV, which implies precise synchronization of oscillations. PLV ranges from zero to one; one indicates perfect synchrony, and zero indicates random phase relationship thus no synchrony. Similar to power time-courses, we converted PLVs into percent signal changes from baseline to estimate task-induced changes in PLVs. For each subject, percent signal changes were then averaged across trials within each condition (AS correct, PS correct, AS incorrect), and pooled across participants for group analyses. Finally, we averaged

PLV time-courses across frequencies within the alpha-, beta-, and gamma-band. Note that to control for performance, correct and incorrect trials were analyzed separately.

PLV has several important advantages compare to other more conventional synchrony measures such as coherence. PLV only considers phase consistency, and is a direct test of theories concerning inter-regional communication (Fries, 2005; Varela, et al., 2001). In contrast, coherence does not quantify phase-relationships, and increases with amplitude covariance. This difference also suggests that oscillatory power will have a larger impact on coherence, but less on PLV.

5.3.12 Statistical Analyses

Oscillatory power estimates and PLVs are non-Gaussian, therefore conventional parametric tests cannot be used. Instead, the significance level was determined by the randomized permutation test (Maris & Oostenveld, 2007). To briefly illustrate, when testing differences between the AS task and the PS task, we first calculated the test statistic of *t*-test comparing the mean of all AS observations from the mean of all PS observations. Then we randomly permuted the AS and PS labels for all observations, and recalculated the test statistic. We repeated this random assignment procedure 1000 times to create a null distribution of *t*-values. This distribution satisfied the null hypothesis, since any differences between AS and PS could only occur by chance as labels were assigned by chance. The proportion of values in the null distribution that was greater than the original "real" test statistic was treated as the significance probability value.

For each contrast of interest, we permuted the task condition label or subject assignment 1000 times to derive an empirical null distribution that satisfied the null hypothesis. To control for family-wise error rate, we calculated cluster level statistics instead of testing the significance

of every time-frequency bin (Maris & Oostenveld, 2007). For both oscillatory power and PLV values, the following contrasts were tested for their significances: AS correct trials vs. PS correct trials and AS correct trials vs. AS incorrect trials. We further tested developmental differences by permuting adults vs. adolescents for AS correct trials, AS incorrect trials, and PS correct trials. Note that we did not test for incorrectly performed PS trials because participants performed at ceiling.

5.3.13 How Preparatory Oscillatory Power Affect AS Task Performance

We performed multi-level (mixed-effect) logistic regressions to examine the relationship between trial-by-trial preparatory oscillatory and AS task performance:

$$P = \frac{\exp(a + bx)}{1 + \exp(a + bx)}, \tag{6}$$

where P is the probability of correct AS task performance, a is the intercept term, b is the regression coefficient (slope) that quantifies the strength of predictive effect of preparatory oscillatory power for AS task performance, x is single trial oscillatory power. A positive slope indicates that the stronger the preparatory oscillatory power, the more likely participants will perform correctly on the AS task. Subjects were entered as random effect, and intercept and slope terms were entered as fixed effects separately for adults and adolescents.

6.0 RESULTS AND DISCUSSION

6.1 BEHAVIOR

As expected, accuracy of AS trial performance was greater for adults (adults, *M* = 74 %, *SD* = 14; adolescents, *M* = 59 %, *SD* = 18; *t*(35) = 2.86, *p* = 0.007; Figure 7A), whereas PS accuracy was at ceiling for both age groups (adults, *M* = 98 %, *SD* = 1.2; adolescents, *M* = 97 %, *SD* = 1.9; *t*(35) = 1.84, *p* = 0.074; Figure 7A). No developmental differences in saccade latencies were found for both AS (adults, *M* = 330 ms, *SD* = 45 ms; adolescents, *M* = 347 ms, *SD* = 65 ms; *t*(35) = -0.92, *p* = 0.36; Figure 7B), and PS (adults, *M* = 235 ms, *SD* = 23; adolescents, *M* = 252 ms, *SD* = 43; *t*(35) = -1.45, *p* = 0.16; Figure 7B).

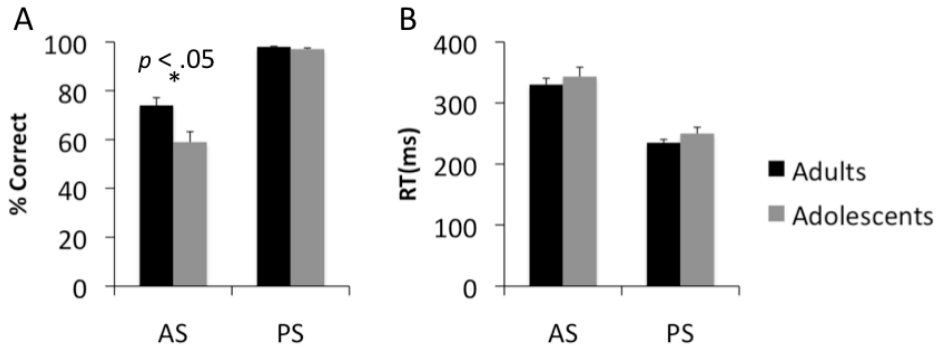

Figure 7. Behavioral performance.
A. Accuracies for AS and PS. B. Saccade latencies for AS and PS. RT = reaction time. Error bar = one *SE*.

To test if participants were able to improve their performances on the AS task through learning, we further compared accuracies and latencies between early and late phases of MEG scanning (Figure 8). We found no significant differences between different quarters of testing, suggesting that AS task performance has minimal learning effect within a session.

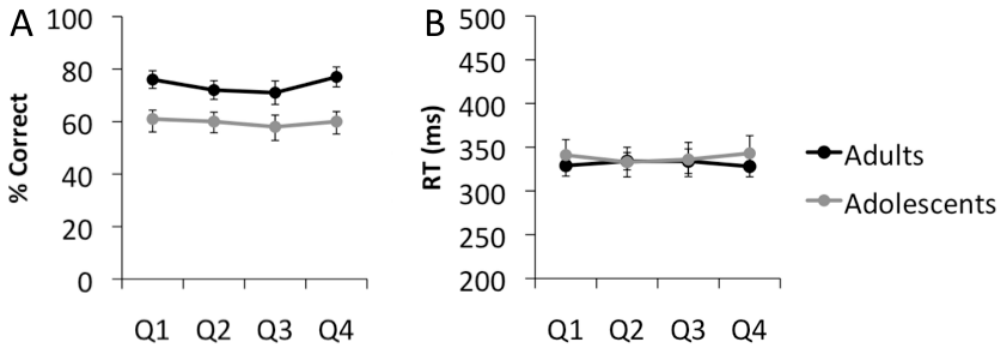

Figure 8. Behavioral performance of AS trials during different quarters of testing.
A. Accuracies of AS at different quarters of MEG testing. B. Saccade latencies of AS at different quarters of MEG testing. No significant differences were found between quarters. Q1 = first quarter of testing, Q2 = second quarter, Q3 = third quarter, Q4 = last quarter. Error bar = one *SE*.

6.2 REGIONS OF INTEREST

The primary aim of this dissertation was to delineate developmental changes in oscillatory neurodynamics of cortical regions associated preparatory inhibitory control. To achieve this aim, we selected *a priori* anatomical structures that were known to be involved in inhibitory and oculomotor processes, and defined ROIs that included dipoles that showed reliable oscillatory activities across all frequencies of interest. As described in the methods (Chapter 5.3.9), ROIs

were defined on each participant's native surface, and all subsequent analyses were performed in native space to reduce spatial smoothing and interpolation error. The following ROIs were defined in both hemispheres: the DLPFC, the VLPFC, the iFEF, the sFEF, the IPS, and the V1. To inspect the spatial location of ROIs, and the degree of overlap between participants, we morphed each participant's ROI into a group average surface (see Chapter 5.3.6), and calculated the percentage of overlap (Figure 9). We found that most ROIs showed a high degree of overlap across participants and age groups, especially for the iFEF, the sFEF, and the IPS. The spatial coverage was slightly more dispersed for prefrontal ROIs. These ROIs were age-neutral, unbiased, and independent with regard to our hypotheses, as they were defined using all trials (AS and PS, correct and incorrect), frequencies (8-60 Hz), and without any group contrasts.

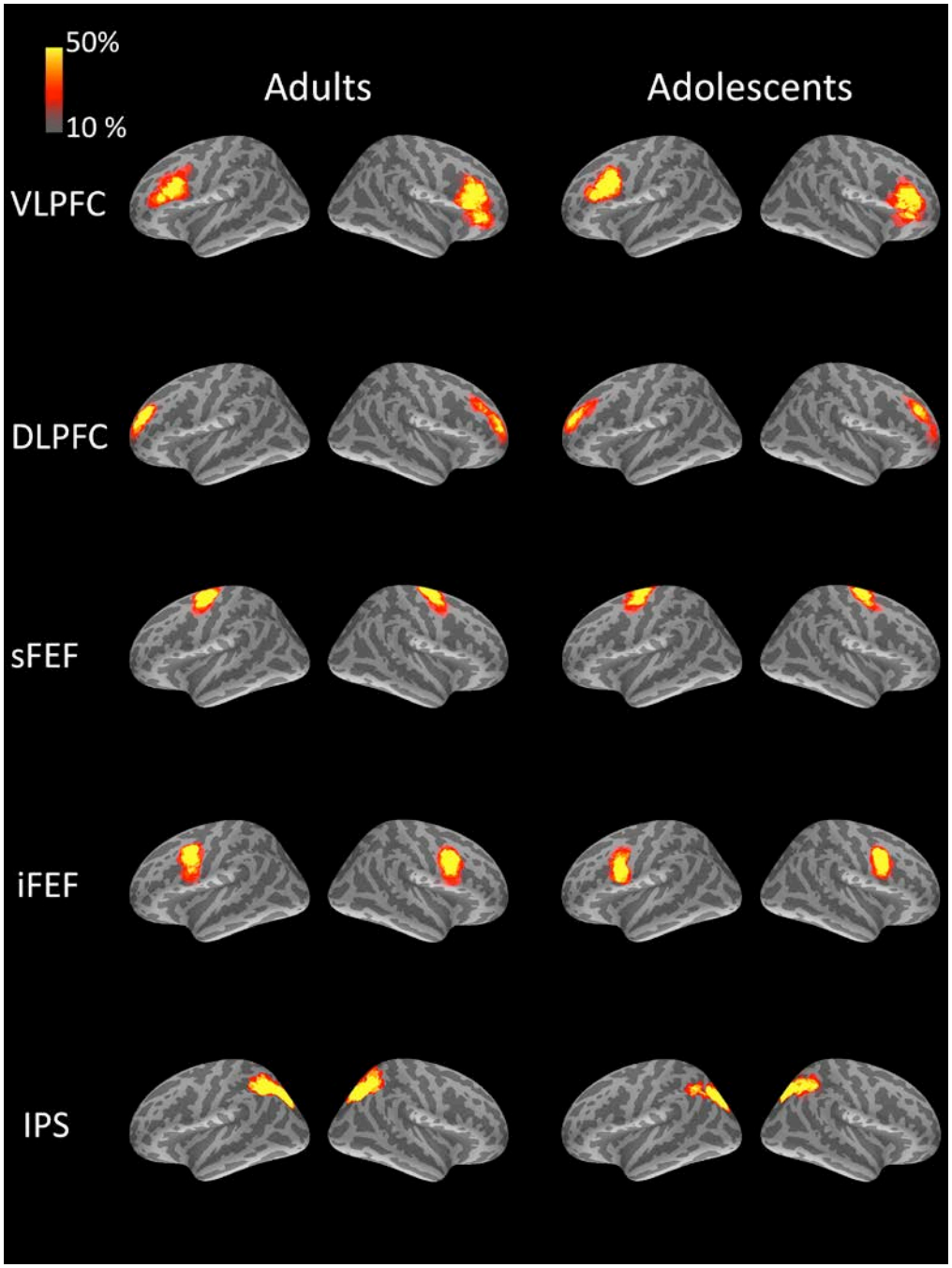

Figure 9. Spatial coverage of ROIs.
Color-scale indicates the percentage of participants within each age group that showed reliable oscillatory activities for alpha-, beta-, and gamma-band at this vertex.

6.2.1 Dynamic Statistical Parametric Maps

To ensure that the ROIs we defined showed reliable activation associated with the AS task, we performed exploratory whole-brain dSPM analysis to characterize the spatiotemporal patterns of evoked activity (Figure 10). Leveraging MEG's superior temporal resolution, we characterized the time-resolved evoked activity during the preparatory period and the response period (prior to the saccade). Note that time-domain evoked activities are phase-locked to the cue and are distinct from our primary interest—induced oscillatory activities that are not necessarily phase-locked to the cue (Jensen & Hesse, 2010). Nevertheless, we performed this analysis to corroborate the veracity of our ROI selection procedure. We found that the ROIs we identified were activated during both the preparatory period and the response period. During the preparatory period, the AS task cue first activated the visual cortex, activity then propagated to frontal and parietal regions, including the IPS, the FEF, and lateral PFC regions (DLPFC and VLPFC). Similar progression of activity was also observed during the response period. These results suggest that MEG has the spatial sensitivity to identify cortical regions known to be involved in inhibitory control processes, and the ROIs we created based on frequency-domain induced oscillatory activities also showed reliable temporal-domain evoked activations.

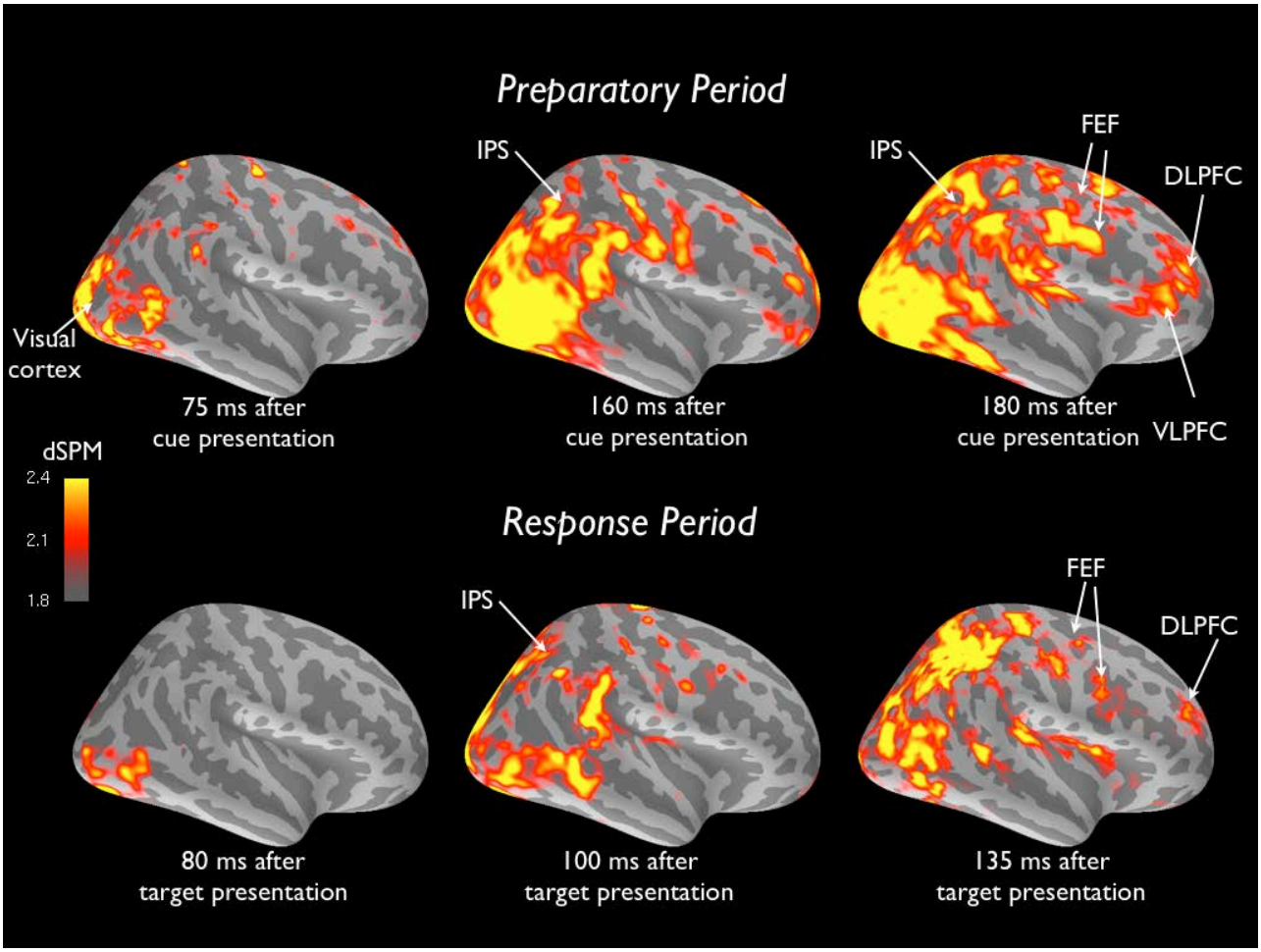

Figure 10. dSPM maps associated with AS task performance.
Temporal evolution of evoked activation associated with AS, averaged across all participants. Note that we did not extend our analysis pass 200 ms into the response period to avoid saccade-artifacts.

6.2.2 Temporal progression of evoked responses

To quantify the temporal progression of evoked activations during the preparatory period, we calculated the time-to-peak for each ROI separately for each condition and each age group (Figure 11). Briefly, for each condition and age group, the averaged task-related evoked response (MNE current estimates) was extracted from each ROI for each participant, and the latency from the onset of cue presentation to the time of maximum neural activity was calculated. We found that across condition and age group, the visual cortex was activated first, peaking around 120 ms, followed by the IPS, peaking around 150 ms, and PFC ROIs, peaking around 150 to 200 ms. We also found considerable individual differences, indicated by the relatively large error bars (one *SE*; Figure 11). As a result, no significant differences were found in the latencies of peak neural activities between ROIs, between conditions, or between age groups. Nevertheless, a pattern of occipital-parietal-frontal progression was observed, pattern that reflect the sequence of time-domain activation evoked by the task cue. We did not perform this analysis for the response period because saccades distort MNE current estimates, making it difficult to separate the peak of neural activities from saccade artifacts.

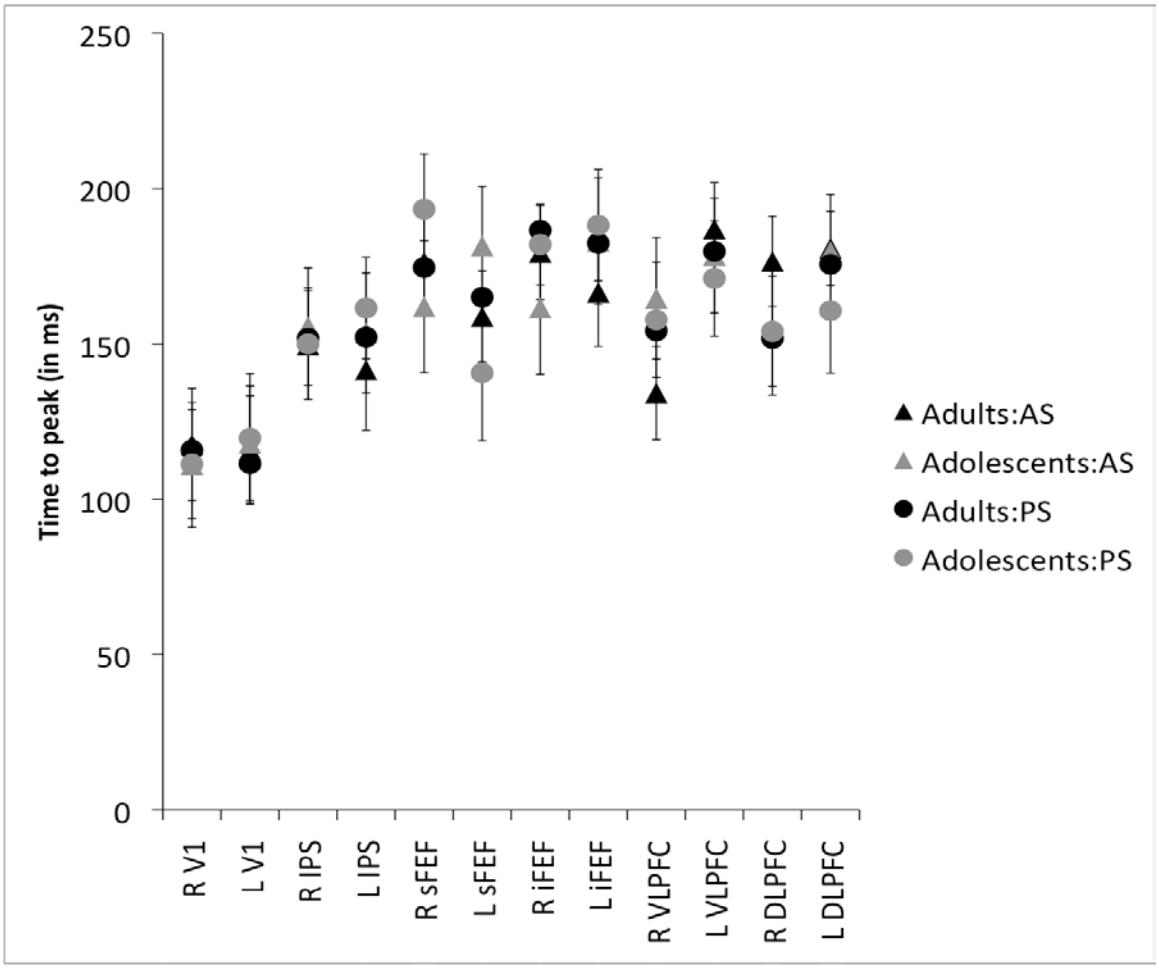

Figure 11. Time-to-peak of cortical activations evoked by the task cue.
R = Right, L = Left, error bar = one *SE*.

6.2.3 Control Analyses

One concern was that adolescents might have weaker signal-to-noise ratio that could bias group analyses. To rule out this possibility, we compared the averaged *z*-score of oscillatory power across the alpha-, beta-, and gamma-band in the V1 between adults and adolescents (see Chapter 5.3.9). Briefly, power values of each frequency were converted to signal-to-noise estimates by subtracting it from the baseline mean and dividing by the baseline variance, then averaging across frequencies and time. V1 was chosen because our previous study found no significant age effect in this region (Velanova et al., 2008), suggesting that basic visual processes are mature by adolescence, and that age-invariant activations in V1 could be used as an indication of comparable signal-to-noise between adolescents and adults. We found no significant age-related differences in the V1 (Figure 12). We further inspected the time-courses of alpha-, beta- and gamma-band power during the AS preparatory period, and no significant age-related differences were found in the V1 (timecourses from the right V1 shown in Figure 13).

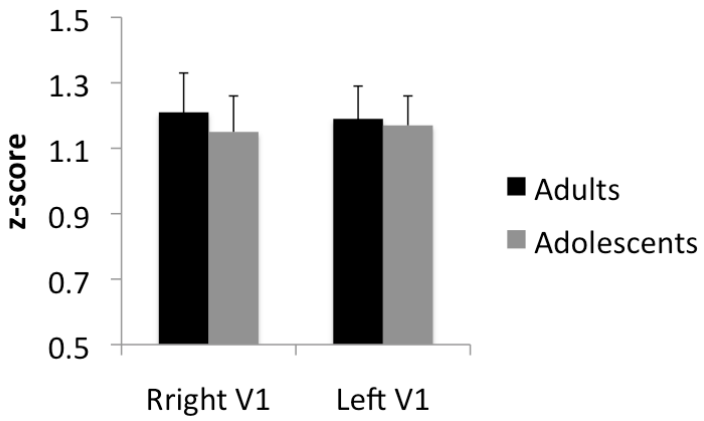

Figure 12. No significant age-related differences in oscillatory power were observed in the primary visual cortex.
Z-scores were averaged across frequencies (8-60 Hz) and time (only during the preparatory period). Error bar = one *SE*.

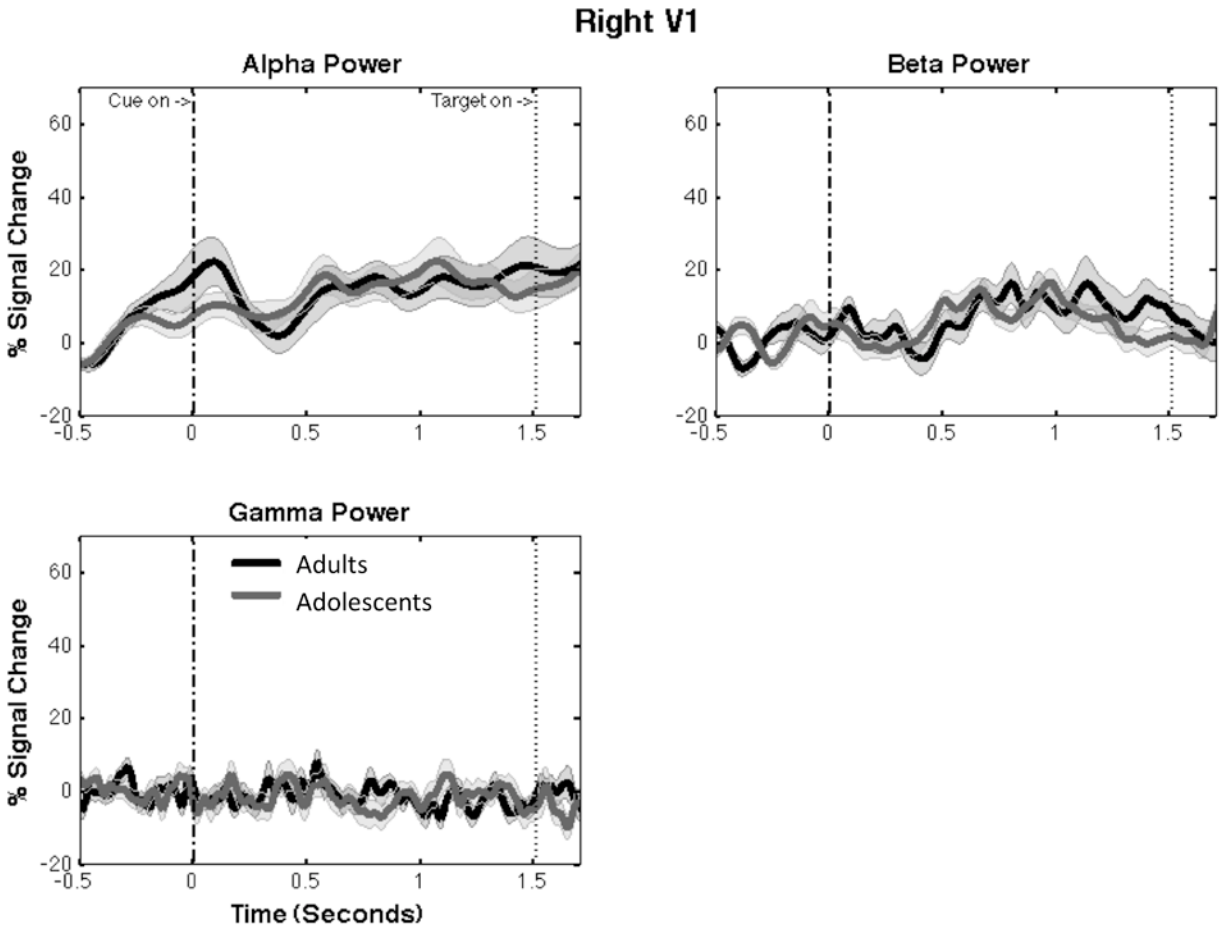

Figure 13. No significant age-related differences in alpha-, beta-, and gamma-band power were found in the right V1.
Y scale is percent signal change from baseline. Shaded areas indicating one *SE*. X axis indicates the time since cue onset. From zero to 1.5 seconds is the preparatory period. Y axis indicates percent signal change from baseline. Only correctly performed AS trials were analyzed.

6.3 GAMMA-BAND POWER

We hypothesized that task-rule maintenance would be associated with increases in gamma-band power. However, we did not find any robust gamma-band activity in any ROIs. Given that fast-spiking GABA interneurons remain immature during adolescence (Lewis & Melchitzky, 2012), we further hypothesized that adolescents would show weaker gamma-band power. However, nor did we find any significant age effects. Figure 14 illustrates this by presenting gamma-band power in the right DLPFC. For all ROIs, we found that gamma-band power fluctuated around zero throughout the task epoch. As a result, we did not find significant task-related or age-related modulation in gamma-band power.

6.3.1 Interim Discussion

There are two possible explanations for the lack of gamma effect. First, it remains controversial whether or not MEG has the sensitivity to reliably measure gamma rhythm. It is well documented that the spectral energy of neural activity follows the $1/f$ power-law scaling (He, Zempel, Snyder, & Raichle, 2010). The implication is that the higher the frequency, the weaker the overall signal will be; gamma-band activity might be too weak to be reliably measured by MEG sensors. This limitation was demonstrated in a simultaneous MEG and iEEG study which reported that while iEEG observed robust alpha-, beta-, and gamma-band activities, MEG was only reliable in measuring alpha- and beta-band activities, but not gamma (Dalal et al., 2009). Second, because we utilized a block design, it is possible that the demand for working memory

maintenance was lessened, resulting in less gamma-band activity. Although memorizing stimuli properties such as memorizing the location of a stimulus (Roux, et al., 2012) or the identity of the stimulus (Howard, et al., 2003) has been associated with increased gamma-band power, it is unclear if gamma activity encodes task-rules (“look away from the dot” vs. “look at the dot”). In support, a recent study showed that neural ensembles encode SR mapping rules through oscillatory synchronization in the beta frequency range, but not gamma (Buschman, et al., in press).

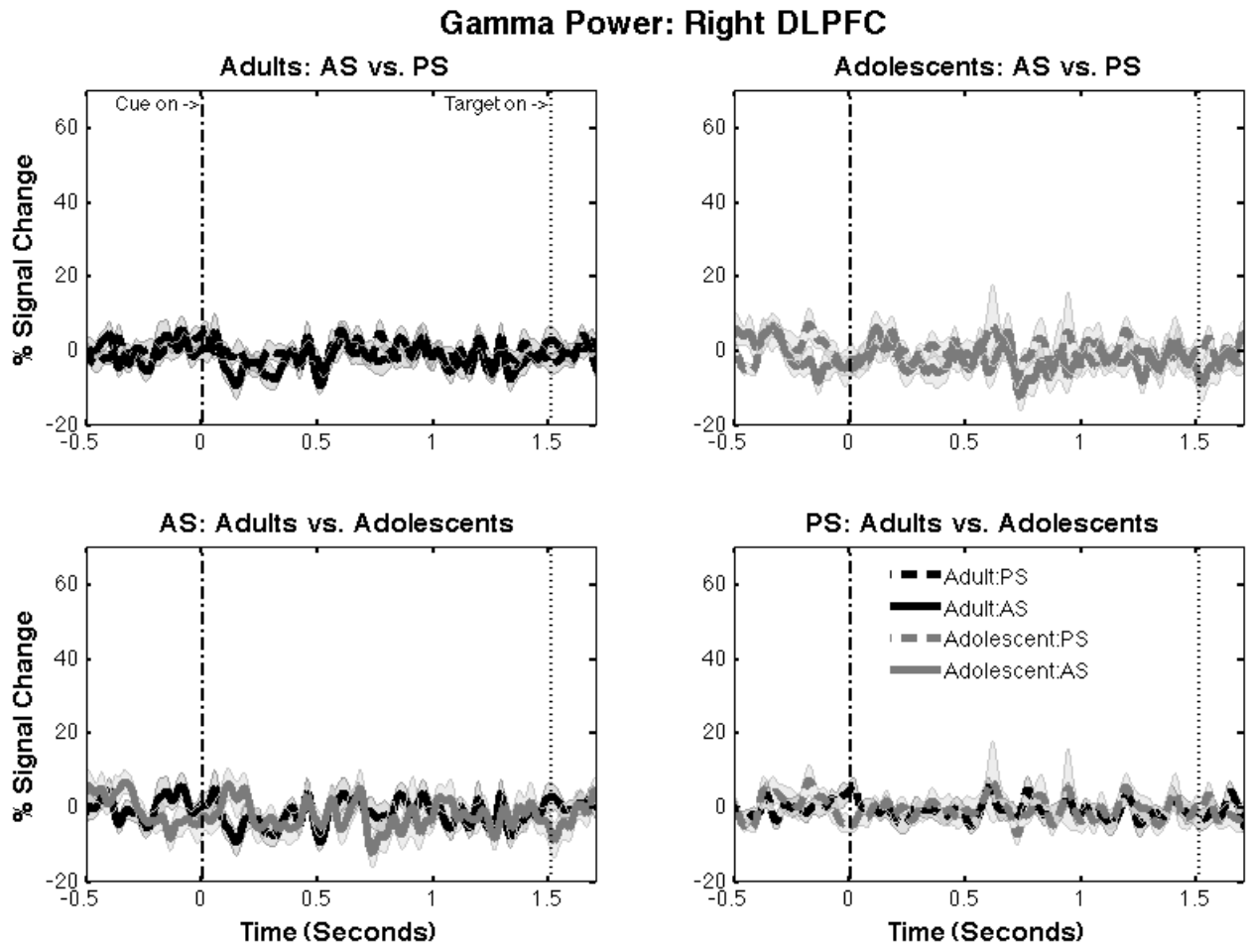

Figure 14. Gamma-band power in the right DLPFC.
Y scale is percent signal change from baseline. Shaded areas indicating one *SE*. X axis indicates the time since cue onset. From zero to 1.5 seconds is the preparatory period. Only correct trials were analyzed.

6.4 BETA-BAND POWER

It has been suggested that the PFC provides top-down control signal to inhibit saccade-related activities in the oculomotor regions (Munoz & Everling, 2004), and we hypothesized that increases in beta-band power in the PFC would reflect top-down signaling. The resulting lessened need for top-down signaling could result in weaker beta-band power when compared to the AS task. Developmentally, we hypothesized that adolescents would show weaker beta-band power in the PFC, reflecting immaturities in top-down signaling processes.

In support of our hypothesis, we found that preparatory beta-band power in the PFC was significantly stronger for the AS task when compared to the PS task. In adults, this effect was observed in the right DLPFC (Figure 15) and the right VLFPC (Figure 16). No task-related modulation of beta-band power was observed in adolescents or any in any other ROIs (see Appendix A). This suggests that increased beta-band power for the correct trials of the AS task is specific to the PFC, but not a global resonance phenomenon.

In support of our developmental hypothesis, we found that for the AS task, beta-band power during the preparatory period was significantly stronger in adults compared to adolescents. This effect was observed in the right DLPFC (Figure 15), the right VLPFC (Figure 16), and the left VLPFC (Figure 17). No age effect was found for the PS task, or in any other ROIs. Note that to control for the behavioral difference, only correct trials were included in the above analyses.

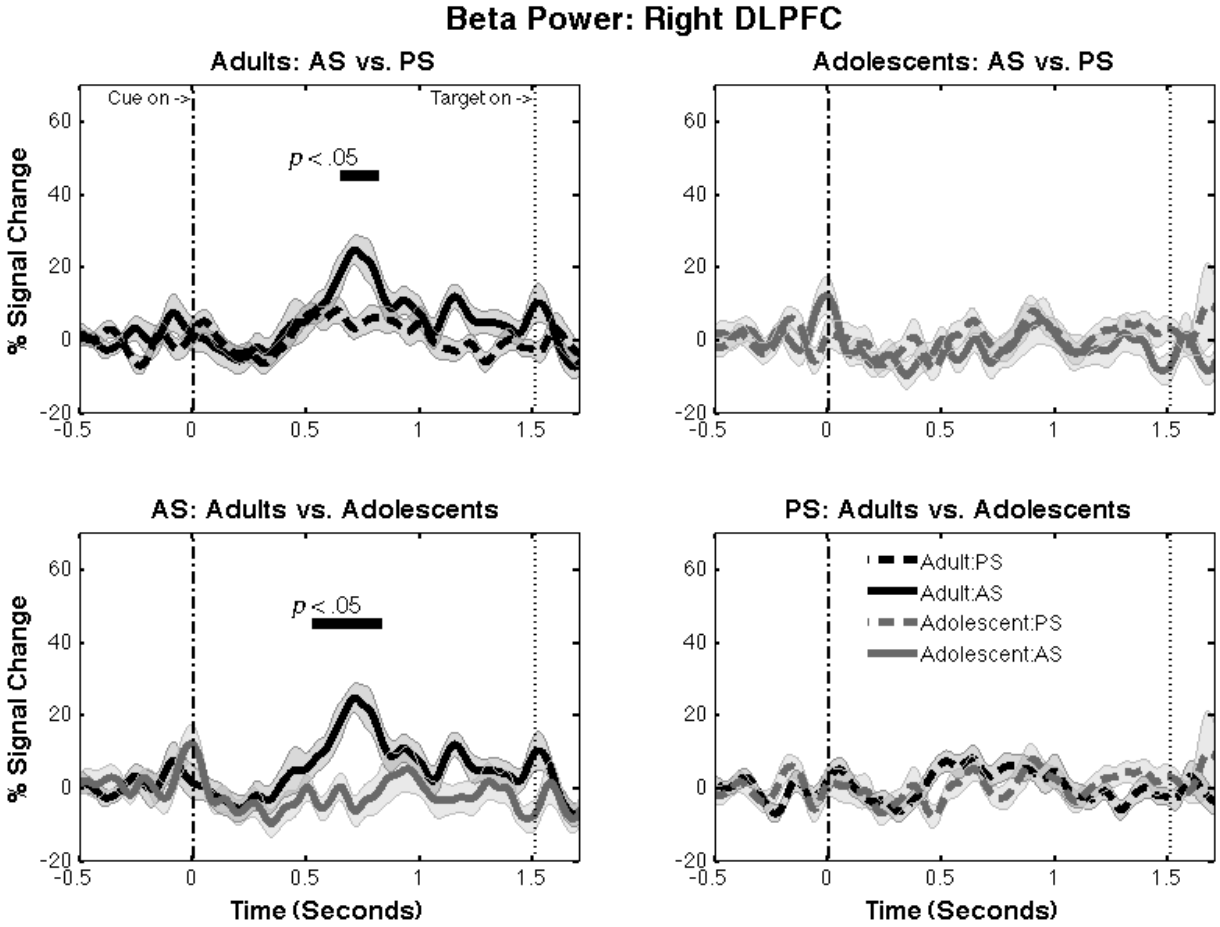

Figure 15. Beta-band power in the right DLPFC.
Y scale is percent signal change from baseline. Shaded areas indicating one *SE*. X axis indicates the time to saccade onset. Horizontal bar indicates task period that showed significant difference between conditions or age groups (p <.05 corrected). Only correct trials were analyzed.

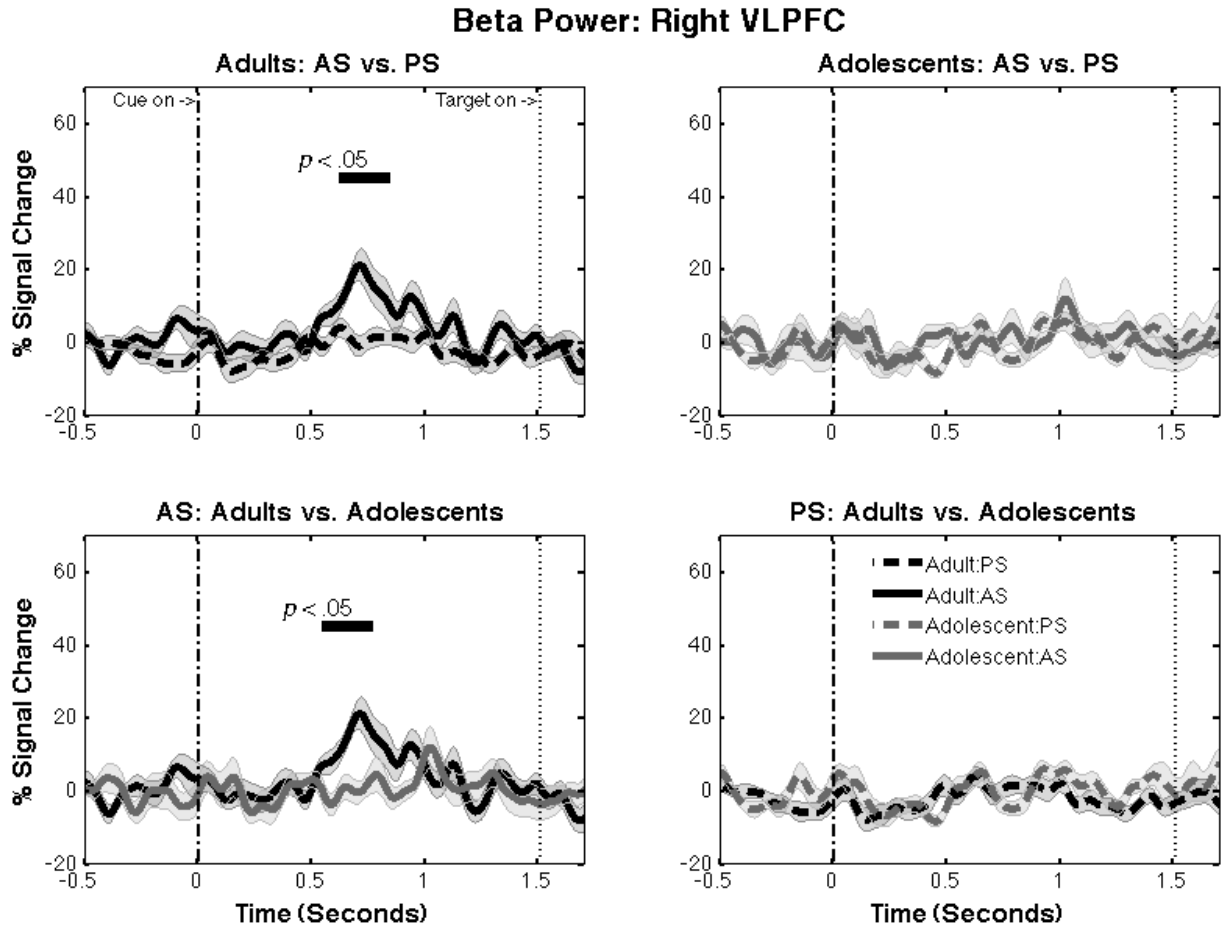

Figure 16. Beta-band power in the right VLPFC.
Y scale is percent signal change from baseline. Shaded areas indicating one *SE*. X axis indicates the time to saccade onset. Horizontal bar indicates task period that showed significant difference between conditions or age groups (p <.05 corrected). Only correct trials were analyzed.

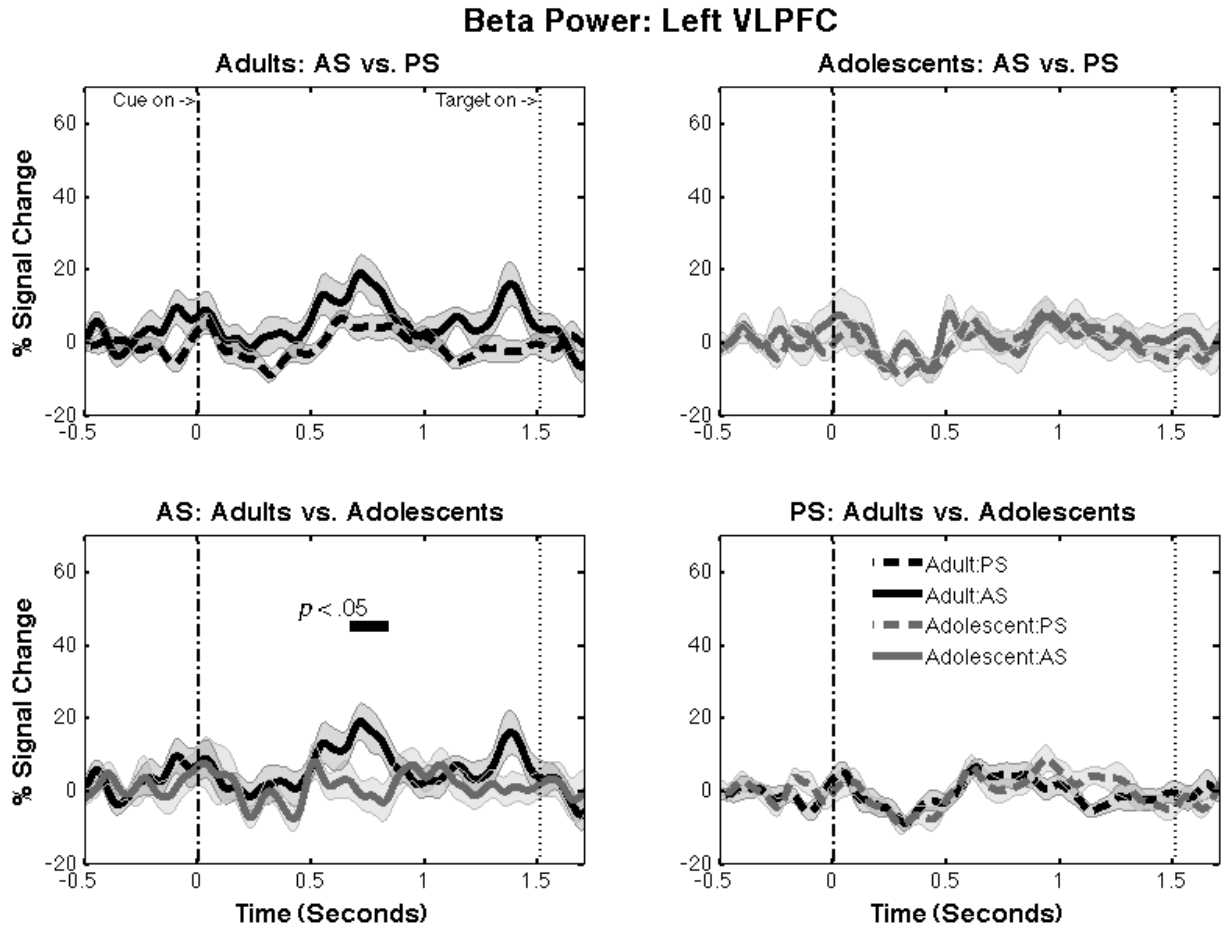

Figure 17. Beta-band power in the left VLPFC.
Y scale is percent signal change from baseline. Shaded areas indicating one *SE*. X axis indicates the time to saccade onset. Horizontal bar indicates task period that showed significant difference between conditions or age groups (p <.05 corrected). Only correct trials were analyzed.

If increased preparatory beta-band power is an indication of enhanced top-down control, it should also affect AS task performance. To test this hypothesis, we performed a logistic regression to assess the trial-by-trial impact of preparatory beta-band power on the probability of correct AS task performance (Figure 18). The independent variable was single-trial beta-band power averaged from 700 ms to 800 ms during the preparatory period (the time-widow when we observed significant task-modulation). Though no statistically significant association was found in the right VLPFC, for adults there was a trend showing that probability of correct AS task performance increased as preparatory beta-band power in the right VLPFC increased (b = 0.046, z = 1.61, p = 0.11). For adolescents no significant association was found (b = -0.013, z = -0.64, p = 0.53). No statistically significant associations between preparatory beta-band power and AS task performance were found in other ROIs for both age groups.

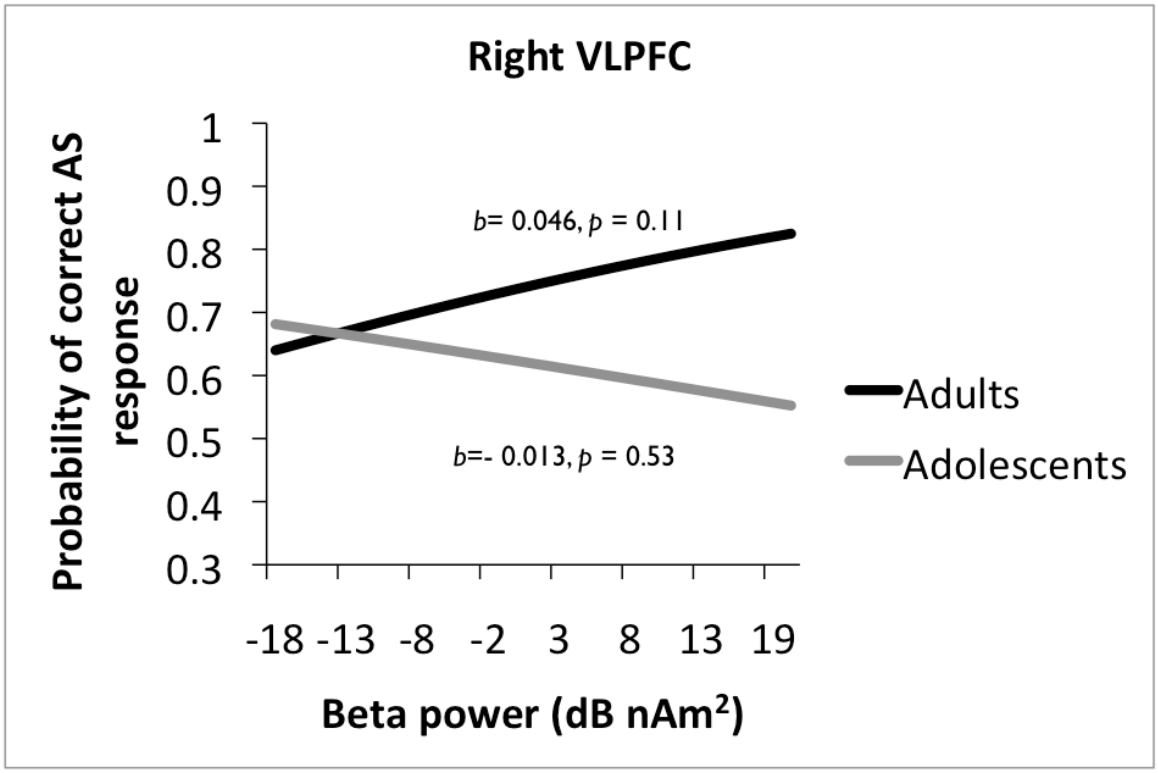

Figure 18. Preparatory beta-band power and AS task performance.

6.4.1 Interim Discussion

We found that in response to the heightened control demand by the AS task, adult participants' beta-band power increased in the right DLPFC and the right VLPFC during the preparatory period, but beta-band power did not increase among adolescents. These results are consistent with the literature suggesting that the PFC sends control signals to inhibit motor responses (Swann, et al., 2009), and to bias sensory and motor processes to generate goal-directed responses (Everling & Johnston, 2011; Miller & Cohen, 2001). Further, it has been found that

compared to the PS task, the right DLPFC is more heavily involved in AS task performance (Ford, Goltz, Brown, & Everling, 2005), and other inhibitory control tasks heavily recruit the right VLPFC (Aron, 2011; Levy & Wagner, 2011). A transcranial magnetic stimulation (TMS) study also found that when used single-pulse TMS to interfere with the right DLPFC during the preparatory period, participants' AS performances suffered, suggesting that the lateral PFC is involved in preparatory inhibitory control processes.

In the PFC, we observed robust task-related modulations in beta-band power, but not in gamma- and alpha-band (see Chapter 6.5 for alpha-band results). Our results are consistent with recent animal and human studies suggesting that beta rhythm is involved in top-down control of goal-directed behavior (Buschman, et al., in press; Buschman & Miller, 2007; Pesaran, Nelson, & Andersen, 2008; Saalmann, et al., 2007; Swann, et al., 2009). We suggest that the increased frontal beta-band power we observed reflect prefrontal top-down signaling through the feedback projection pathways to oculomotor regions. This top-down signaling process could serve to inhibit preparatory saccade-related activities, and to decrease the likelihood of generating reflexive saccades (Munoz & Everling, 2004).

Consistent with the literature, we only found significant task-related modulations of beta-band power in the right DLPFC and the right VLPFC, but not in the left PFC. One study found that patients with damages in the right VLPFC made more AS errors, compared to patients with left VLPFC lesions (Hodgson, et al., 2007). Our results are also consistent with other imaging studies, suggesting that compared to the left PFC, the right PFC is more heavily involved in inhibitory motor responses (Aron, et al., 2003; Rubia, et al., 2003).

Another observation is that the shapes of beta-band timecourses were similar between the right DLPFC, the right VLPDC, and the right iFEF (Figure 30). Because MNE source estimates

are essentially linear combinations of all sensor signals (Hamalainen, et al., 2010), this similarity could reflect the inherent correlation between source estimates (Schoffelen & Gross, 2009). We addressed this issue by interpreting task-related modulations in beta-band power, since volume conduction does not change across conditions. However, because of this limitation, it is difficult to dissociate the functions of DLPFC and VLPFC. One iEEG study suggests that the right DLPFC is associated with task-goal maintenance, and the right VLPFC implements inhibition over the motor system (Swann, Tandon, Pieters, & Aron, 2012). Because MEG does not have the same spatial acuity as iEEG, we tentatively conclude that increased beta-band power in the right DLPFC and the right VLPFC collectivity reflect top-down signaling process related to preparatory inhibitory control, and also potentially task-rule representation for AS. This interpretation is consistent with findings suggesting that increased beta-band activity (but not gamma) is associated with forming arbitrary SR mapping rules in the PFC (Buschman, et al., in press), and to inhibit motor-related activities (Swann, et al., 2009).

In contrast to adults, we did not find any statistically significant task-related beta-band modulations in adolescents. Group comparisons showed that compared to adults, adolescents showed significantly weaker beta-band power in the right DLPFC, the right VLPFC, and the left DLPFC. We propose that these age-related differences reflect weaker prefrontal top-down signaling function in adolescents. Specifically, immaturities in control signal output that bias preparatory saccade-related activities in down-stream oculomotor cortices (Hwang, et al., 2010).

What is the specific neural mechanism that might contribute to age-related increases in beta-band power from adolescence to adulthood? Existing models suggest that the expression of local beta-band activity could reflect neural circuits sending outputs from the deep layers of cortical columns (Roopun, et al., 2010; Wang, 2010), or interactions between feedback and

feedforward inputs into cortical columns (Jones, et al., 2009). Extending these models to the PFC, it is possible that after a prefrontal microcircuit generates an output, it receives feedbacks from non-specific thalamic nuclei or other prefrontal microcircuits, and this recurrent interaction generates rhythmic oscillation (Bollimunta, et al., 2011; Steriade, Gloor, Llinas, Lopes de Silva, & Mesulam, 1990). Based on these models, we suggest that decreased beta-band power in the PFC during adolescence might reflect immaturities in PFC outputting control signals through cortical-BG-thalamocortical interactions (Vokoun, Mahamed, & Basso, 2011).

Another possibility is that decreased beta-band power in adolescents reflects immaturities in the interaction between excitatory and inhibitory neurons within prefrontal microcircuits. To further constrain and specify the neural mechanisms associated age-related changes in beta rhythm expression, we need to first understand what type of (and how) inhibitory interneurons are involved in beta rhythm genesis in the PFC, and specify details of how cortical-BG-thalamocortical interactions might drive PFC beta rhythm. Such details are currently unavailable, which points to the critical need for future investigations. For example optogenitically drive different inhibitory populations in the cortex or different subcortical structures to test how PFC beta rhythm could be generated.

6.5 ALPHA-BAND POWER

To successfully perform an AS trial, saccade-related activity during the preparatory period would need to be sufficiently suppressed (Everling, et al., 1999; Everling & Munoz, 2000; Munoz & Everling, 2004). We hypothesized that during the preparatory period, alpha-band power would increase in oculomotor regions for the AS task when compared to the PS task, reflecting

functional inhibition of saccade-related activities. Furthermore, due to the known decreased white matter integrity in the thalamic radiata during adolescence (Asato et al., 2010), and projection tracts' hypothesized involvement in alpha rhythm genesis (Bollimunta, et al., 2011; Hughes & Crunelli, 2005; Jones, et al., 2009), we hypothesized that alpha-band power would increase from adolescence to adulthood.

In support of our hypothesis, we found that preparatory alpha-band power in several oculomotor ROIs was significantly stronger for the AS task when compared to the PS task. In adults, this effect was observed in the left iFEF (Figure 19), the right sFEF (Figure 20), and the left IPS (Figure 21). For adolescents, alpha-band power was higher for the AS task in the left iFEF (Figure 19) and the right iFEF (Figure 22). Unexpectedly, for adolescents alpha-band power was significantly stronger in the right sFEF for the PS task (Figure 20). In addition, no task-related modulation of alpha-band power was observed in the DLPFC and the VLPFC (see Appendix B), suggesting that increased alpha-band power for the AS task is specific to oculomotor regions, but not a global resonance phenomenon.

In support of our developmental hypothesis, we found that for the AS task, alpha-band power during the preparatory period was significantly stronger in adults compared to adolescents. This effect was observed in the left iFEF (Figure 19) and the right sFEF (Figure 20). No age effect was found for the PS task, or in any other ROIs. Note that to control for behavioral difference, only correct trials were included in the above analyses.

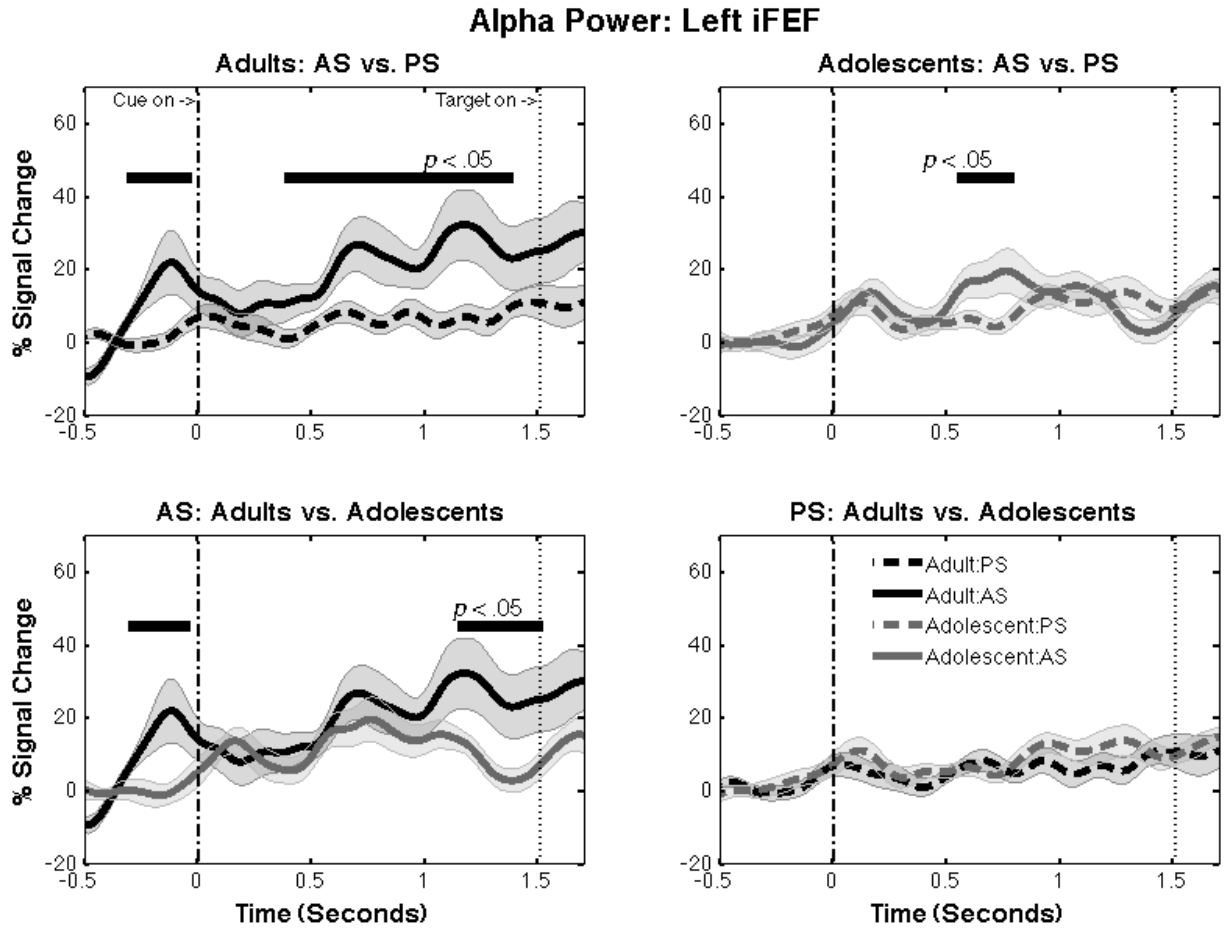

Figure 19. Alpha-band power in the left iFEF.
Y scale is percent signal change from baseline. Shaded areas indicating one *SE*. X axis indicates the time since cue onset. From zero to 1.5 seconds is the preparatory period. Horizontal bar indicates task period that showed significant difference between conditions or age groups (p <.05 corrected). Only correct trials were analyzed.

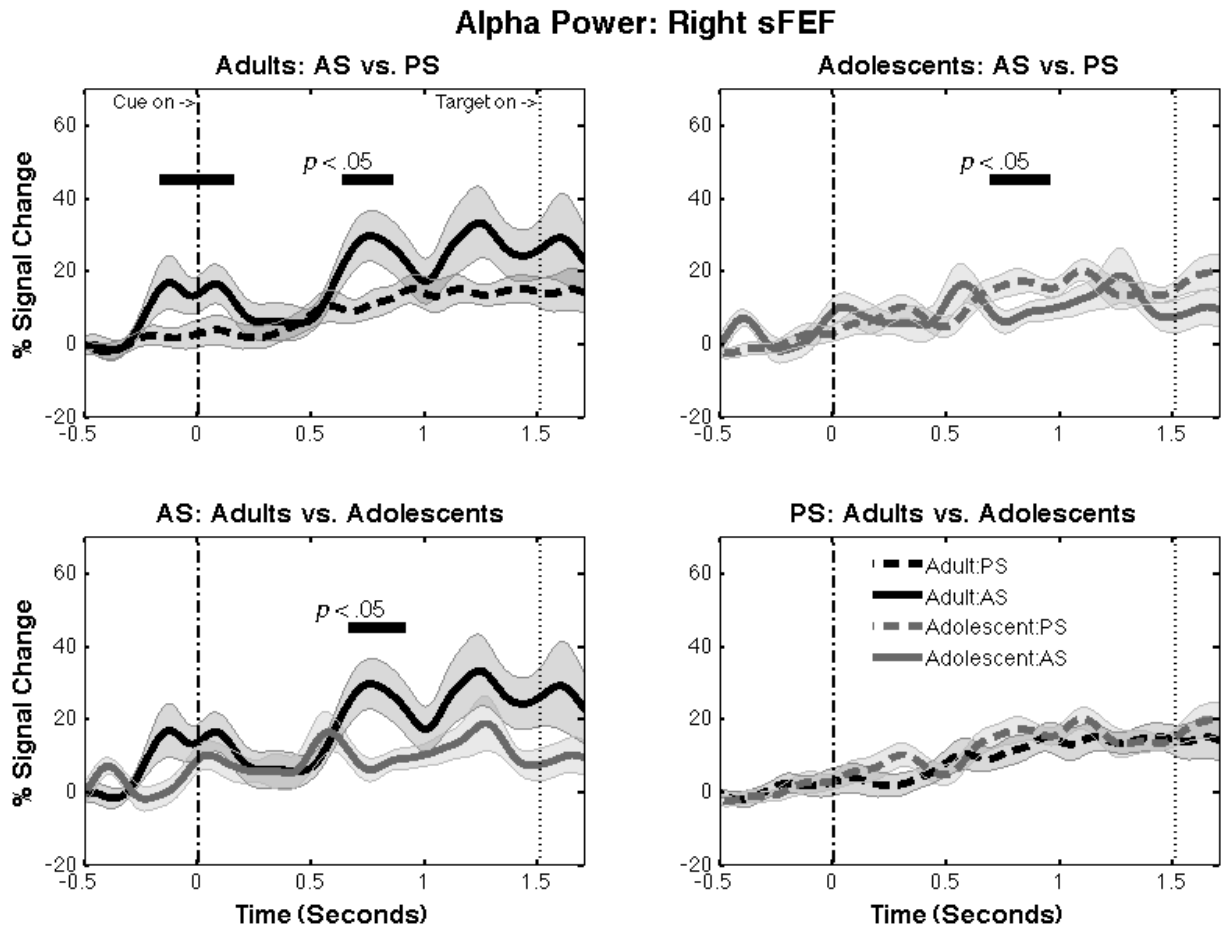

Figure 20. Alpha-band power in the right sFEF.
Y scale is percent signal change from baseline. Shaded areas indicating one *SE*. X axis indicates the time since cue onset. From zero to 1.5 seconds is the preparatory period. Horizontal bar indicates task period that showed significant difference between conditions or age groups ($p < .05$ corrected). Only correct trials were analyzed.

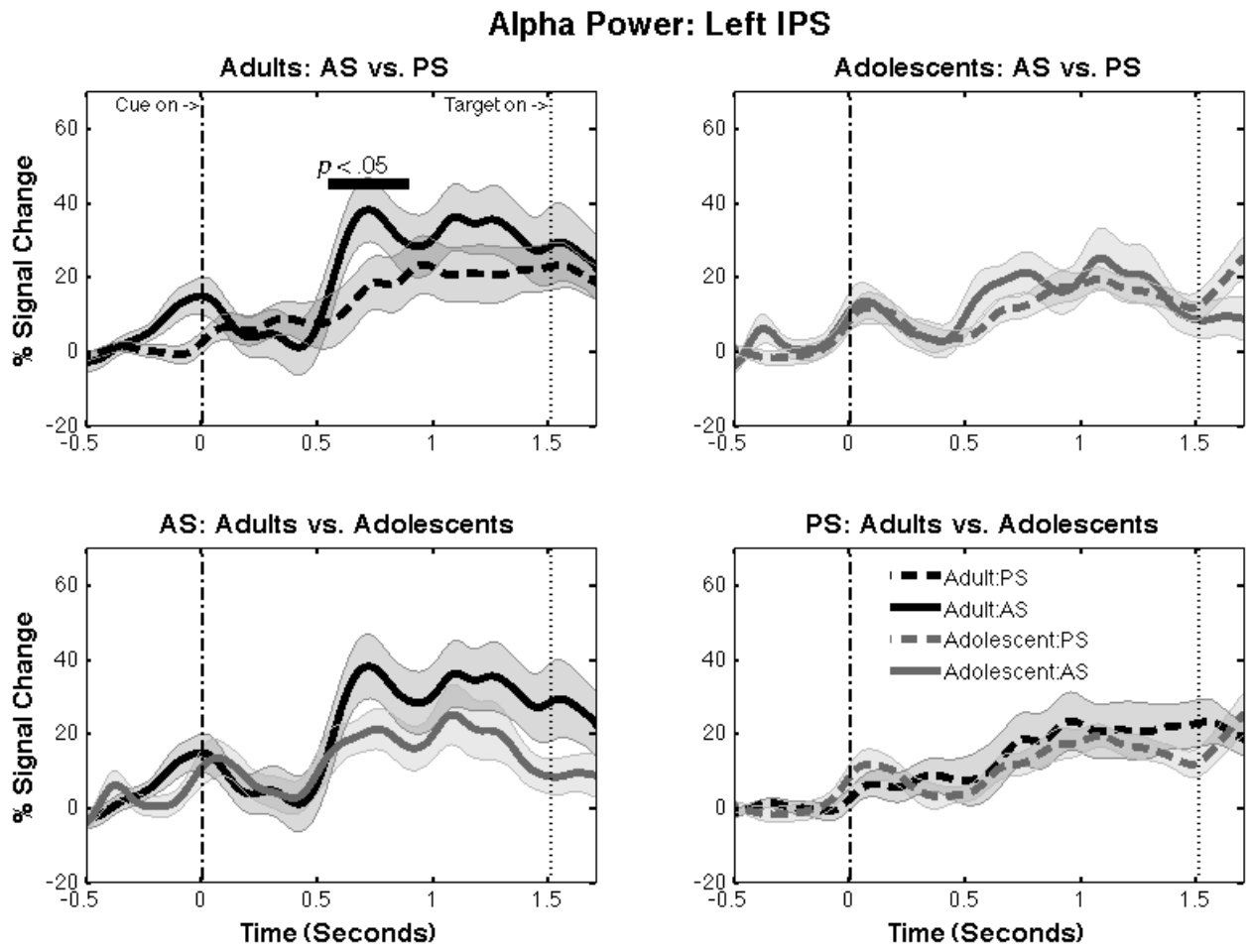

Figure 21. Alpha-band power in the left IPS.
Y scale is percent signal change from baseline. Shaded areas indicating one *SE*. X axis indicates the time since cue onset. From zero to 1.5 seconds is the preparatory period. Horizontal bar indicates task period that showed significant difference between conditions or age groups (p <.05 corrected). Only correct trials were analyzed.

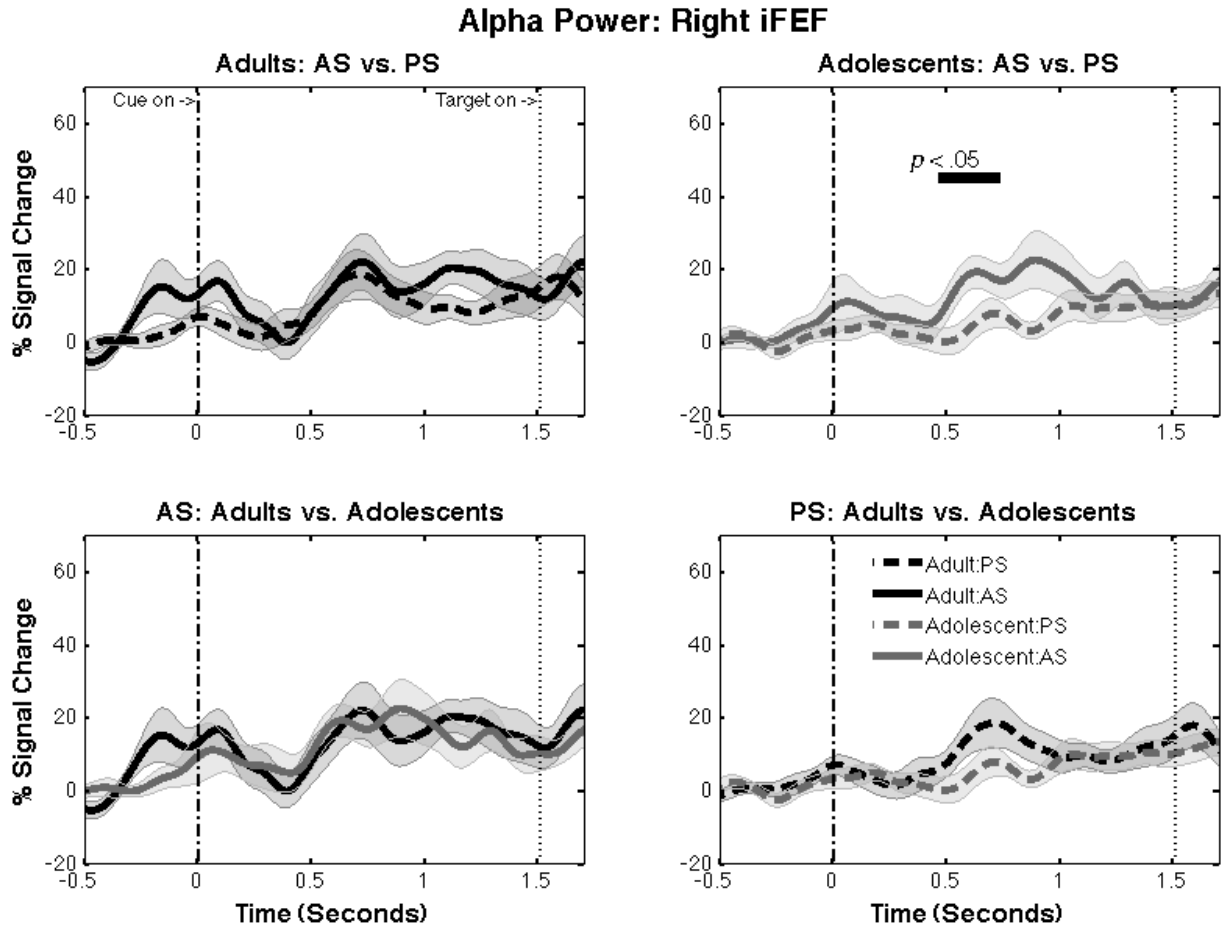

Figure 22. Alpha-band power in the right iFEF.
Y scale is percent signal change from baseline. Shaded areas indicating one *SE*. X axis indicates the time since cue onset. From zero to 1.5 seconds is the preparatory period. Horizontal bar indicates task period that showed significant difference between conditions or age groups ($p < .05$ corrected). Only correct trials were analyzed.

If increased alpha-band power does reflect inhibition of saccade mechanism, it should decrease when participants are ready to make a saccade. We re-arranged the timing of AS trials to the onset of the saccade, and analyzed timecourses of alpha-band power prior to the onset of saccades. As expected, alpha-band power decreased right before saccade onset in all four FEF ROIs (Figure 19).

Further, if increased alpha-band power is an indication of enhanced functional inhibition of saccade-related activities in oculomotor cortices, it should also correlate with better AS tasks performance. To test this hypothesis, we performed a logistic regression to assess the trial-by-trial impact of preparatory alpha-band power on the probability of correct AS task performance (Figure 24). The independent variable was single-trial alpha-band power averaged from 700 ms to 1500 ms during the preparatory period (the time-widow when we observed significant task-modulation). We found that for adults there was a significant association: as preparatory alpha-band power in the right sFEF increased, the probability of performing a correct AS trial increased (b = 0.061, z = 2.04, p = 0.04). Whereas for adolescents no significant association was found, though there was a trend showing negative association (b = -0.038, z = -1.65, p = 0.09). No statistically significant associations between preparatory alpha-band power and AS task performance were found in other ROIs for adults and adolescents, although for adults the associations approached trend in other FEF ROIs.

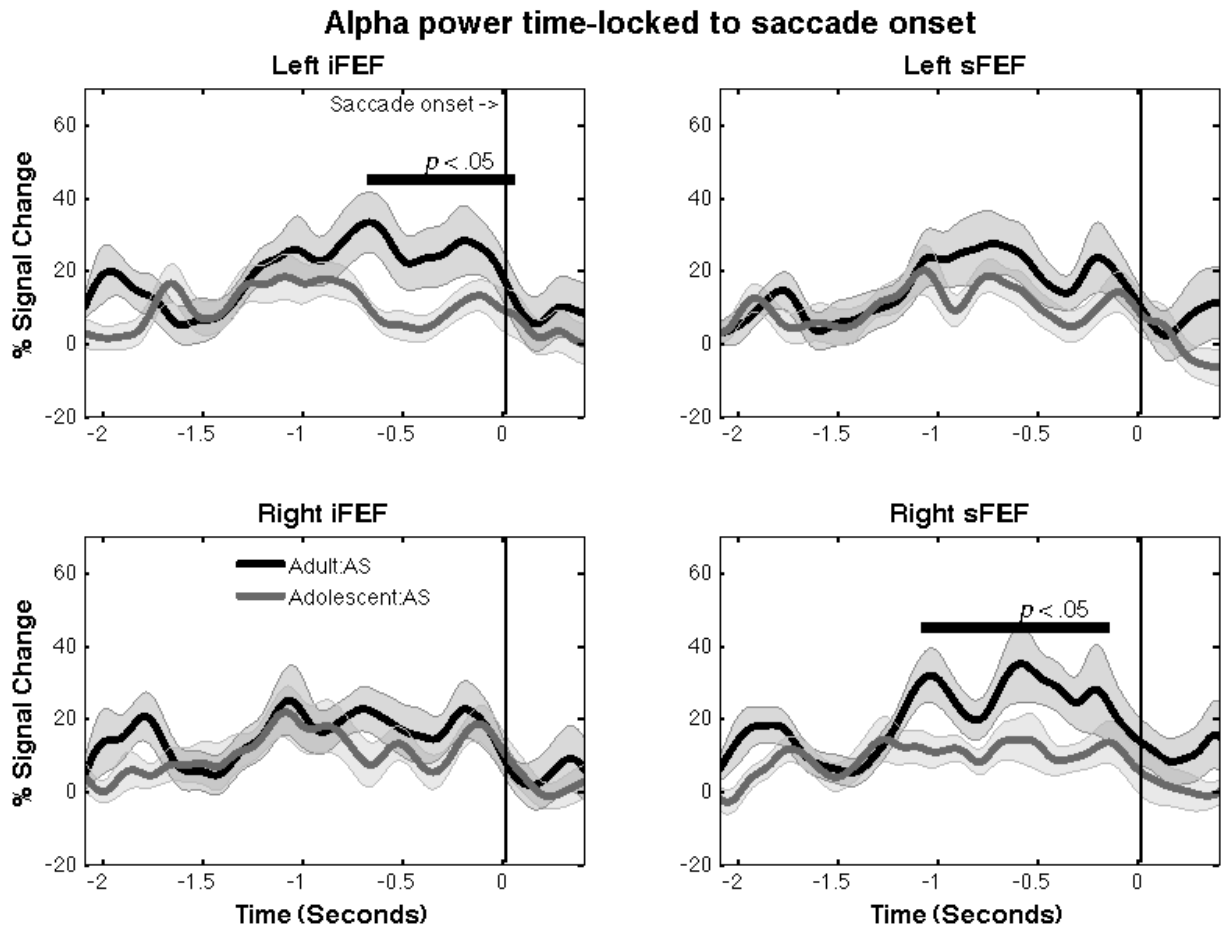

Figure 23. Alpha-band power time-locked to saccade onset.
Y scale is percent signal change from baseline. Shaded areas indicating one *SE*. X axis indicates the time to saccade onset. Horizontal bar indicates task period that showed significant difference between conditions or age groups (p <.05 corrected). Only correct trials were analyzed.

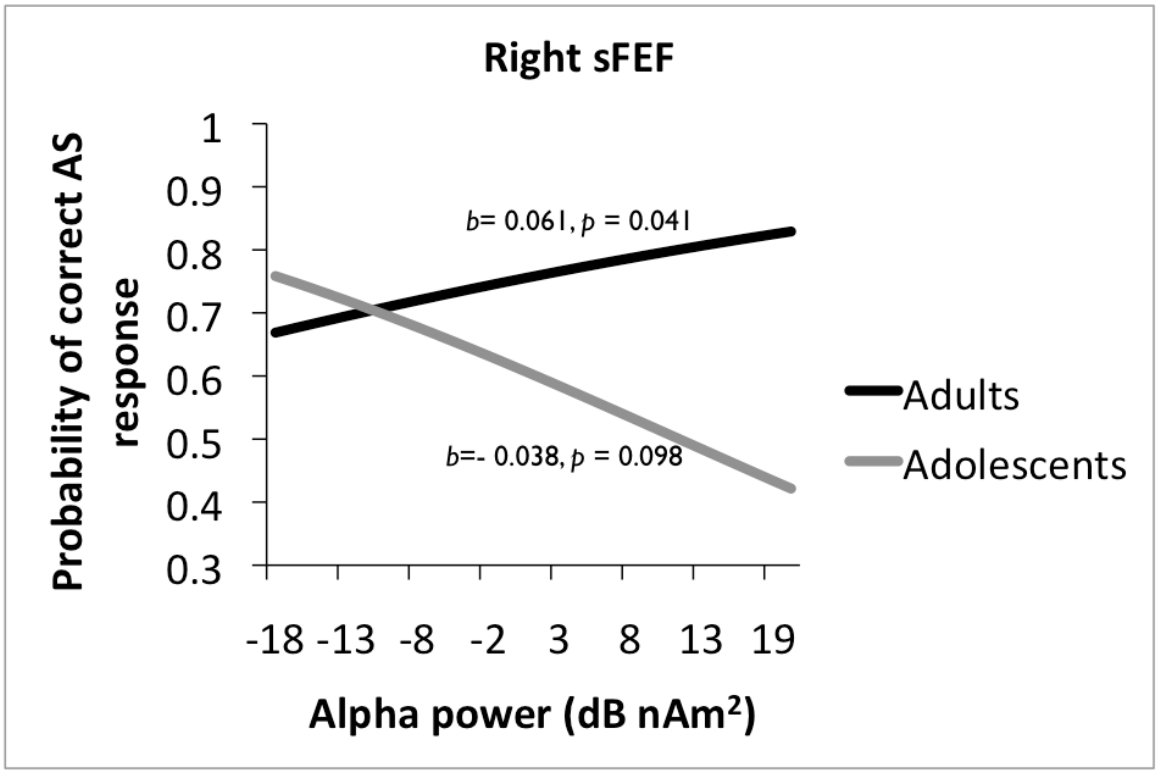

Figure 24. Preparatory alpha-band power and AS task performance.

6.5.1 Interim Discussion

In adults, we found that when compared to the PS task, alpha-band power was significantly stronger for the AS task in the left iFEF and the right sFEF. Further, stronger alpha-band power was correlated with better AS task performance, suggesting that stronger inhibition of saccade-related activity could lead to better AS task performance. In adolescents, increased alpha-band power for the AS task was found in the bilateral iFEF.

Historically, alpha-band activity was thought to reflect “idling” or “inattentive” states. This conception was based on observations that alpha rhythm is most pronounced when participants are awake but not engaging in any task. However, it has been demonstrated that alpha activity can be modulated by different task conditions, and thus require an alternate interpretation (Jensen & Mazaheri, 2010; S. Palva & Palva, 2007). One increasingly influential hypothesis suggests that increased alpha-band activity reflects functional inhibition of cortical activity (Jensen & Mazaheri, 2010; Klimesch, et al., 2007), and has received strong empirical support (Bonnefond & Jensen, 2012; Haegens, et al., 2011). Our results are consistent with this hypothesis, suggesting that inhibition of preparatory saccade-related activity in the FEF is associated with increased alpha-band power. These results are consistent with Everling and Munoz’s FEF recording study (2000), and their model (2004) suggesting that pretarget saccade-related activity has to be inhibited for successful AS task performance.

The superior portion of the precentral sulcus (sFEF) has long been suggested to be the human homologue of monkey FEF (Curtis, 2011; Luna, et al., 1998). Human functional imaging studies also found the inferior portion of the precentral sulcus (iFEF) associated with oculomotor control (Berman et al., 1999; Lee, et al., 2010; Luna, et al., 1998; Moon, et al., 2007). We interpreted our results in both the sFEF and the iFEF as an indication of functional inhibition of saccade-related activity. Because the iFEF partially overlaps with the inferior frontal junction, a region that has been hypothesized to be involved in stimulus-driven attention orienting (Asplund, Todd, Snyder, & Marois, 2010; Levy & Wagner, 2011), it is possible that the iFEF activity is associated with attention processing of visual cues (the red X), whereas the increased alpha-band power in the sFEF is associated with inhibition of saccadic motor control. Since we observed increased alpha-band power late in the preparatory period, long after the salient cue was

presented, we suggest that increased alpha-band power is not related to attention processing of visual stimuli. Nevertheless, the functional role of the inferior precentral sulcus in oculomotor paradigms remains to be explored.

In adults, we also found significant task-related modulation of alpha-band power in the left IPS. Although pretarget suppression of saccade-related activities in the SC (Everling, et al., 1999) and the FEF (Everling & Munoz, 2000) have been found to be critical for successful AS task performance, similar effect has not been reported in the monkey LIP. Unlike the FEF and the SC, electric stimulation of LIP neurons does not induce saccades (Curtis, 2011), suggesting that the IPS is not directly involved in the motor production of saccades. Therefore, the increased alpha-band power we observed in the left IPS is probably not functionally equivalent with the elevated alpha-band power in the FEF. It has been suggested that the IPS is involved in transforming the stimulus location vector into a saccade direction vector (Van Der Werf, Jensen, Fries, & Medendorp, 2008; Zhang & Barash, 2000). Because the possible target locations were fixed in our paradigm (four locations), it is possible that participants memorized target locations, and the increased alpha-band power in the left IPS reflects functional inhibition of reflexive saccade direction vectors.

We noticed that for the AS task, alpha-band power in the FEF and the IPS started to increase around 500 ms into the preparatory period, sustained throughout the later half of the preparatory period, and lasted through the first 200 ms of the response period. Could this alpha activity reflect temporal prediction of the timing of the target onset, rather then functional inhibition of saccade-related activity? We consider this scenario unlikely for the following two reasons. First, the sustained alpha effect continued past target presentation, and decreased right before the onset of the saccade (Figure 23), suggesting that this effect is associated with saccades

but not target presentation. Second, alpha-band power was significantly higher for the AS task when compared to the PS task, suggesting that the increased alpha-band power is associated the increased control demand for the AS task, but not temporal prediction of the timing of target onset.

It is possible that perhaps participants have acquired task contingencies, and withheld inhibition until late into the preparatory period when it was most needed. Before the MEG sessions, participants performed practice trials and other similar oculomotor tasks in the MRI environment; in such a case, the late peaking alpha-band power we observed could reflect task familiarity. To test if learning of trial timing occurred during the MEG testing, we contrasted alpha-band power timecourses from trials administered in the first half of the testing, versus trials administered in the second half. If learning had occurred, we would expect to see stronger alpha-band power in the beginning versus the end of the session. We did not find such effect in our MEG data (see Appendix C), and our behavioral data (Figure 8) suggest that no learning occurred during MEG testing.

We also found significant increases in alpha-band power around the time when the task cue was presented, or even before the start of the preparatory period. Could this activity reflect participants were predicating the onset of task cues? This is unlikely because inter-trial-intervals were jittered; instead, we suspect this effect reflects task-set related functional inhibition (Velanova, et al., 2009), whereby an overall heightened level of inhibition was maintained throughout the AS task blocks.

If beta-band activity reflects top-down signaling that transmits control signals to inhibit saccade-related activities in oculomotor regions, and if alpha-band activity represents functional inhibition of saccade-related activity, then we would expect these two signals to have a temporal

relationship. Indeed, we found that beta-band power showed significant task modulation around the time when alpha-band activity started to peak (500 ms into the preparatory period). Because we did not find sustained beta increase, this further suggests that after the initial increases in both alpha- and beta-band power, the prolonged functional inhibition as indicated by sustain increases in alpha-band power was probably sustained by sources other than the PFC. One possibility is that recurrent thalamocortical pathway may be cable of sustaining inhibition signal after the initial signaling from the PFC.

Although we observed robust task-related modulation in beta-band activity, increased beta-band power in the PFC was only weakly correlated with better AS task performance. In contrast, in adults we found significant associations between alpha-band power in the right sFEF and AS task performance. This suggests that though increased cognitive control demand for the AS task modulates prefrontal top-down signaling, the success vs. failure of AS task performance depends more heavily on how effective saccade-related activity is inhibited in the oculomotor regions.

Consistent with our developmental hypothesis, compared to adolescents, adults showed significantly stronger alpha-band power in the right sFEF and the left iFEF. Studies have shown that even when instructed in advance, adolescents still have difficulties in inhibiting upcoming prepotent motor responses (Luna, et al., 2004; Munoz, et al., 1998). Our results suggest that his behavioral difference could be related to immaturities in sustaining inhibitory neural signals that functionally inhibit preparatory saccade-related activities (Everling, et al., 1998; Everling & Munoz, 2000).

Similar to beta activity, the genesis of alpha rhythm is still not well understood, and at this point we can only postulate on why adolescents showed weaker alpha-band power. Most

studies agree that alpha rhythm involves cortical-thalamic interaction (Bollimunta, et al., 2011; Jones, et al., 2009; Saalmann, et al., 2012), and decreased alpha-band power during adolescence could suggest immature functioning of deep-layer thalamocortical cells. Similarly, decreased myelination of thalamic-cortical projection tracts during adolescence (Asato, et al., 2010; Lebel, Walker, Leemans, Phillips, & Beaulieu, 2008) could also affect cortical-thalamic interactions. For example, it has been found that the thalamus innervates low-threshold spiking inhibitory neurons (Tan, et al., 2008) that provide sustained inhibition on excitatory cells to reduce spiking outputs (Gentet, et al., 2012). Decreased myelination during adolescence could reduce the effectiveness of driving interneuron activities, ultimately leading to lower levels of cortical inhibition. Although direct physiological evidence is still lacking, one computational modeling study further suggests that alpha rhythm recruits low-threshold spiking interneurons (Vierling-Claassen, et al., 2010), finding which supports our interpretation that decreased alpha-band power during adolescence reflects immaturities in functional inhibition.

It is also possible that weaker frontal top-down signaling during adolescence, as indicated by decreased beta-band power, could led to insufficient inhibition in the FEF. Because wavelet analyses require a longer wavelet window to achieve a reasonable spectral resolution, the power timecourses were temporally smoothed, making it difficult to make conclusive assessment on temporal causality based on power timecourses. In the next section (Chapter 6.6), we directly tested the phase synchrony between the PFC and the FEF.

6.6 NEURAL SYNCHRONY

We have presented results suggesting that top-down signaling is associated with increased beta-band power in the PFC, and that functional inhibition is associated with increased alpha-band power in oculomotor regions. We further hypothesized that beta neural synchrony between the PFC and oculomotor regions will increase to communicate top-down biasing signals for the AS task, and that adolescents will show weaker long-range beta neural synchrony, indicating ineffective cortical-cortical communication.

To test these hypotheses, we calculated PLVs in the beta-band between PFC ROIs (bilateral DLPFC and bilateral VLPFC) and oculomotor ROIs. Because we observed robust alpha-band power modulation in the FEF, we first focused on PFC-FEF synchrony. For adults, we did not find any significant task-related modulations in PLVs between the PFC and all FEF ROIs. Instead, we found that beta neural synchrony between the right DLPFC and the right IPS was significantly stronger for the AS task compared to the PS task (Figure 25). Unexpectedly, for adolescents we found that beta neural synchrony was significantly higher for the PS task compared to the AS task, between the right DLPFC and the left sFEF (Figure 26), and between the right VLPFC and the right sFEF (Figure 27). In support of our developmental hypothesis, for the AS task, Adults' beta-band neural synchrony between the right DLPFC and the right IPS was significantly stronger compared to adolescents (Figure 25). Similar age effect was also observed between the right DLPFC and the left sFEF (Figure 26), and between the right VLPFC and the right sFEF (Figure 27). To control for performance differences, only correct trials were analyzed.

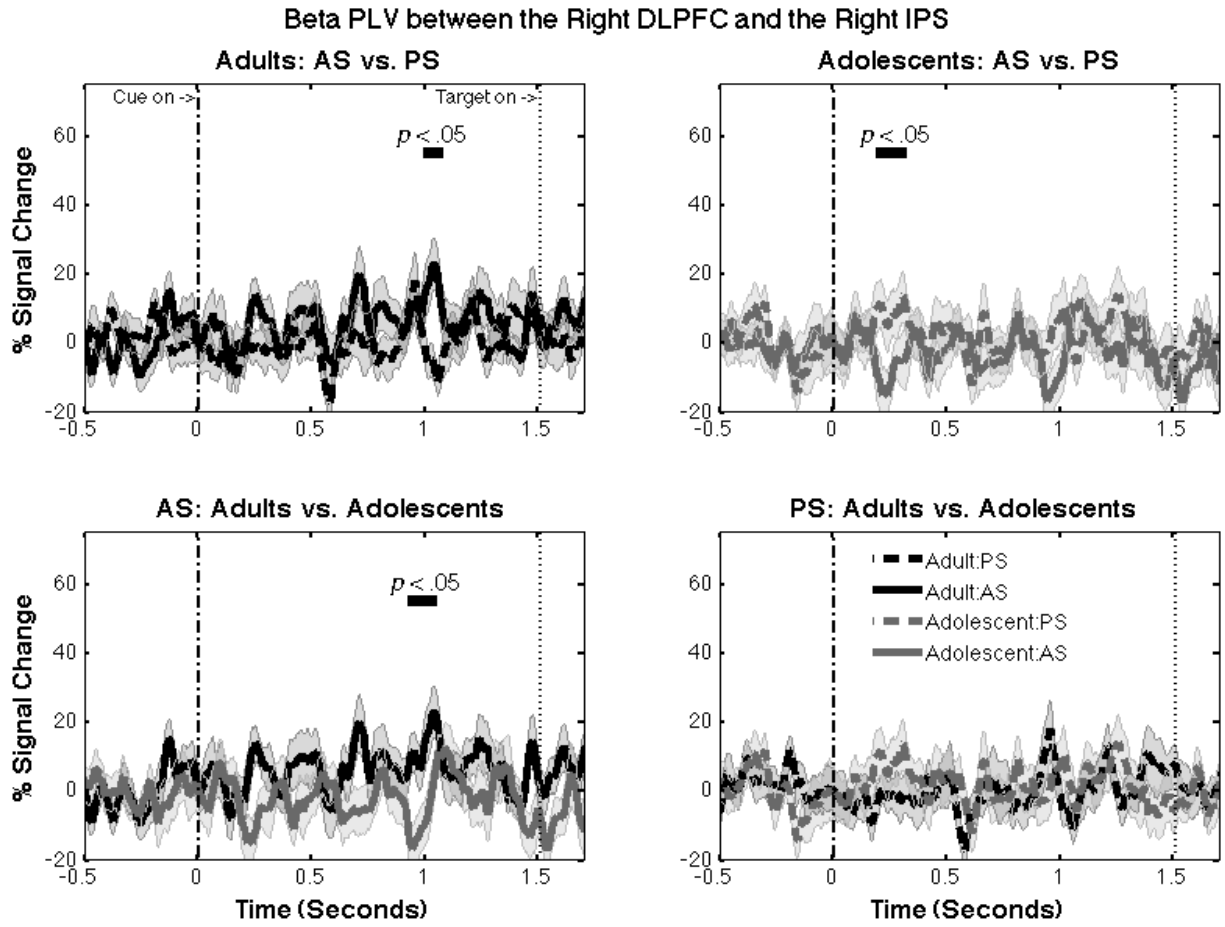

Figure 25. Beta-band neural synchrony between the right DLPFC and the right IPS.
Y scale is percent signal change in PLVs from baseline. Shaded areas indicating one *SE*. X axis indicates the time since cue onset. From zero to 1.5 seconds is the preparatory period. Horizontal bar indicates task period that showed significant difference between conditions or age groups (p <.05 corrected). Only correct trials were analyzed.

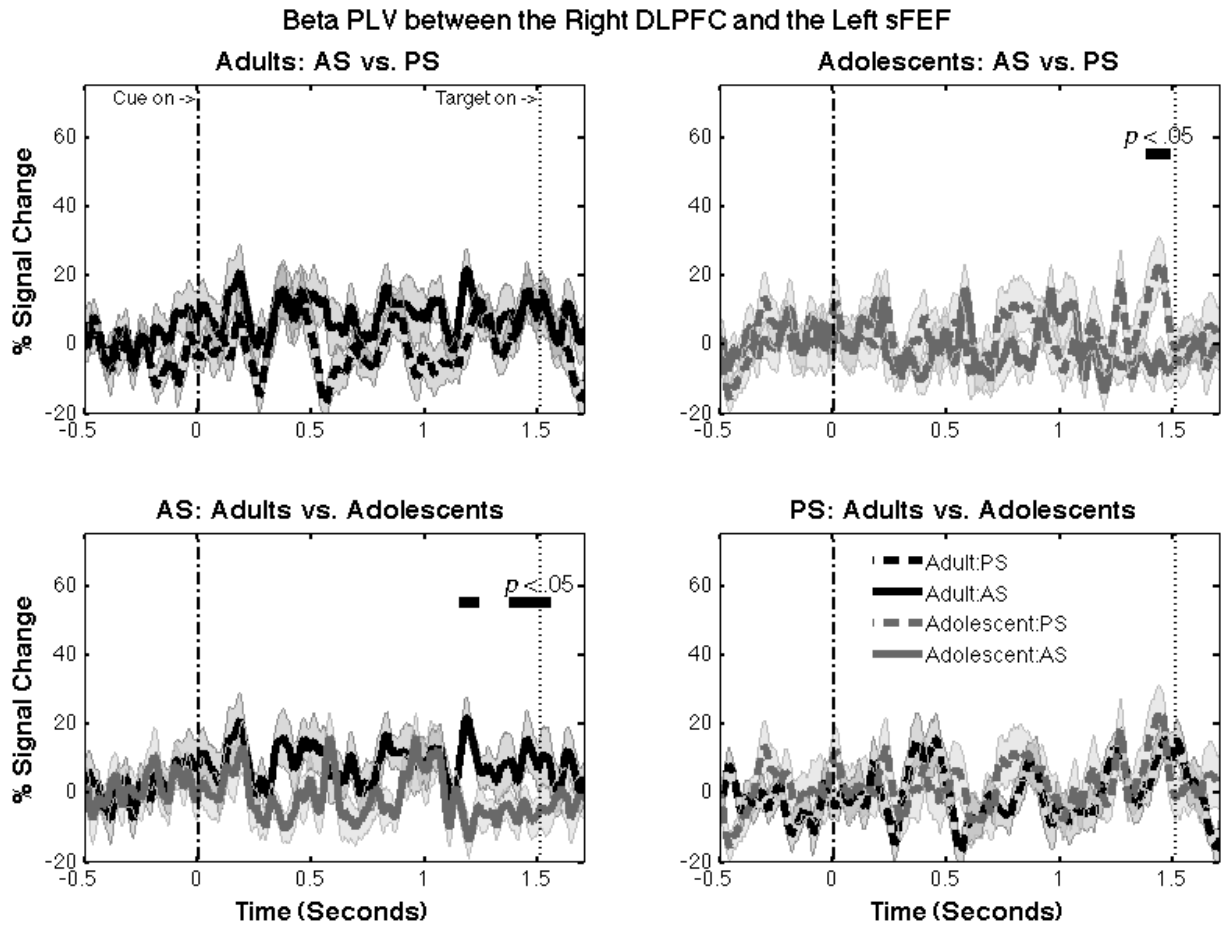

Figure 26. Beta-band neural synchrony between the right DLPFC and the left sFEF.
Y scale is percent signal change in PLVs from baseline. Shaded areas indicating one *SE*. X axis indicates the time since cue onset. From zero to 1.5 seconds is the preparatory period. Horizontal bar indicates task period that showed significant difference between conditions or age groups (p <.05 corrected). Only correct trials were analyzed.

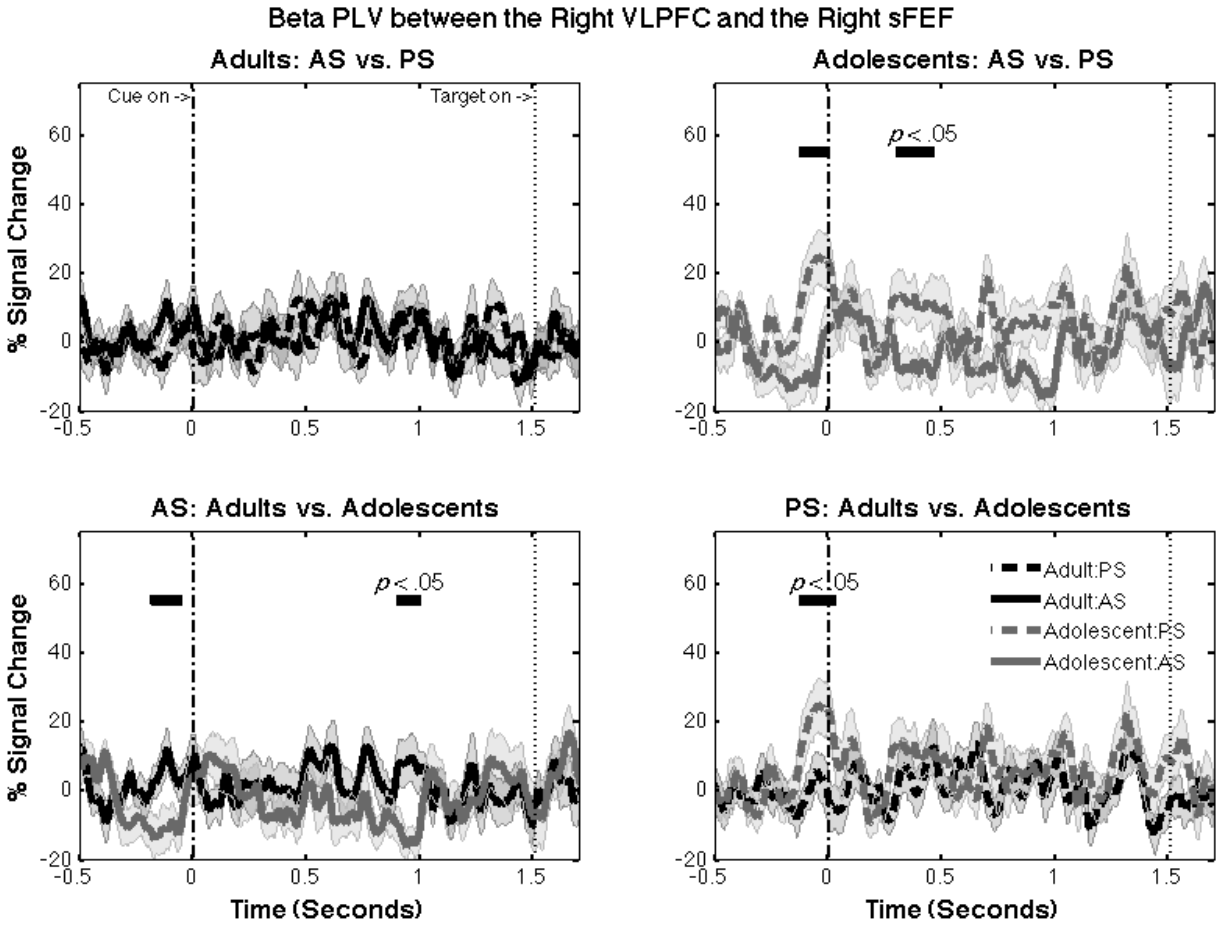

Figure 27. Beta-band neural synchrony between the right VLPFC and the right sFEF.
Y scale is percent signal change in PLVs from baseline. Shaded areas indicating one *SE*. X axis indicates the time since cue onset. From zero to 1.5 seconds is the preparatory period. Horizontal bar indicates task period that showed significant difference between conditions or age groups (p <.05 corrected). Only correct trials were analyzed.

Could inter-regional communication be supported by synchrony in frequencies other than beta-band? To address this question, we examined both alpha- and gamma-band neural synchrony between ROIs. We did not find any significant task-related modulations in alpha- and gamma-band neural synchrony. However, for the AS task, alpha-band neural synchrony between the left sFEF and the right IPS was higher for adults when compared to adolescents (Figure 28).

Because PLV measures the phase consistency across trials, we were not able to repeat the trial-by-trial analysis that we did to assess the impact of preparatory alpha- and beta-band power on task performance. To investigate the association between preparatory neural synchrony and AS task performance, we repeated PLV analyses by including both correct and incorrect trials. Then for each participant, we extracted the averaged preparatory PLV values from all the significant time-clusters we reported above, and correlated with behavioral performance. We did not find any significant correlations, with r ranging from -0.12 to 0.21, and all p values were greater than 0.16.

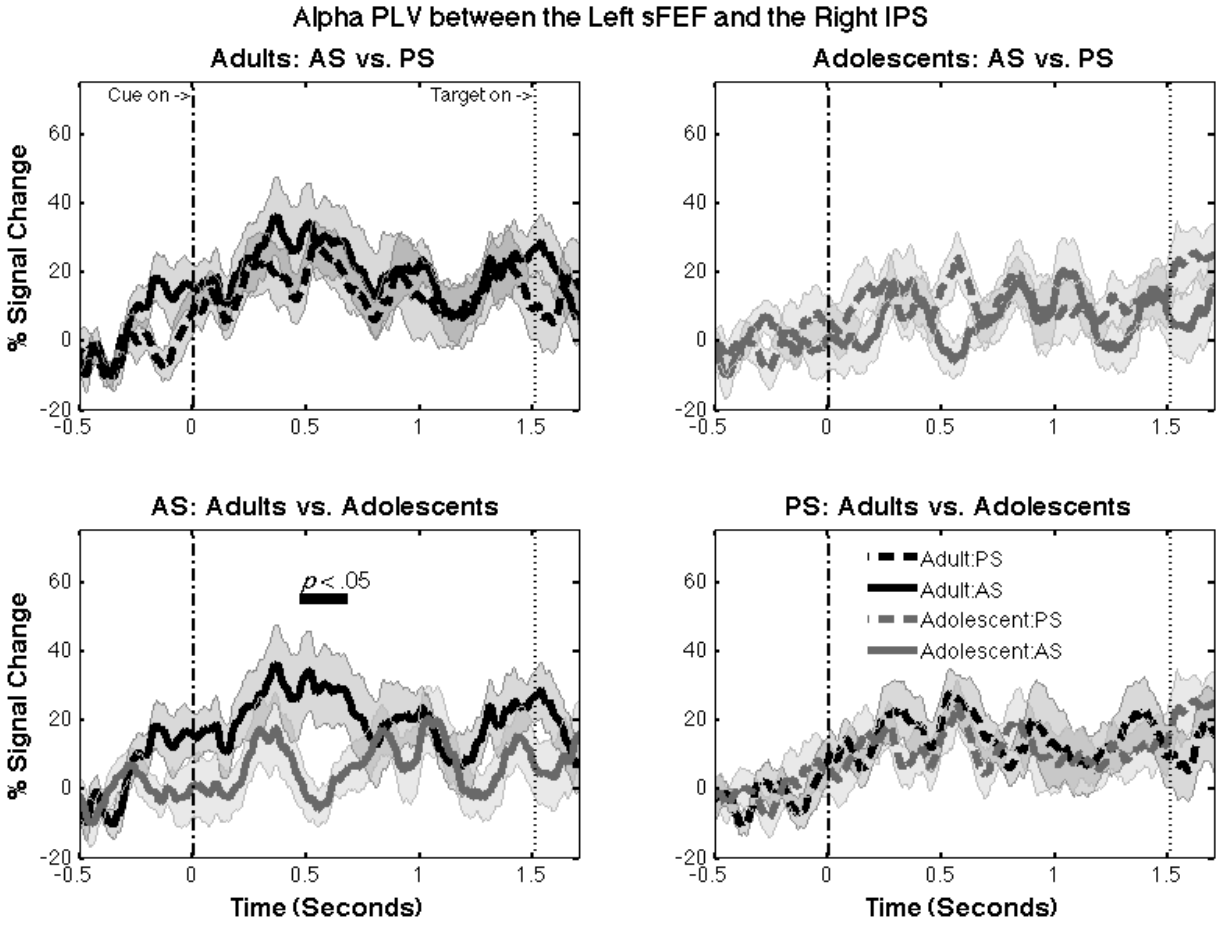

Figure 28. Alpha-band neural synchrony between the left sFEF and the right IPS.
Y scale is percent signal change in PLVs from baseline. Shaded areas indicating one *SE*. X axis indicates the time since cue onset. From zero to 1.5 seconds is the preparatory period. Horizontal bar indicates task period that showed significant difference between conditions or age groups (p <.05 corrected). Only correct trials were analyzed.

6.6.1 Interim Discussion

It has been long hypothesized that the PFC provides inhibitory signals to suppress saccade-related activity in the FEF (Munoz & Everling, 2004). We hypothesized that beta-band neural synchrony between the PFC and the FEF would increase for the AS task, reflecting enhanced communication between frontal cognitive control regions and oculomotor regions for top-down inhibition of saccade-related activity. However, we did not find evidence that supports this hypothesis. Instead, for adults we found that beta-band neural synchrony between the right DLPFC and the right IPS increased for the AS task, when compared to the PS task. As previously discussed, increased alpha-band power in the parietal cortex is probably associated with the inhibition of reflexive saccade direction vector, but not functional inhibition of saccade generation. We suggest this increased synchrony pattern could reflect be related to the preparation of the vector inversion process. Because we did not find significant task-related modulation in alpha-band power in the right IPS, it is also possible that the DLPFC-IPS connectivity is not related to functional inhibition, but related to other preparatory cognitive control processes such as working memory maintenance. One study has found increased beta-band neural synchrony between frontal and parietal cortices when working memory load increased (J. M. Palva, Monto, Kulashekhar, & Palva, 2010).

Since we did not find any significant task-related increases in phase synchrony between the PFC and FEF ROIs, it remains an open question how functional inhibition in the FEF was initiated. Because the thalamus could be involved in both inhibition (Tan, et al., 2008) and alpha rhythm (Jones, et al., 2009; Saalmann, et al., 2012), it is possible that signals were transmitted

through indirect connectivity, such as cortical-BG-thalamocortical pathways (Vokoun, et al., 2011) or the cortical-thalamic-cortical pathways (Saalmann, et al., 2012; Sherman & Guillery, 2011). For example, the global pallidus and the substantia nigra are composed of mainly GABAergic neurons that inhibit the thalamocortical pathway to prevent saccade generation (Hikosaka, Takikawa, & Kawagoe, 2000). Outputs from the PFC could be transmitted to the caudate, then from the caudate to the global pallidus and the substantia nigra, and then to the thalamus and to the FEF (Alexander, et al., 1986). Cortical-cortical interaction could also be mediated by indirect cortical-thalamic-cortical pathways (Sherman & Guillery, 2011). Particularly, non-specific thalamic nuclei (such as the pulvinar) are known to have widespread cortical connectivity, well situated to mediate inter-cortical communication (Saalmann, et al., 2012). Unfortunately, these hypotheses are difficult to test with MEG, given its insensitivity to subcortical sources.

Another possibility is that the FEF receives inhibition input from regions other than the PFC, such as the SEF or the ACC (Everling & Johnston, 2011; Schlag-Rey, et al., 1997). One recent study showed that temporally deactivating the monkey DLPFC reduced the suppression of stimulus-related activity in the SC, and eliminated the differences in activity between PS and AS trials (Koval, et al., 2011). These results strongly suggest that the DLFPC is critically involved in providing control signal to bias saccade-related activity, at least to the SC. It is also possible that PFC control signals are first transmitted to the SEF, and in turn SEF provides inhibition of the FEF and the SC. Future studies should clarify if DLPFC directly influences preparatory activity in the FEF, and if the SEF or the ACC provides top-down inhibition signal.

Beta-band neural synchrony between the right DLPFC and the right IPS, the right VLPFC and the right sFEF, the right DLPFC and the left sFEF, and alpha-band neural synchrony

between the left sFEF and the right IPS all increased from adolescence to adulthood. However, because only the DLPFC-IPS connections showed stronger PLV measure for the AS task compared to the PS task, we cannot confidently suggest all these connections were involved in preparatory inhibitory control processes. We tentatively suggest that these age-related differences reflect overall immaturities in coordinating distributed activities during adolescence.

Decreased synchrony during adolescence could be associated with decreased white-matter integrity in direct cortical-cortical association tracts and subcortical-cortical projection tracts (Asato, et al., 2010; Ashtari, et al., 2007; Barnea-Goraly, et al., 2005; Lebel, et al., 2008; Schmithorst, et al., 2002). Decreased myelination affects the speed and validity of neuronal transmission (Stufflebeam, et al., 2008), and may further impede the effectiveness of entraining distributed brain regions into the same oscillating frequency and to maintain a consistent phase relationship. Note that the synchrony measure we used, PLV is calculated by only considering phase information but not frequency amplitudes (Lachaux, et al., 1999), therefore weaker alpha- and beta-band power during adolescence should not have confounded our synchrony analyses.

7.0 GENERAL DISCUSSION

Perhaps one of the most striking findings from the adolescent development literature is that even when instructed in advance, adolescents still have difficulties inhibiting an anticipated prepotent motor response, and that although adolescents can sometimes successfully inhibit single responses, the rate of correct inhibitory responses continues to increase into adulthood. This is repeatedly demonstrated by studies showing that compared to adults, adolescents consistently showed higher AS error rates across studies (e.g., Klein & Foerster, 2001; Klein, Foerster, Hartnegg, & Fischer, 2005; Luna, et al., 2004; Munoz & Everling, 2004), even when the preparatory time was extended to six seconds (Ordaz, et al., 2010). Collectively these studies suggest that there are critical immaturities in the preparatory neurocognitive processes being engaged in preparation to inhibit reflexive saccades.

We have presented results providing novel insights into what these immaturities might be. First, we found that compared to adults, adolescents could not initiate and sustain the same level of functional inhibition to inhibit preparatory saccade-related activity, as indicated by decreased alpha-band power in the FEF. Second, we found that compared to adults, adolescents showed less robust top-down signaling, as indicated by weaker beta-band power in the right DLPFC and the right VLPFC. Lastly, flexible coupling between task-relevant regions have been suggested to be critical for goal-directed behaviors (Siegel, et al., 2012), yet we found that

compared to adults adolescents showed decreased levels of synchrony between task-relevant regions, reflecting immaturities in coordinating distributed cortical activities.

These results extend our previous fMRI studies (Hwang, et al., 2010; Velanova, et al., 2008, 2009) and provide additional evidence illuminating the nature of immature inhibitory control during adolescence. Consistent with our previous effective connectivity study (Hwang, et al., 2010), we found that adolescents showed weaker fronto-parietal synchrony associated with correct AS trial performance, indicating that our fMRI results were not biased by performance differences. However, we were unable to replicate our increased frontal-FEF fMRI connectivity findings. As discussed in Chapter 6.6.1, we suspect this was because subcortical structures were involved in mediating inhibitory signal (Hikosaka, et al., 2000; Vokoun, et al., 2011) and rhythm genesis (Jones, et al., 2009; Steriade, et al., 1990). Because MEG is not sensitive to subcortical sources, and because pairwise GCA between cortical ROIs could discount contributions from subcortical ROIs, other connectivity methods that can specifically model the contribution from subcortical structures are needed.

In our previous fMRI studies (Velanova, et al., 2008, 2009), we could not separate preparatory vs. response signals in our trial-locked, evoked BOLD analyses. When compared transient activations associated with correct trials, we did not find significant differences between adolescents and adults in the FEF and the DLPFC (Velanova, et al., 2008). Nevertheless, when comparing sustained task-set related activities between adolescents and adults, we found decreased sustain activation in the PFC and other temporal/parietal regions for adolescents (Velanova, et al., 2009). Building on these findings, by using high temporal resolution MEG, we found that immaturities persist in transient (trial-related) preparatory control signals during adolescence, indicating weaker top-down signaling and functional inhibition.

Because BOLD infers neuronal activity summated across slow and fast neural oscillations, we gained more sensitivity in detecting transient signals by using MEG. Indeed, studies have reported complex and nonlinear relationship between BOLD and trial-related neural synchronization/desynchornization (Scheeringa et al., 2011; Winterer et al., 2007). It is possible that when contrasting microcircuit activities of adolescents and adults, adolescents' activity was not as synchronous as adults', yet had similar metabolic demand, as indicated by similar transient BOLD responses. When considered together, our results suggest that adolescents have immaturities in transient, trial-related preparatory neurocognitive processes, in addition to immature sustained, task-set related function (Velanova, et al., 2009).

Although our hypotheses and results were specific to the oculomotor paradigm, they could be generalized to inhibitory control of other behaviors, not just saccadic responses. In a broader context, we found that adolescents showed evidence of decreased levels of functional inhibition of task-irrelevant or task-inappropriate processes, and less robust top-down control of goal-directed behaviors. Immature functional inhibition could lead to inhibitory failure because if task-irrelevant or task in-inappropriate processes are not sufficiently suppressed, they could override the weaker goal-directed or contextually-driven behavior. Our results suggest that adolescents have immaturities in generating and sustaining inhibition signal, and if contextually inappropriate behavior has a much stronger representation, adolescents could have difficulties suppressing it. Similarly, immaturities in top-down signaling could affect how processes in the sensory and motor regions could be effectively biased toward accomplishing a behavioral goal.

Overall, we found that adolescents did not show the same pattern of oscillatory neurodynamics as adults—weaker local oscillatory power and weaker phase synchrony between distant regions. It is possible the immaturities in neural circuits' functions will not only reduce

spectral energy, but also decrease long-range synchronization between distant oscillating neurons. These immaturities could have important translational implications. As discussed in the introduction, impaired inhibitory control is a prominent clinical syndrome in several psychiatric disorders, such as schizophrenia and Attention Deficit/Hyperactivity Disorder (Sweeney, et al., 2002; Sweeney, et al., 2004). More recently, abnormal oscillatory activities have also been reported in patients with neuropsychiatric disorders (Uhlhaas & Singer, 2006, 2012). Whether or not the neural mechanisms associated with decreased oscillatory power and decreased phase synchrony that we observed in adolescents overlaps with disorders' underlying etiologies is an open question that needs to be empirically investigated. The first step is to pinpoint the neural mechanisms involved in alpha and beta rhythms in healthy developing adolescents. Although specifics remain elusive, our findings provide a context for future directions.

Inhibitory interneurons are known to be critical for rhythm genesis and regulating activities within microcircuits (Moore, et al., 2010). Initial studies suggest that GABA interneurons undergo important changes through adolescence that could affect microcircuit processing (Lewis & Melchitzky, 2012). How different types of inhibitory neurons develop through adolescence, and their functional role in regulating cortical activities need to be further investigated. Studies suggest that certain inhibitory populations, such as the SOM interneurons, could be involved in amplifying alpha rhythm (Vierling-Claassen, et al., 2010), and provide sustain inhibition over pyramidal neurons (Gentet, et al., 2012). It is possible that weaker functional inhibition during adolescence could be related to immaturities in interneuron functioning within microcircuits. How SOM interneurons function over the course of adolescence, and its abnormality in psychiatric disorders, should be further investigated.

Other candidates are the thalamocortical and BG-thalamocortical pathways. Existing models prominently highlight the thalamus's role in both alpha and beta rhythm geneses (Bollimunta, et al., 2011; Jones, et al., 2009), yet direct physiological evidence remains sparse. Similarly, how the BG-thalamocortical loop could be involved in transmitting control signal and sustaining inhibitory signal need to be further investigated. As discussed above, age-related increases in white matter integrity of fronto-cortical and fronto-subcortical tracts would support developmental enhancements in thalamocortical and BG-thalamocortical pathways. Interestingly, one theory proposed that several psychopathologies could be characterized by abnormal resonant interactions between the thalamus and the cortex, giving rise to abnormal oscillatory neurodynamics (Schulman et al., 2011). Given the adolescent emergence of major neurpsychiatric disorders, underscores the potential translational significance of this area of research.

Behaviorally, we found that adolescents failed to inhibit reflexive saccades 40% of the time. Although this performance was significantly worse than adults', on average adolescents were still able to inhibit reflexive saccades on more than half of the trials. A big dilemma is that our results indicated that adolescents were able to generate correct inhibitory responses *despite* weaker top-down control and preparatory inhibition. One possibility is through compensation; perhaps adolescents were utilizing other regions we did not examine. However, our previous fMRI studies showed that adolescents and adults utilized largely overlapping sets of brain regions for AS task performance (Velanova, et al., 2008, 2009), and we consider this possibility unlikely.

Another possibility is that perhaps adolescents' inhibitory control system functions at a level slightly above the threshold of successful inhibition, but well below the level utilized by

adults. In this proposed model, there would be a threshold of required functioning level of top-down signaling and functional inhibition for successful inhibitory control. If system's functioning level dips below the threshold, errors will be made. On a trial-by-trial basis, adolescents' immature system would frequently dip below the threshold, resulting in higher number of error trials (Figure 29). In contrast, adults' system functions at a more mature and robust level. On a trial-by-trial basis, the system's functioning level also varies, but because it is mature and well above the critical threshold, fewer errors are made (Figure 29).

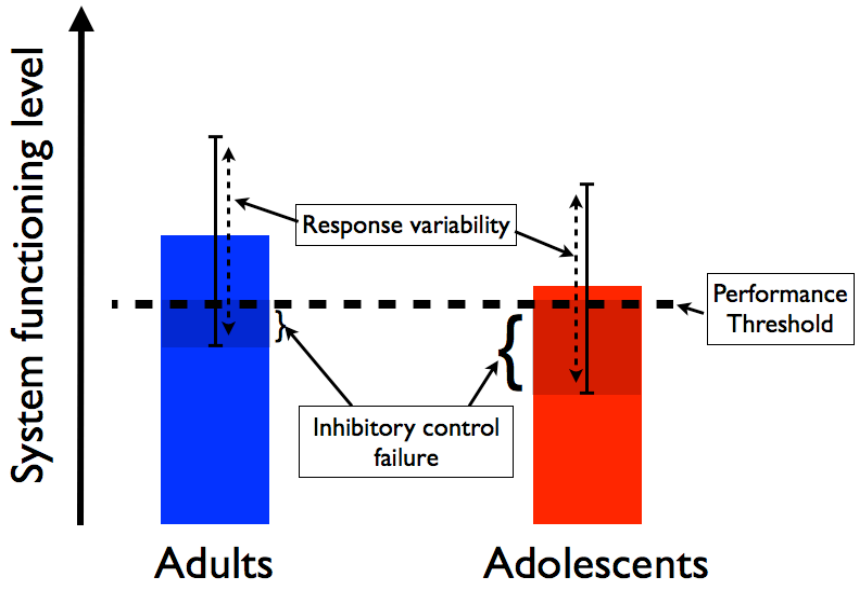

Figure 29. System functioning level.

It has been long recognized that heightened risk-taking behaviors during adolescence is a multi-factor construct, and numerous social and affective factors play significant roles (Crone & Dahl, 2012). Similarly, the need to exert inhibitory control does not only apply to simple motor

responses, but also emotion, motivation, complex behaviors, and thoughts. In this dissertation, we investigated how reflexive motor response could be inhibited in order to generate a voluntary goal-directed response. Despite using a basic model, we found important immaturities in functional inhibition and top-down signaling. It is possible that when placed in emotionally and socially challenging contexts, adolescents' system could be further challenged, resulting in the inhibitory failures and impulsive behaviors that we commonly observe in society.

APPENDIX A

BETA POWER IN THE OCULOMOTOR ROIS

Statistically significant task-related and age-related modulations in beta-band power were only observed in PFC ROIs. For completeness, beta-band power timecourses from other ROIs are presented in this appendix.

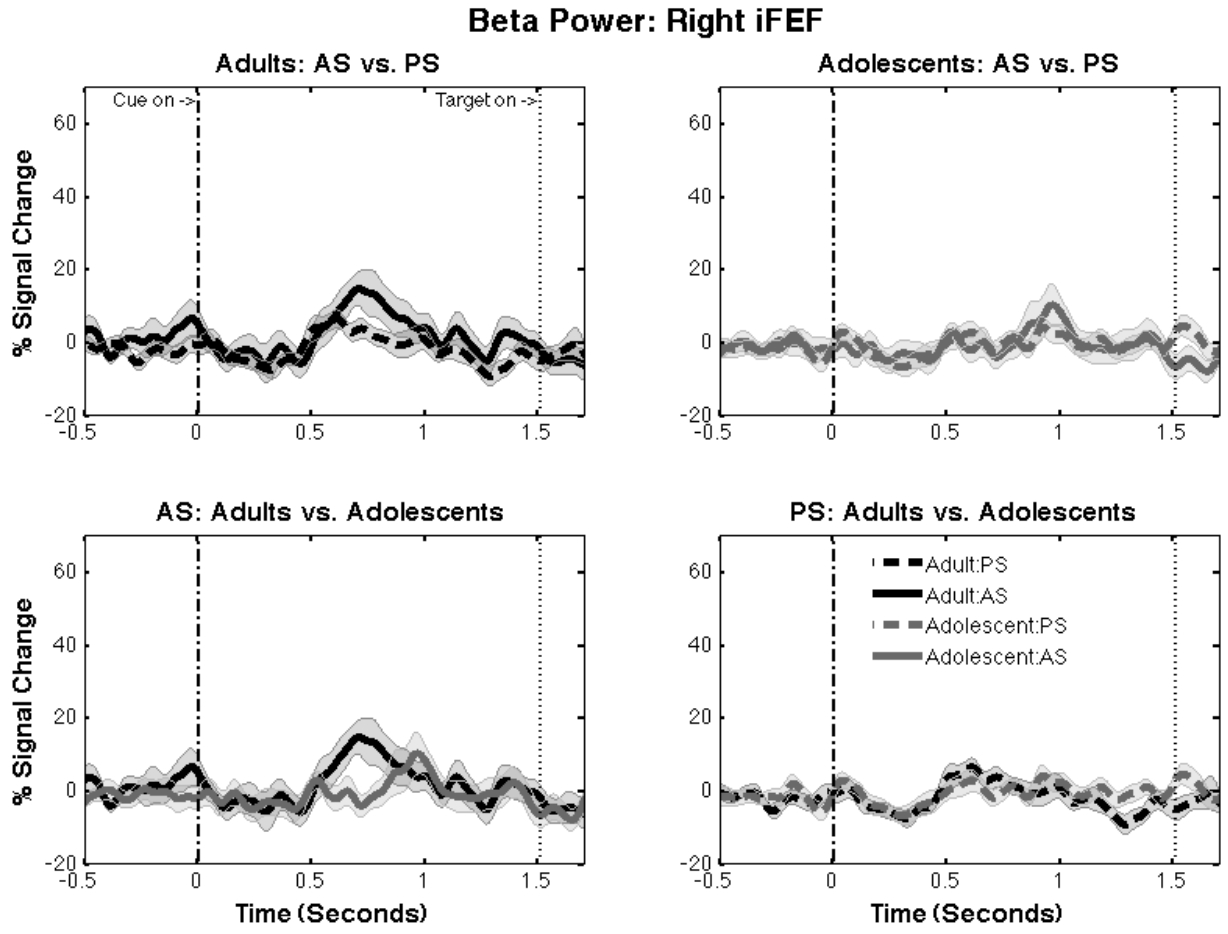

Figure 30. Beta-band power in the right iFEF.
Y scale is percent signal change from baseline. Shaded areas indicating one *SE*. X axis indicates the time since cue onset. From zero to 1.5 seconds is the preparatory period. Horizontal bar indicates task period that showed significant difference between conditions or age groups ($p < .05$ corrected). Only correct trials were analyzed.

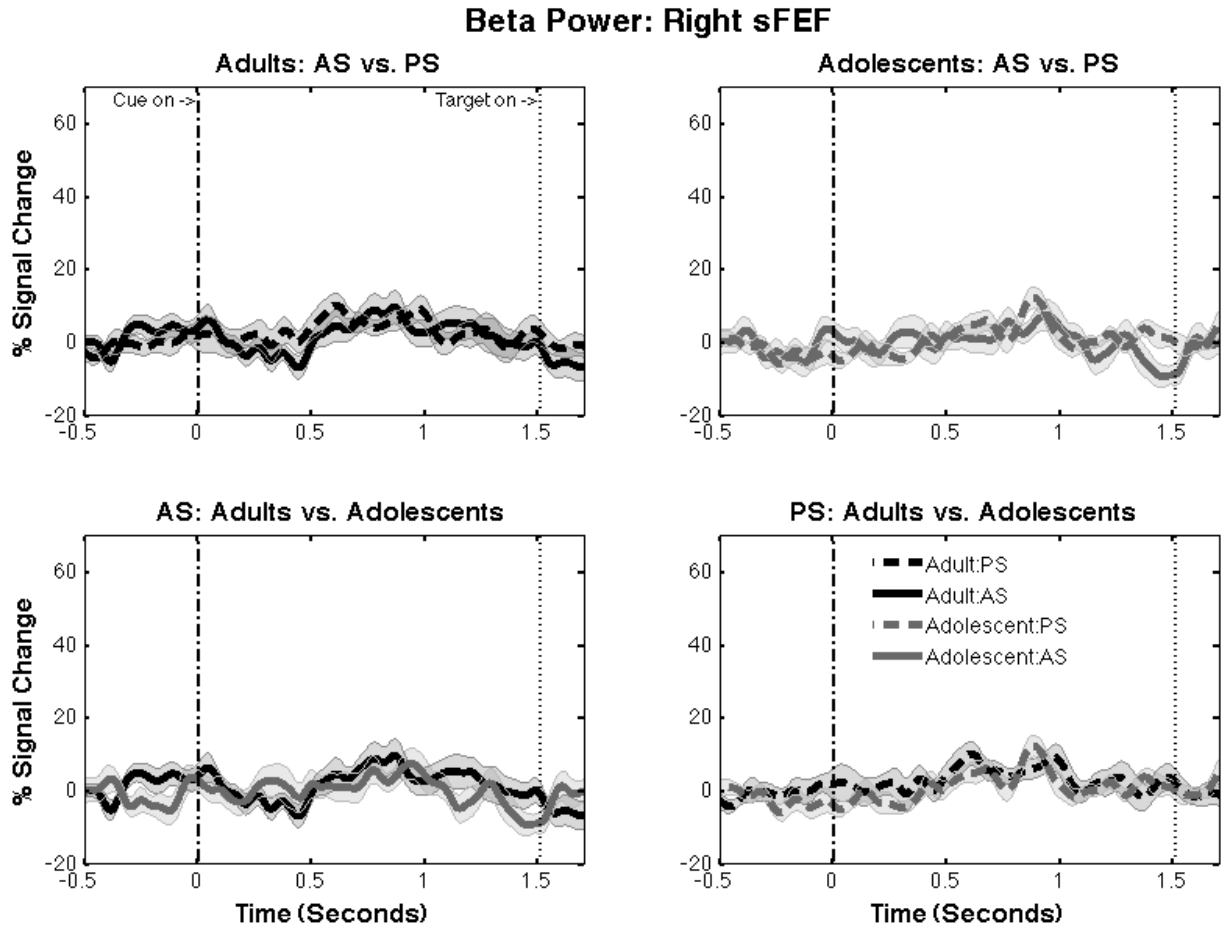

Figure 31. Beta-band power in the right sFEF.
Y scale is percent signal change from baseline. Shaded areas indicating one *SE*. X axis indicates the time since cue onset. From zero to 1.5 seconds is the preparatory period. Horizontal bar indicates task period that showed significant difference between conditions or age groups ($p < .05$ corrected). Only correct trials were analyzed.

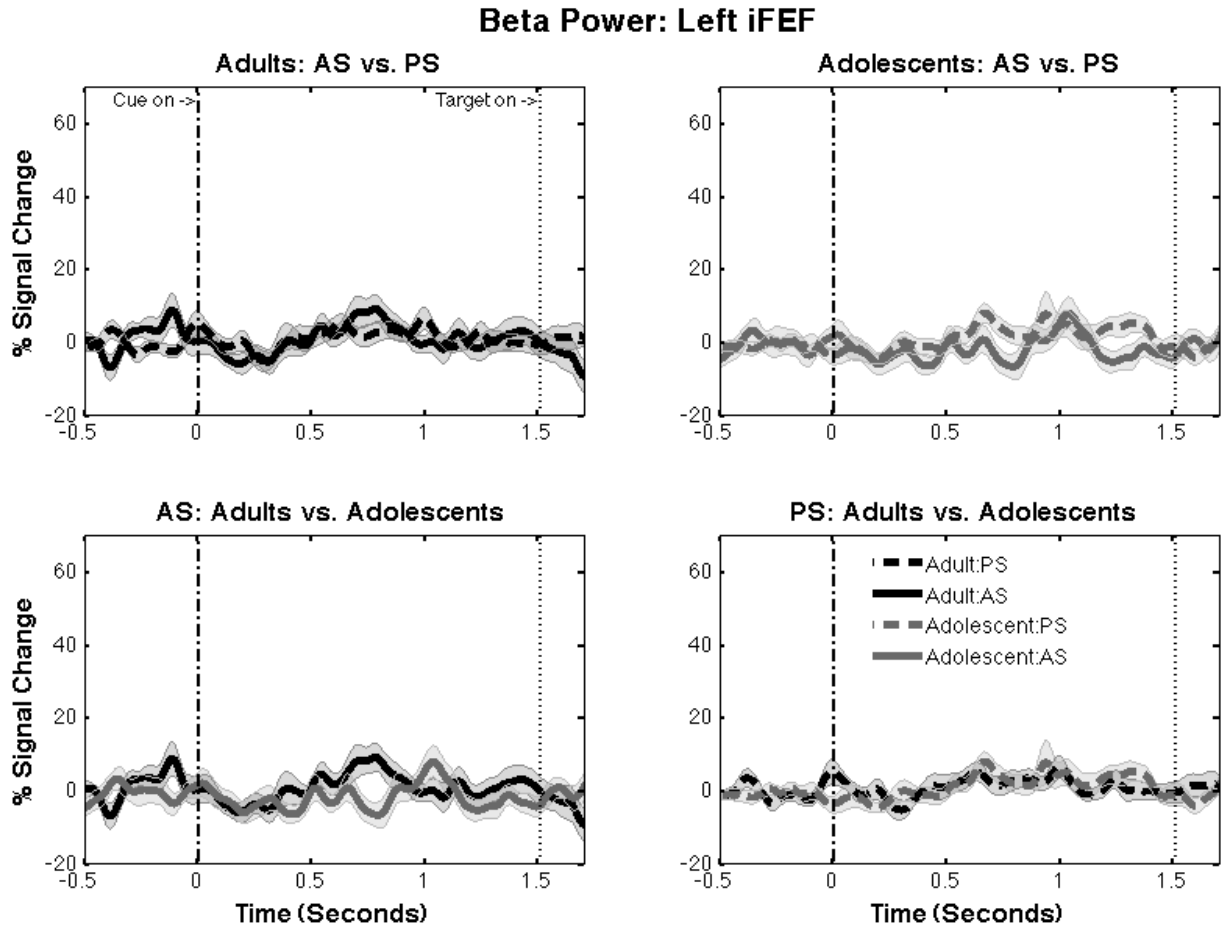

Figure 32. Beta-band power in the left iFEF.
Y scale is percent signal change from baseline. Shaded areas indicating one *SE*. X axis indicates the time since cue onset. From zero to 1.5 seconds is the preparatory period. Horizontal bar indicates task period that showed significant difference between conditions or age groups ($p < .05$ corrected). Only correct trials were analyzed.

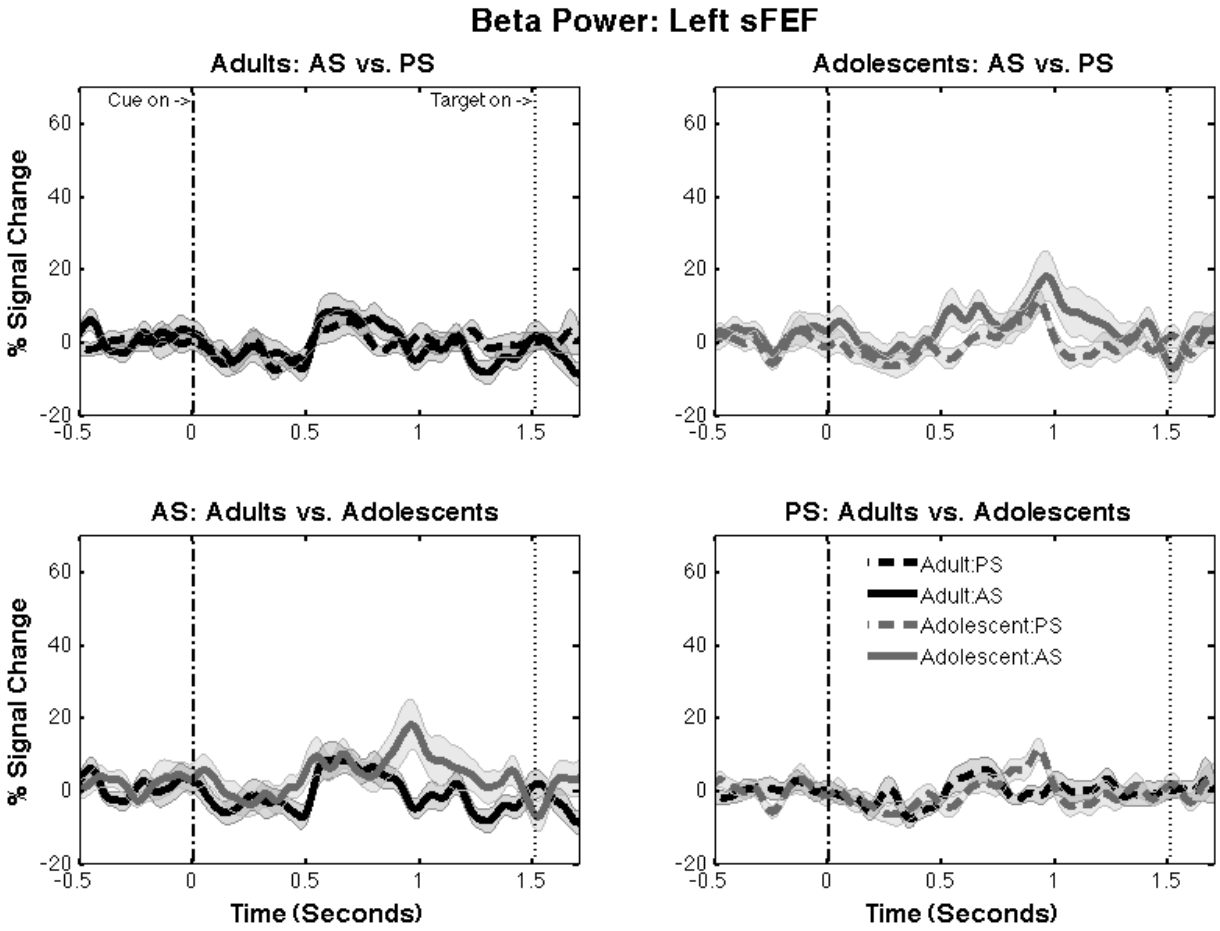

Figure 33. Beta-band power in the left sFEF.
Y scale is percent signal change from baseline. Shaded areas indicating one *SE*. X axis indicates the time since cue onset. From zero to 1.5 seconds is the preparatory period. Horizontal bar indicates task period that showed significant difference between conditions or age groups ($p < .05$ corrected). Only correct trials were analyzed.

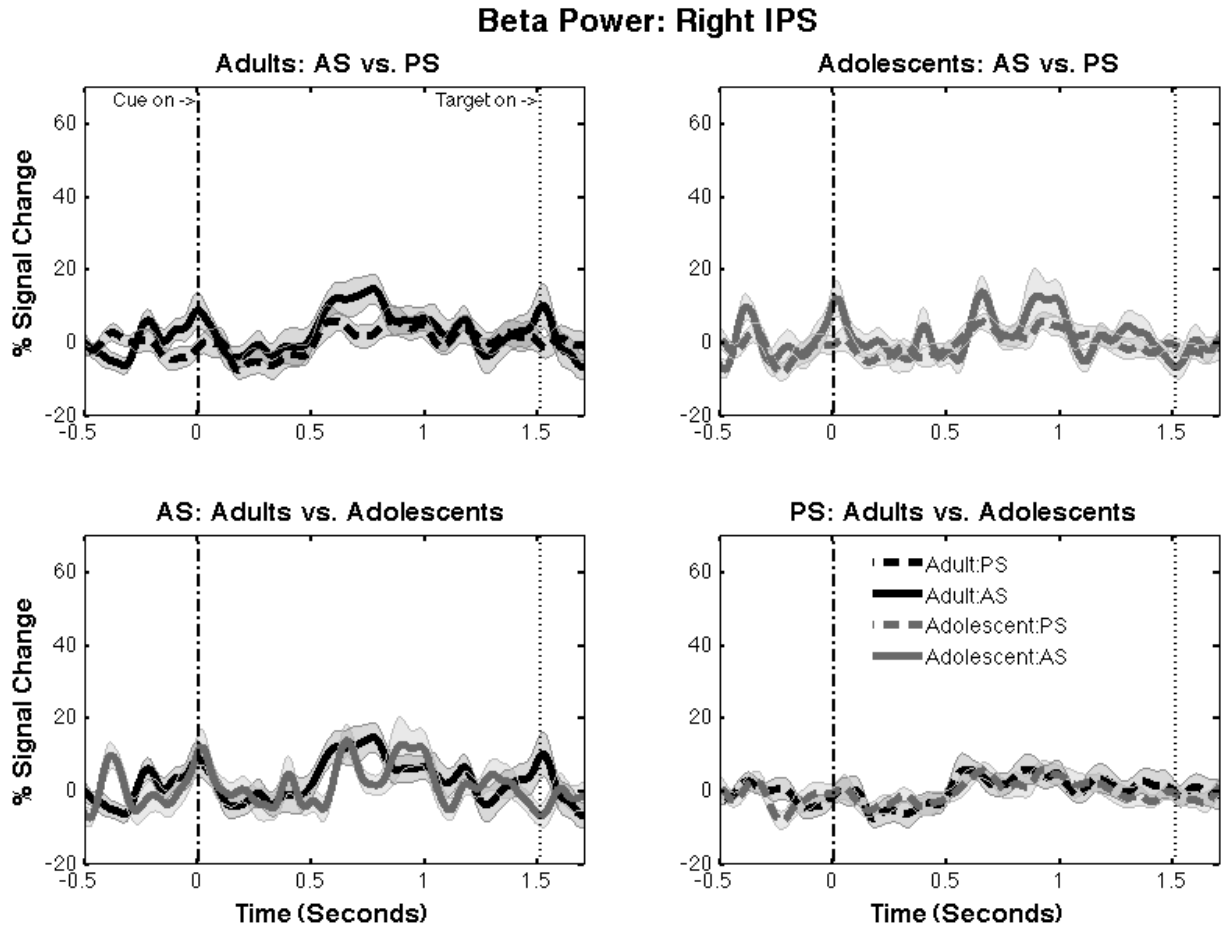

Figure 34. Beta-band power in the right IPS.
Y scale is percent signal change from baseline. Shaded areas indicating one *SE*. X axis indicates the time since cue onset. From zero to 1.5 seconds is the preparatory period. Horizontal bar indicates task period that showed significant difference between conditions or age groups ($p < .05$ corrected). Only correct trials were analyzed.

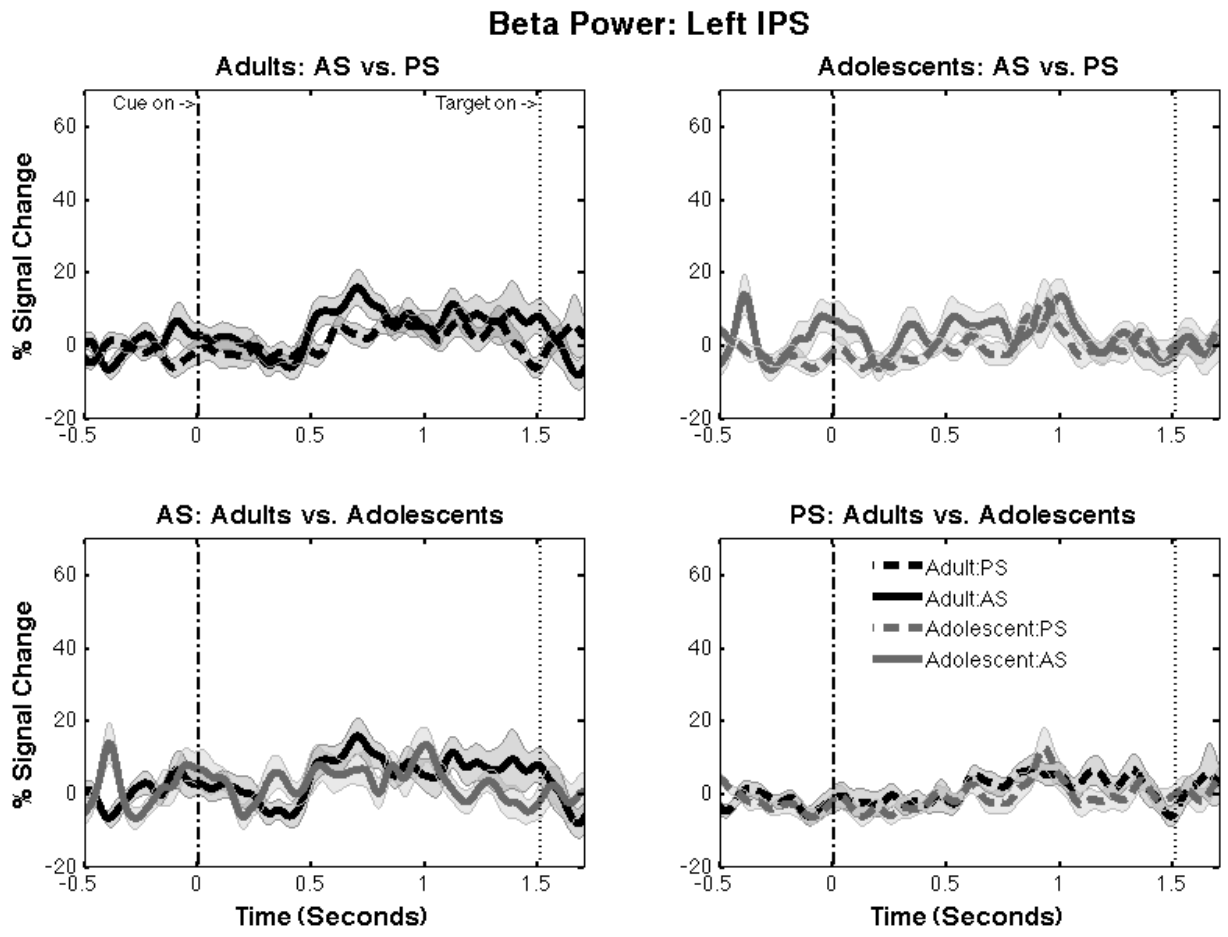

Figure 35. Beta-band power in the left IPS.
Y scale is percent signal change from baseline. Shaded areas indicating one *SE*. X axis indicates the time since cue onset. From zero to 1.5 seconds is the preparatory period. Horizontal bar indicates task period that showed significant difference between conditions or age groups ($p < .05$ corrected). Only correct trials were analyzed.

APPENDIX B

ALPHA POWER IN THE RIGHT PFC ROIS

Statistically significant task-related and age-related modulations in alpha-band power were only observed in oculomotor ROIs. For completeness, alpha-band power timecourses from the right PFC ROIs are presented in this appendix.

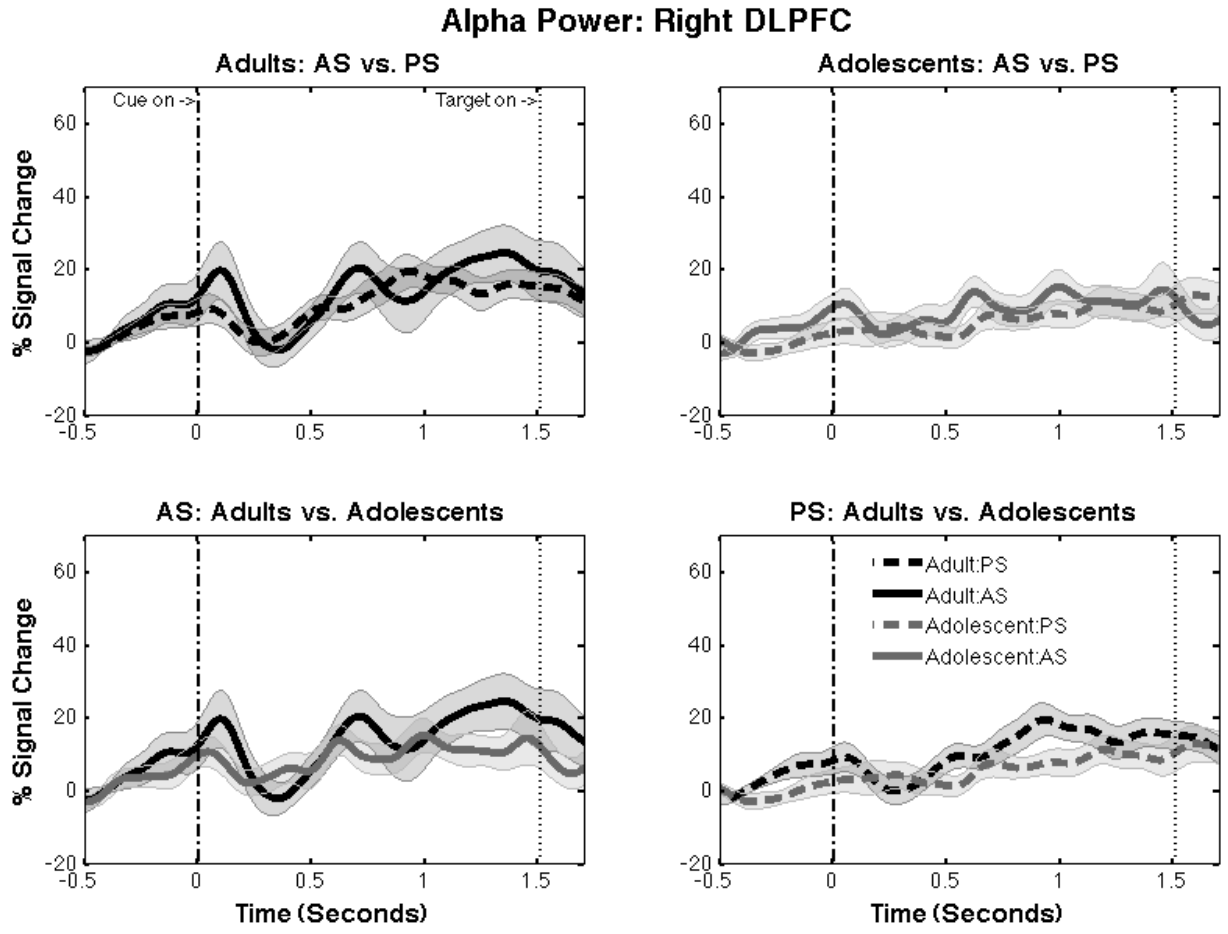

Figure 36. Alpha-band power in the right DLPFC.
Y scale is percent signal change from baseline. Shaded areas indicating one *SE*. X axis indicates the time since cue onset. From zero to 1.5 seconds is the preparatory period. Horizontal bar indicates task period that showed significant difference between conditions or age groups ($p < .05$ corrected). Only correct trials were analyzed.

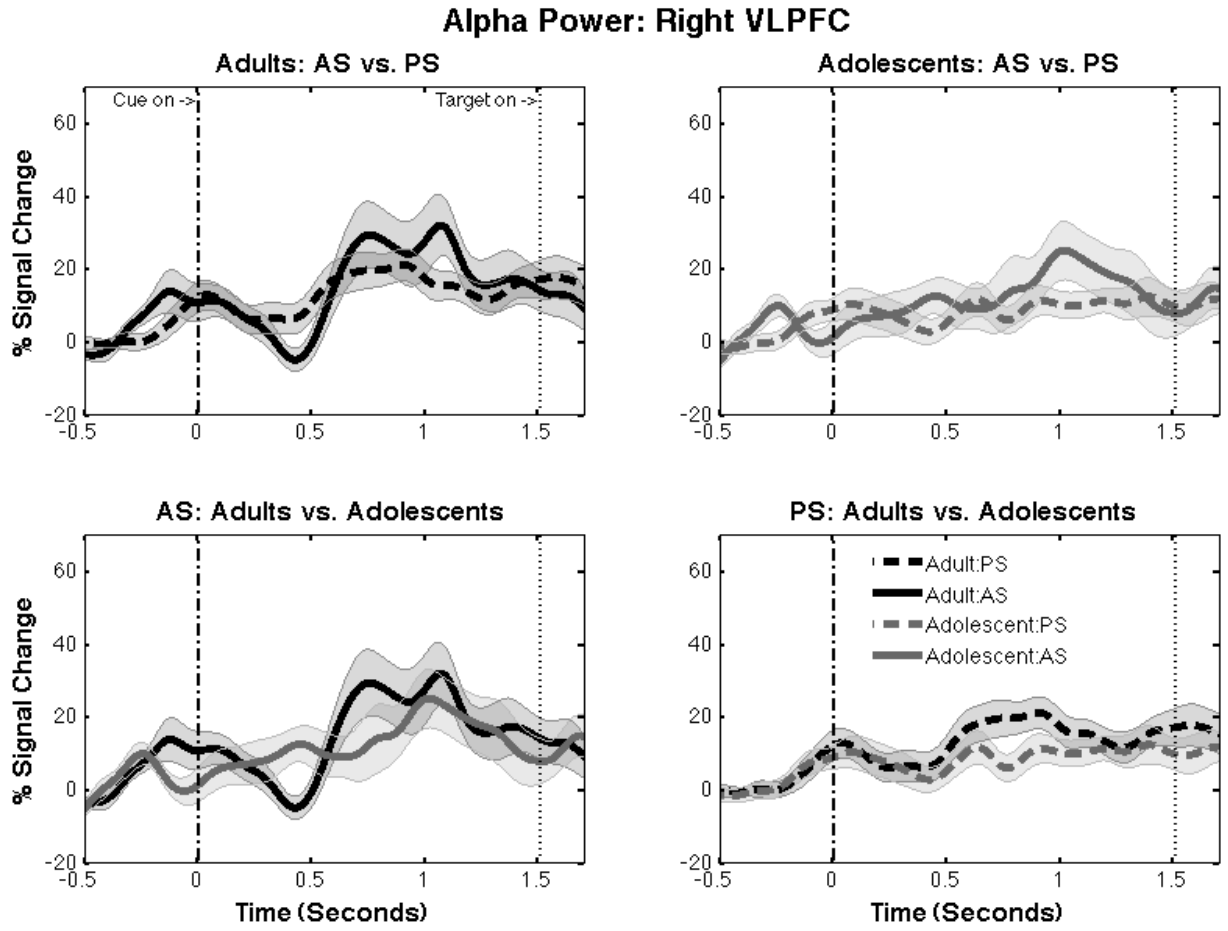

Figure 37. Alpha-band power in the right VLPFC.
Y scale is percent signal change from baseline. Shaded areas indicating one *SE*. X axis indicates the time since cue onset. From zero to 1.5 seconds is the preparatory period. Horizontal bar indicates task period that showed significant difference between conditions or age groups (p <.05 corrected). Only correct trials were analyzed.

APPENDIX C

CONTRASTING ALPHA-BAND POWER DURING DIFFERENT PARTS OF THE TESTING

Here we present results contrasting alpha-band power during the first half of the testing session, versus the second half. No significant differences were found. Specifically, alpha-band power timecourses of AS trials from the first half of the testing were not statistically different when compared to the second half of the testing, for both adults and adolescents.

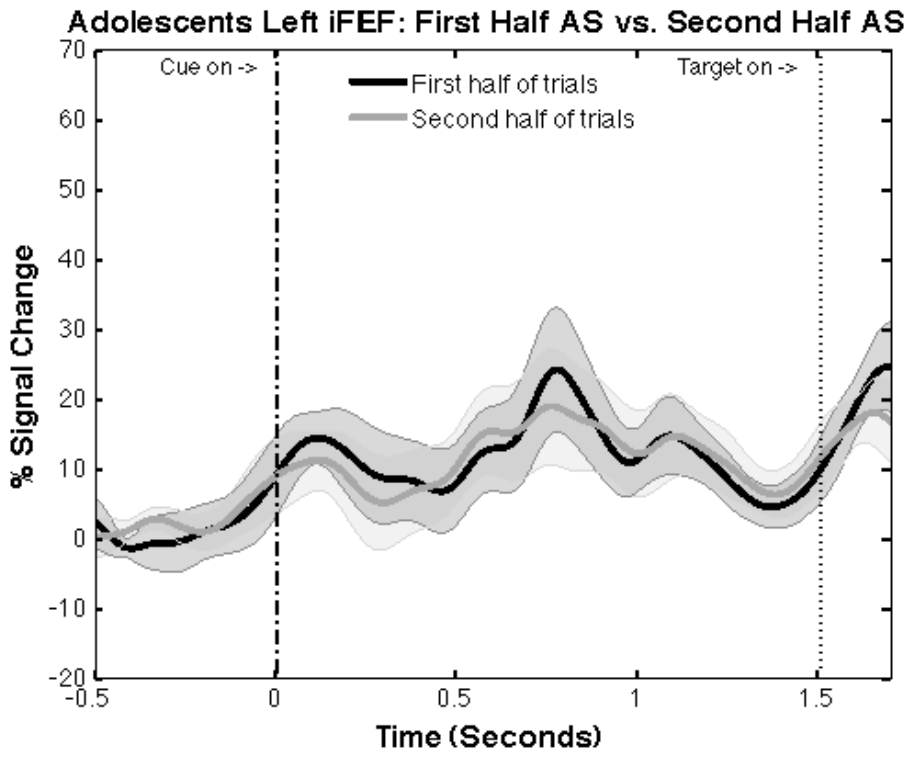

Figure 38. Adolescents' alpha-band power timecourses during different halfs of the testing. Y scale is percent signal change from baseline. Shaded areas indicating one *SE*. X axis indicates the time since cue onset. From zero to 1.5 seconds is the preparatory period. Horizontal bar indicates task period that showed significant difference between conditions or age groups ($p < .05$ corrected). Only correct trials were analyzed.

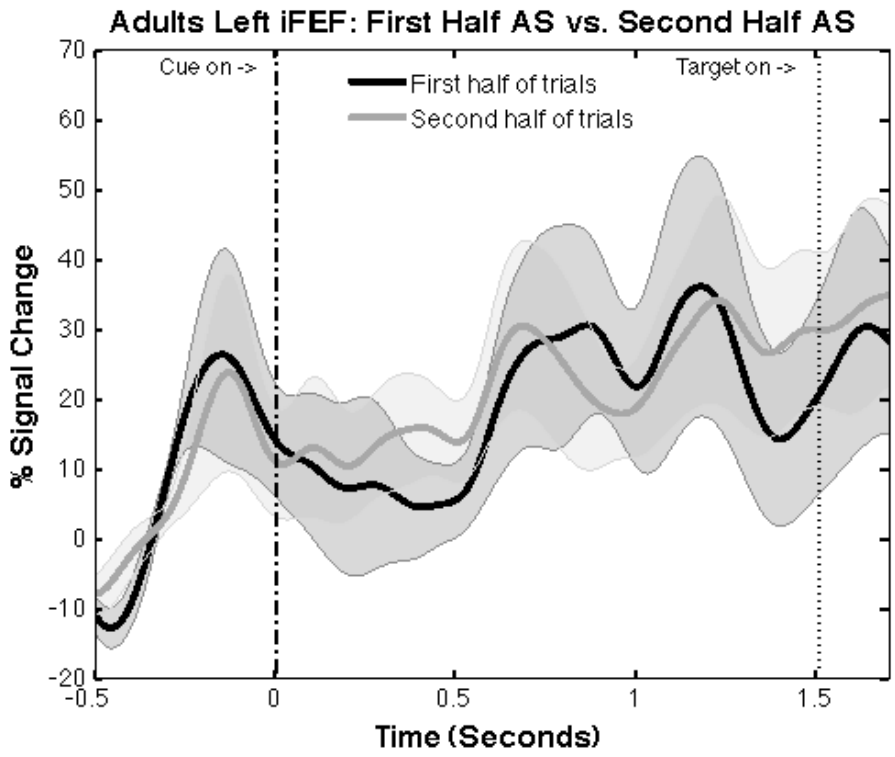

Figure 39. Adults' alpha-band power timecourses during different halfs of the testing.
Y scale is percent signal change from baseline. Shaded areas indicating one *SE*. X axis indicates the time since cue onset. From zero to 1.5 seconds is the preparatory period. Horizontal bar indicates task period that showed significant difference between conditions or age groups (p <.05 corrected). Only correct trials were analyzed.

BIBLIOGRAPHY

Akaishi, R., Morishima, Y., Rajeswaren, V. P., Aoki, S., & Sakai, K. (2010). Stimulation of the frontal eye field reveals persistent effective connectivity after controlled behavior. *Journal of Neuroscience, 30*(12), 4295-4305.

Akam, T., & Kullmann, D. M. (2010). Oscillations and filtering networks support flexible routing of information. *Neuron, 67*(2), 308-320.

Alexander, G. E., DeLong, M. R., & Strick, P. L. (1986). Parallel organization of functionally segregated circuits linking basal ganglia and cortex. *Annual Review of Neuroscience, 9*, 357-381.

Amso, D., & Johnson, S. P. (2005). Selection and inhibition in infancy: evidence from the spatial negative priming paradigm. *Cognition, 95* (2), B27-B36.

Aron, A. R. (2011). From reactive to proactive and selective control: developing a richer model for stopping inappropriate responses. *Biological Psychiatry, 69*(12), 55-68.

Aron, A. R., Fletcher, P. C., Bullmore, E. T., Sahakian, B. J., & Robbins, T. W. (2003). Stop-signal inhibition disrupted by damage to right inferior frontal gyrus in humans. *Nature Neuroscience, 6*(2), 115-116.

Aron, A. R., Robbins, T. W., & Poldrack, R. A. (2004). Inhibition and the right inferior frontal cortex. *Trends in Cognitive Sciences, 8*(4), 170-177.

Asato, M. R., Terwilliger, R., Woo, J., & Luna, B. (2010). White matter development in adolescence: a DTI study. *Cerebral Cortex, 20*(9), 2122-2131.

Ashtari, M., Cervellione, K. L., Hasan, K. M., Wu, J., McIlree, C., Kester, H., et al. (2007). White matter development during late adolescence in healthy males: a cross-sectional diffusion tensor imaging study. *NeuroImage, 35* (2), 501-510.

Asplund, C. L., Todd, J. J., Snyder, A. P., & Marois, R. (2010). A central role for the lateral prefrontal cortex in goal-directed and stimulus-driven attention. *Nature Neuroscience, 13*(4), 507-512.

Badre, D., & D'Esposito, M. (2009). Is the rostro-caudal axis of the frontal lobe hierarchical? *Nature Reviews Neuroscience, 10*(9), 659-669.

Barnea-Goraly, N., Menon, V., Eckert, M., Tamm, L., Bammer, R., Karchemskiy, A., et al. (2005). White matter development during childhood and adolescence: a cross-sectional diffusion tensor imaging study. *Cerebral Cortex, 15* (12), 1848-1854.

Barton, J. J., Greenzang, C., Hefter, R., Edelman, J., & Manoach, D. S. (2006). Switching, plasticity, and prediction in a saccadic task-switch paradigm. *Experimental Brain Research, 168*(1-2), 76-87.

Bedard, A. C., Nichols, S., Barbosa, J. A., Schachar, R., Logan, G. D., & Tannock, R. (2002). The development of selective inhibitory control across the life span. *Developental Neuropsychology, 21*(1), 93-111.

Berman, R. A., Colby, C. L., Genovese, C. R., Voyvodic, J. T., Luna, B., Thulborn, K. R., et al. (1999). Cortical networks subserving pursuit and saccadic eye movements in humans: an fMRI study. *Human Brain Mapping, 8*, 209-225.

Bollimunta, A., Mo, J., Schroeder, C. E., & Ding, M. (2011). Neuronal mechanisms and attentional modulation of corticothalamic alpha oscillations. *Journal of Neuroscience, 31*(13), 4935-4943.

Bonnefond, M., & Jensen, O. (2012). Alpha oscillations serve to protect working memory maintenance against anticipated distracters. *Current Biology*.

Braver, T. S. (2012). The variable nature of cognitive control: a dual mechanisms framework. *Trends in Cognitive Sciences, 16*(2), 106-113.

Brown, M. R., Vilis, T., & Everling, S. (2007). Frontoparietal activation with preparation for antisaccades. *Journal of Neurophysiology, 98* (3), 1751-1762.

Buehlmann, A., & Deco, G. (2010). Optimal information transfer in the cortex through synchronization. *Plos Computational Biology, 6*(9).

Buffalo, E. A., Fries, P., Landman, R., Buschman, T. J., & Desimone, R. (2011). Laminar differences in gamma and alpha coherence in the ventral stream. *Proceedings of the National Academy of the United States of America, 108*(27), 11262-11267.

Bunge, S. A., Dudukovic, N. M., Thomason, M. E., Vaidya, C. J., & Gabrieli, J. D. E. (2002). Immature frontal lobe contributions to cognitive control in children: evidence from fMRI. *Neuron, 33*(2), 301-311.

Burchell, T. R., Faulkner, H. J., & Whittington, M. A. (1998). Gamma frequency oscillations gate temporally coded afferent inputs in the rat hippocampal slice. *Neuroscience Letters, 255*(3), 151-154.

Buschman, T. J., Denovellis, E. L., Diogo, C., Bullock, D., & Miller, E. K. (in press). Synrhonous oscillatory neural ensembles for rules in the prefrontal cortex. *Neuron*.

Buschman, T. J., & Miller, E. K. (2007). Top-down versus bottom-up control of attention in the prefrontal and posterior parietal cortices. *Science, 315*(5820), 1860-1862.

Buzsaki, G. (2006). *Rhythms of the brain*. Oxford ; New York: Oxford University Press.

Buzsaki, G., & Draguhn, A. (2004). Neuronal oscillations in cortical networks. *Science, 304*(5679), 1926-1929.

Canolty, R. T., Ganguly, K., Kennerley, S. W., Cadieu, C. F., Koepsell, K., Wallis, J. D., et al. (2010). Oscillatory phase coupling coordinates anatomically dispersed functional cell assemblies. *Proceedings of the National Academy of Sciences of the United States of America, 107*(40), 17356-17361.

Cardin, J., Carlén, M., Meletis, K., Knoblich, U., Zhang, F., Deisseroth, K., et al. (2009). Driving fast-spiking cells induces gamma rhythm and controls sensory responses. *Nature*.

Casey, B. J., Trainor, R. J., Orendi, J. L., Schubert, A. B., Lystrom, L. E., Giedd, J. N., et al. (1997). A developmental functional MRI study of prefrontal activation during performance of a go-no-go task. *Journal of Cognitive Neuroscience, 9*(6), 835-847.

Cicchetti, D., & Rogosch, F. A. (1999). Psychopathology as risk for adolescent substance use disorders: a developmental psychopathology perspective. *Journal of Clinical Child & Adolescent Psychology, 28*(3), 355-365.

Cicchetti, D., & Rogosch, F. A. (2002). A developmental psychopathology perspective on adolescence. *Journal of Consulting and Clinical Psychology, 70*(1), 6-20.

Cicchetti, D., & Toth, S. L. (1998). The development of depression in children and adolescents. *American Psychologist, 53*(2), 221-241.

Cohen, M. X. (2011). It's about time. *Frontiers in Human Neuroscience, 5*, 2.

Cole, M. W., Bagic, A., Kass, R., & Schneider, W. (2010). Prefrontal dynamics underlying rapid instructed task learning reverse with practice. *Journal of Neuroscience, 30*(42), 14245-14254.

Connolly, J. D., Goodale, M. A., Menon, R. S., & Munoz, D. P. (2002). Human fMRI evidence for the neural correlates of preparatory set. *Nature Neuroscience, 5*(12), 1345-1352.

Crone, E. A., & Dahl, R. E. (2012). Understanding adolescence as a period of social-affective engagement and goal flexibility. *Nature Reviews Neuroscience, 13*(9), 636-650.

Curtis, C. E. (2011). Testing animal models of human oculomotor control with neuroimaging. In S. P. Liversedge, I. D. Gilchrist & S. Everling (Eds.), *The Oxford Handbook of Eye Movements* (pp. 383-398). New York, NY: Oxford University Press.

Curtis, C. E., Cole, M. W., Rao, V. Y., & D'Esposito, M. (2005). Canceling planned action: an FMRI study of countermanding saccades. *Cerebral Cortex, 15* (9), 1281-1289.

Curtis, C. E., & D'Esposito, M. (2003a). Persistent activity in the prefrontal cortex during working memory. *Trends in Cognitive Sciences, 7*(9), 415-423.

Curtis, C. E., & D'Esposito, M. (2003b). Success and failure suppressing reflexive behavior. *Journal of Cognitive Neuroscience, 15*(3), 409-418.

Dalal, S. S., Baillet, S., Adam, C., Ducorps, A., Schwartz, D., Jerbi, K., et al. (2009). Simultaneous MEG and intracranial EEG recordings during attentive reading. *NeuroImage, 45*(4), 1289-1304.

Dale, A. M., Fischl, B., & Sereno, M. I. (1999). Cortical surface-based analysis. I. Segmentation and surface reconstruction. *NeuroImage, 9*(2), 179-194.

Dale, A. M., Liu, A. K., Fischl, B. R., Buckner, R. L., Belliveau, J. W., Lewine, J. D., et al. (2000). Dynamic statistical parametric mapping: combining fMRI and MEG for high-resolution imaging of cortical activity. *Neuron, 26*(1), 55-67.

Dale, A. M., & Sereno, M. I. (1993). Improved localizadon of cortical activity by combining EEG and MEG with MRI cortical surface reconstruction: a linear approach. *Journal of Cognitive Neuroscience, 5*(2), 162-176.

Delorme, A., & Makeig, S. (2004). EEGLAB: an open source toolbox for analysis of single-trial EEG dynamics including independent component analysis. *Journal of Neuroscience Methods, 134*(1), 9-21.

DeSouza, J., Menon, R., & Everling, S. (2003). Preparatory set associated with pro-saccades and anti-saccades in humans investigated with event-related fMRI. *Journal of Neurophysiology, 89*, 1016-1023.

Destrieux, C., Fischl, B., Dale, A., & Halgren, E. (2010). Automatic parcellation of human cortical gyri and sulci using standard anatomical nomenclature. *NeuroImage, 53*(1), 1-15.

Diamond, A. (1989). Developmental progression in human infants and infant monkeys, and the neural bases of, inhibitory control of reaching *The development and neural bases of higher cognitive functions*. New York: Academy of Science Press.

Donner, T. H., & Siegel, M. (2011). A framework for local cortical oscillation patterns. *Trends in Cognitive Sciences, 15*(5), 191-199.

Douglas, R. J., & Martin, K. A. (2004). Neuronal circuits of the neocortex. *Annual Review of Neuroscience, 27*, 419-451.

Durston, S., Thomas, K. M., Yang, Y. H., Ulug, A. M., Zimmerman, R. D., & Casey, B. J. (2002). A neural basis for the development of inhibitory control. *Developmental Science, 5*(4), F9-F16.

Dustman, R. E., Shearer, D. E., & Emmerson, R. Y. (1999). Life-span changes in EEG spectral amplitude, amplitude variability and mean frequency. *Clinical Neurophysiology, 110*(8), 1399-1409.

Erickson, S. L., & Lewis, D. A. (2002). Postnatal development of parvalbumin- and GABA transporter-immunoreactive axon terminals in monkey prefrontal cortex. *Journal of Comparative Neurology, 448*(2), 186-202.

Everling, S., Dorris, M. C., Klein, R. M., & Munoz, D. P. (1999). Role of primate superior colliculus in preparation and execution of anti-saccades and pro-saccades. *Journal of Neuroscience, 19*(7), 2740-2754.

Everling, S., Dorris, M. C., & Munoz, D. P. (1998). Reflex suppression in the anti-saccade task is dependent on prestimulus neural processes. *Journal of Neurophysiology, 80*, 1584-1589.

Everling, S., & Johnston, K. (2011). Frontal cortex and saccadic control. In S. P. Liversedge, I. D. Gilchrist & S. Everling (Eds.), *The Oxford handbook of eye movements* (pp. 279-302). Oxford ; New York: Oxford University Press.

Everling, S., & Munoz, D. P. (2000). Neuronal correlates for preparatory set associated with pro-saccades and anti-saccades in the primate frontal eye field. *Journal of Neuroscience, 20*(1), 387-400.

Fischer, B., Biscaldi, M., & Gezeck, S. (1997). On the development of voluntary and reflexive components in human saccade generation. *Brain Research, 754*(1-2), 285-297.

Fischer, B., & Boch, R. (1983). Saccadic eye movements after extremely short reaction times in monkey. *Brain Research, 260*, 21-26.

Fischl, B., Sereno, M. I., & Dale, A. M. (1999). Cortical surface-based analysis. II: Inflation, flattening, and a surface-based coordinate system. *Neuroimage, 9*(2), 195-207.

Ford, K. A., Goltz, H. C., Brown, M. R. G., & Everling, S. (2005). Neural processes associated with antisaccade task performance investigated with event-related FMRI. *Journal of Neurophysiology, 94*(1), 429-440.

Fries, P. (2005). A mechanism for cognitive dynamics: neuronal communication through neuronal coherence. *Trends in Cognitive Sciences, 9*(10), 474-480.

Fung, S. J., Webster, M. J., Sivagnanasundaram, S., Duncan, C., Elashoff, M., & Weickert, C. S. (2010). Expression of interneuron markers in the dorsolateral prefrontal cortex of the developing human and in schizophrenia. *American Journal of Psychiatry, 167*(12), 1479-1488.

Geier, C. F., & Luna, B. (2012). Developmental effects of incentives on response inhibition. *Child Development, 83*(4), 1262-1274.

Gentet, L. J., Kremer, Y., Taniguchi, H., Huang, Z. J., Staiger, J. F., & Petersen, C. C. (2012). Unique functional properties of somatostatin-expressing GABAergic neurons in mouse barrel cortex. *Nature Neuroscience, 15*(4), 607-612.

Ghuman, A. S., McDaniel, J. R., & Martin, A. (2011). A wavelet-based method for measuring the oscillatory dynamics of resting-state functional connectivity in MEG. *NeuroImage, 56*(1), 69-77.

Gitelman, D. R. (2002). ILAB: A program for postexperimental eye movement analysis. *Behavior Research Methods Instruments & Computers, 34*(4), 605-612.

Gogtay, N., Giedd, J. N., Lusk, L., Hayashi, K. M., Greenstein, D., Vaituzis, A. C., et al. (2004). Dynamic mapping of human cortical development during childhood through early

adulthood. *Proceedings of the National Academy of the United States of America, 101*(21), 8174-8179.

Gross, J., Schmitz, F., Schnitzler, I., Kessler, K., Shapiro, K., Hommel, B., et al. (2006). Anticipatory control of long-range phase synchronization. *European Journal of Neuroscience, 24*(7), 2057-2060.

Haegens, S., Nacher, V., Luna, R., Romo, R., & Jensen, O. (2011). Alpha-Oscillations in the monkey sensorimotor network influence discrimination performance by rhythmical inhibition of neuronal spiking. *Proceedings of the National Academy of Sciences of the United States of America, 108*(48), 19377-19382.

Haider, B., & McCormick, D. A. (2009). Rapid neocortical dynamics: cellular and network mechanisms. *Neuron, 62*(2), 171-189.

Hallett, P. E. (1978). Primary and secondary saccades to goals defined by instructions. *Vision Research, 18*, 1279-1296.

Hamalainen, M. S. (2010). MNE software user's guide. Massachusetts General Hospital.

Hamalainen, M. S., Hari, R., Ilmoniemi, R. J., Knuutila, J., & Lounasmaa, O. V. (1993). Magnetoencephalography-theory, instrumentation, and applications to noninvasive studies of the working human brain. *Reviews of Modern Physics, 65*(2), 413-497.

Hamalainen, M. S., & Ilmoniemi, R. J. (1994). Interpreting magnetic fields of the brain: minimum norm estimates. *Medical & Biological Engineering & Computing, 32*(1), 35-42.

Hamalainen, M. S., Lin, F. H., & Mosher, J. C. (2010). Anatomically and functionally constrained minimum-norm estimates. In P. C. Hansen, M. L. Kringelbach & R. Salmelin (Eds.), *MEG : an introduction to methods* (pp. 186-215). New York: Oxford University Press.

Hamalainen, M. S., & Sarvas, J. (1989). Realistic conductivity geometry model of the human head for interpretation of neuromagnetic data. *IEEE Transactions on Biomedical Engineering, 36*(2), 165-171.

Handel, B. F., Haarmeier, T., & Jensen, O. (2011). Alpha oscillations correlate with the successful inhibition of unattended stimuli. *Journal of Cognitive Neuroscience, 23*(9), 2494-2502.

Hanes, D. P., & Schall, J. D. (1996). Neural control of voluntary movement initiation. *Science, 274*, 427-430.

Hashimoto, T., Nguyen, Q. L., Rotaru, D., Keenan, T., Arion, D., Beneyto, M., et al. (2009). Protracted developmental trajectories of GABAA receptor alpha1 and alpha2 subunit expression in primate prefrontal cortex. *Biological Psychiatry, 65*(12), 1015-1023.

He, B. J., Zempel, J. M., Snyder, A. Z., & Raichle, M. E. (2010). The temporal structures and functional significance of scale-free brain activity. *Neuron, 66*(3), 353-369.

Hikosaka, O., Takikawa, Y., & Kawagoe, R. (2000). Role of the basal ganglia in the control of purposive saccadic eye movements. *Physiological Reviews, 80* (3), 953-978.

Hipp, J. F., Engel, A. K., & Siegel, M. (2011). Oscillatory synchronization in large-scale cortical networks predicts perception. *Neuron, 69*(2), 387-396.

Hodgson, T., Chamberlain, M., Parris, B., James, M., Gutowski, N., Husain, M., et al. (2007). The role of the ventrolateral frontal cortex in inhibitory oculomotor control. *Brain, 130*(Pt 6), 1525-1537.

Howard, M. W., Rizzuto, D. S., Caplan, J. B., Madsen, J. R., Lisman, J., Aschenbrenner-Scheibe, R., et al. (2003). Gamma oscillations correlate with working memory load in humans. *Cerebral Cortex, 13*(12), 1369-1374.

Hughes, S. W., & Crunelli, V. (2005). Thalamic mechanisms of EEG alpha rhythms and their pathological implications. *The Neuroscientist, 11*(4), 357-372.

Huttenlocher, P. R. (1979). Synaptic density in human frontal cortex - developmental changes and effects of aging. *Brain Research, 163*(2), 195-205.

Huttenlocher, P. R., & Dabholkar, A. S. (1997). Regional differences in synaptogenesis in human cerebral cortex. *Journal of Comparative Neurology, 387*(2), 167-178.

Huttenlocher, P. R., de Courten, C., Garey, L. J., & Van der Loos, H. (1982). Synaptogenesis in human visual cortex--evidence for synapse elimination during normal development. *Neuroscience Letters, 33*(3), 248-252.

Hwang, K., & Luna, B. (2012). The development of brain connectivity supporting prefrontal cortical functions. In D. T. Stuss & R. T. Knight (Eds.), *Principles of Frontal Lobe Function, 2nd Edition*. New York, NY: Oxford University Press.

Hwang, K., Velanova, K., & Luna, B. (2010). Strengthening of top-down frontal cognitive control networks underlying the development of inhibitory control: a functional magnetic resonance imaging effective connectivity study. *Journal of Neuroscience, 30*(46), 15535-15545.

Jensen, O., & Hesse, C. (2010). Estimating distributed representations of evoked responses and oscillatory brain activity. In P. C. Hansen, M. L. Kringelbach & R. Salmelin (Eds.), *MEG : an introduction to methods* (pp. 156-185). New York: Oxford University Press.

Jensen, O., Kaiser, J., & Lachaux, J.-P. (2007). Human gamma-frequency oscillations associated with attention and memory. *Trends in Neurosciences, 30*(7), 317-324.

Jensen, O., & Mazaheri, A. (2010). Shaping functional architecture by oscillatory alpha activity: gating by inhibition. *Frontiers in Human Neuroscience, 4*, 186.

Jones, S. R., Kerr, C. E., Wan, Q., Pritchett, D. L., Hamalainen, M., & Moore, C. I. (2010). Cued spatial attention drives functionally relevant modulation of the mu rhythm in primary somatosensory cortex. *Journal of Neuroscience, 30*(41), 13760-13765.

Jones, S. R., Pritchett, D. L., Sikora, M. A., Stufflebeam, S. M., Hamalainen, M., & Moore, C. I. (2009). Quantitative analysis and biophysically realistic neural modeling of the MEG mu rhythm: rhythmogenesis and modulation of sensory-evoked responses. *Journal of Neurophysiology, 102*(6), 3554-3572.

Kaas, J. H. (2010). Cortical circuits: Consistency and variability across cortical areas and species. In C. v. d. Malsburg, W. A. Phillips & W. Singer (Eds.), *Dynamic coordination in the brain : from neurons to mind* (pp. 25-36). Cambridge, Mass.: MIT Press.

Klein, C., & Foerster, F. (2001). Development of prosaccade and antisaccade task performance in participants aged 6 to 26 years. *Psychophysiology, 38*(2), 179-189.

Klein, C., Foerster, F., Hartnegg, K., & Fischer, B. (2005). Lifespan development of pro- and anti-saccades: multiple regression models for point estimates. *Developmental Brain Research, 160* (2), 113-123.

Klimesch, W., Sauseng, P., & Hanslmayr, S. (2007). EEG alpha oscillations: the inhibition-timing hypothesis. *Brain research reviews, 53*(1), 63-88.

Kopell, N., Ermentrout, G. B., Whittington, M. A., & Traub, R. D. (2000). Gamma rhythms and beta rhythms have different synchronization properties. *Proceedings of the National Academy of the United States of America, 97*(4), 1867-1872.

Kopell, N., Kramer, M. A., Malerba, P., & Whittington, M. A. (2010). Are different rhythms good for different functions? *Frontiers in Human Neuroscience, 4*, 187.

Koval, M. J., Lomber, S. G., & Everling, S. (2011). Prefrontal cortex deactivation in macaques alters activity in the superior colliculus and impairs voluntary control of saccades. *Journal of Neuroscience, 31*(23), 8659-8668.

Lachaux, J. P., Rodriguez, E., Martinerie, J., & Varela, F. J. (1999). Measuring phase synchrony in brain signals. *Human Brain Mapping, 8*(4), 194-208.

Lakatos, P., Karmos, G., Mehta, A., Ulbert, I., & Schroeder, C. (2008). Entrainment of neuronal oscillations as a mechanism of attentional selection. *Science, 320*(5872), 110-113.

Lakatos, P., Shah, A. S., Knuth, K. H., Ulbert, I., Karmos, G., & Schroeder, C. E. (2005). An oscillatory hierarchy controlling neuronal excitability and stimulus processing in the auditory cortex. *Journal of Neurophysiology, 94*(3), 1904-1911.

Lebel, C., Walker, L., Leemans, A., Phillips, L., & Beaulieu, C. (2008). Microstructural maturation of the human brain from childhood to adulthood. *NeuroImage, 140* (3), 1044-1055.

Lee, A. K., Hamalainen, M. S., Dyckman, K. A., Barton, J. J., & Manoach, D. S. (2010). Saccadic preparation in the frontal eye field Is modulated by distinct trial history effects as revealed by magnetoencephalography. *Cerebral Cortex*.

Levy, B. J., & Wagner, A. D. (2011). Cognitive control and right ventrolateral prefrontal cortex: reflexive reorienting, motor inhibition, and action updating. *Annals of the New York Academy of Sciences, 1224*, 40-62.

Lewis, D. A., & Melchitzky, D. (2012). Postnatal development of neural circuits in the primate prefrontal cortex. In D. T. Stuss & R. T. Knight (Eds.), *Principles of Frontal Lobe Function, 2nd Edition*. New York, NY: Oxford University Press.

Lin, F. H., Belliveau, J. W., Dale, A. M., & Hamalainen, M. S. (2006). Distributed current estimates using cortical orientation constraints. *Human Brain Mapping, 27*(1), 1-13.

Lin, F. H., Witzel, T., Hämäläinen, M. S., Dale, A. M., Belliveau, J. W., & Stufflebeam, S. M. (2004). Spectral spatiotemporal imaging of cortical oscillations and interactions in the human brain. *NeuroImage, 23*(2), 582-595.

Logothetis, N. K. (2008). What we can do and what we cannot do with fMRI. *Nature, 453* (7197), 869-878.

Logothetis, N. K., Paulsen, J., Augath, M., Trinath, T., & Oeltermann, A. (2001). Neurophysiological investigation of the basis of the fMRI signal. *Nature, 412*, 150-157.

Lopes da Silva, F. H. (2010). Electrophysiological basis of MEG signals. In P. C. Hansen, M. L. Kringelbach & R. Salmelin (Eds.), *MEG : an introduction to methods* (pp. 1-23). New York: Oxford University Press.

Luna, B., Garver, K. E., Urban, T. A., Lazar, N. A., & Sweeney, J. A. (2004). Maturation of cognitive processes from late childhood to adulthood. *Child Development, 75*(5), 1357-1372.

Luna, B., Padmanabhan, A., & O'Hearn, K. (2010). What has fMRI told us about the development of cognitive control through adolescence? *Brain and Cognition, 72*(1), 101-113.

Luna, B., & Sweeney, J. A. (2004). The emergence of collaborative brain function: fMRI studies of the development of response inhibition. *Annals of the New York Academy of Sciences, 1021*(1), 296-309.

Luna, B., Thulborn, K. R., Munoz, D. P., Merriam, E. P., Garver, K. E., Minshew, N. J., et al. (2001). Maturation of widely distributed brain function subserves cognitive development. *NeuroImage, 13*(5), 786-793.

Luna, B., Thulborn, K. R., Strojwas, M. H., McCurtain, B. J., Berman, R. A., Genovese, C. R., et al. (1998). Dorsal cortical regions subserving visually-guided saccades in humans: an fMRI study. *Cerebral Cortex, 8*, 40-47.

Luna, B., Velanova, K., & Geier, C. F. (2010). Methodological approaches in developmental neuroimaging studies. *Human Brain Mapping, 31*(6), 863-871.

Maris, E., & Oostenveld, R. (2007). Nonparametric statistical testing of EEG- and MEG-data. *Journal of Neuroscience Methods, 164*(1), 177-190.

Miller, E. K., & Cohen, J. D. (2001). An integrative theory of prefrontal cortex function. *Annual Review of Neuroscience, 24*, 167-202.

Moon, S., Barton, J., Mikulski, S., Polli, F., Cain, M., Vangel, M., et al. (2007). Where left becomes right: A magnetoencephalographic study of sensorimotor transformation for antisaccades. *NeuroImage, 36*(4), 1313-1323.

Moore, C. I., Carlen, M., Knoblich, U., & Cardin, J. A. (2010). Neocortical interneurons: from diversity, strength. *Cell, 142*(2), 189-193.

Mountcastle, V. B. (1997). The columnar organization of the neocortex. *Brain, 120*(4), 701-722.

Muller, V., Gruber, W., Klimesch, W., & Lindenberger, U. (2009). Lifespan differences in cortical dynamics of auditory perception. *Developmental Science, 12*(6), 839-853.

Munoz, D. P., Broughton, J. R., Goldring, J. E., & Armstrong, I. T. (1998). Age-related performance of human subjects on saccadic eye movement tasks. *Experimental Brain Research, 121*(4), 391-400.

Munoz, D. P., & Everling, S. (2004). Look away: the anti-saccade task and the voluntary control of eye movement. *Nature Reviews Neuroscience, 5*(3), 218-228.

Nenonen, J., Nurminen, J., Kicic, D., Bikmullina, R., Lioumis, P., Jousmaki, V., et al. (2012). Validation of head movement correction and spatiotemporal signal space separation in magnetoencephalography. *Clinical Neurophysiology, 123*(11), 2180-2191.

Oostenveld, R., Fries, P., Maris, E., & Schoffelen, J. M. (2011). FieldTrip: Open source software for advanced analysis of MEG, EEG, and invasive electrophysiological data. *Computational Intelligence and Neuroscience, 2011*, 156869.

Ordaz, S., Davis, S., & Luna, B. (2010). Effects of response preparation on developmental improvements in inhibitory control. *ACTA Psychologica (Amsterdam), 134*(3), 253-263.

Palva, J. M., Monto, S., Kulashekhar, S., & Palva, S. (2010). Neuronal synchrony reveals working memory networks and predicts individual memory capacity. *Proceedings of the National Academy of Sciences of the United States of America, 107*(16), 7580-7585.

Palva, S., & Palva, J. M. (2007). New vistas for alpha-frequency band oscillations. *Trends in Neurosciences, 30*(4), 150-158.

Palva, S., & Palva, J. M. (2012). Discovering oscillatory interaction networks with M/EEG: challenges and breakthroughs. *Trends in Cognitive Sciences, 16*(4), 219-230.

Pesaran, B., Nelson, M. J., & Andersen, R. A. (2008). Free choice activates a decision circuit between frontal and parietal cortex. *Nature, 453*(7193), 406-409.

Pesaran, B., Pezaris, J. S., Sahani, M., Mitra, P. P., & Andersen, R. A. (2002). Temporal structure in neuronal activity during working memory in macaque parietal cortex. *Nature Neuroscience, 5*(8), 805-811.

Pfurtscheller, G., & Lopes da Silva, F. H. (1999). Event-related EEG/MEG synchronization and desynchronization: basic principles. *Clinical Neurophysiology, 110*(11), 1842-1857.

Pierrot-Deseilligny, C., Muri, R. M., Ploner, C. J., Gaymard, B., Demeret, S., & Rivaud-Pechoux, S. (2003). Decisional role of the dorsolateral prefrontal cortex in ocular motor behaviour. *Brain, 126*(Pt 6), 1460-1473.

Pierrot-Deseilligny, C., Rivaud, S., Gaymard, B., & Agid, Y. (1991). Cortical control of reflexive visually-guided saccades. *Brain, 114 (Pt 3)*, 1473-1485.

Rakic, P., Bourgeois, J. P., Eckenhoff, M. F., Zecevic, N., & Goldman-Rakic, P. S. (1986). Concurrent overproduction of synapses in diverse regions of the primate cerebral cortex. *Science, 232*, 232-235.

Resnick, M. D., Bearman, P. S., Blum, R. W., Bauman, K. E., Harris, K. M., Jones, J., et al. (1997). Protecting adolescents from harm. Findings from the national longitudinal study on adolescent health. *Journal of American Medical Association, 278*(10), 823-832.

Rodriguez, E., George, N., Lachaux, J. P., Martinerie, J., Renault, B., & Varela, F. J. (1999). Perception's shadow: long-distance synchronization of human brain activity. *Nature, 397*(6718), 430-433.

Roebroeck, A., Formisano, E., & Goebel, R. (2005). Mapping directed influence over the brain using Granger causality and fMRI. *NeuroImage, 25*(1), 230-242.

Roopun, A. K., Lebeau, F. E., Ramell, J., Cunningham, M. O., Traub, R. D., & Whittington, M. A. (2010). Cholinergic neuromodulation controls directed temporal communication in neocortex in vitro. *Frontiers in Neural Circuits, 4*, 8.

Roux, F., Wibral, M., Mohr, H. M., Singer, W., & Uhlhaas, P. J. (2012). Gamma-band activity in human prefrontal cortex codes for the number of relevant items maintained in working memory. *Journal of Neuroscience, 32*(36), 12411-12420.

Rubia, K., Smith, A. B., Brammer, M. J., & Taylor, E. (2003). Right inferior prefrontal cortex mediates response inhibition while mesial prefrontal cortex is responsible for error detection. *NeuroImage, 20*(1), 351-358.

Rubia, K., Smith, A. B., Taylor, E., & Brammer, M. (2007). Linear age-correlated functional development of right inferior fronto-striato-cerebellar networks during response inhibition and anterior cingulate during error-related processes. *Human Brain Mapping, 28*(11), 1163-1177.

Rubia, K., Smith, A. B., Woolley, J., Nosarti, C., Heyman, I., Taylor, E., et al. (2006). Progressive increase of frontostriatal brain activation from childhood to adulthood during event-related tasks of cognitive control. *Human Brain Mapping, 27*(12), 973-993.

Saalmann, Y. B., Pigarev, I. N., & Vidyasagar, T. R. (2007). Neural mechanisms of visual attention: how top-down feedback highlights relevant locations. *Science, 316*(5831), 1612-1615.

Saalmann, Y. B., Pinsk, M. A., Wang, L., Li, X., & Kastner, S. (2012). The pulvinar regulates information transmission between cortical areas based on attention demands. *Science, 337*(6095), 753-756.

Sakai, K. (2008). Task set and prefrontal cortex. *Annual Review of Neuroscience, 31*, 219-245.

Scheeringa, R., Fries, P., Petersson, K. M., Oostenveld, R., Grothe, I., Norris, D. G., et al. (2011). Neuronal dynamics underlying high- and low-frequency EEG oscillations contribute independently to the human BOLD signal. *Neuron, 69*(3), 572-583.

Schlag-Rey, M., Amador, N., Sanchez, H., & Schlag, J. (1997). Antisaccade performance predicted by neuronal activity in the supplementary eye field. *Nature, 390*(6658), 398-401.

Schmithorst, V. J., Wilke, M., Dardzinski, B. J., & Holland, S. K. (2002). Correlation of white matter diffusivity and anisotropy with age during childhood and adolescence: a cross-sectional diffusion-tensor MR imaging study. *Radiology, 222*(1), 212-218.

Schoffelen, J.-M., & Gross, J. (2009). Source connectivity analysis with MEG and EEG. *Human Brain Mapping, 30*(6), 1857-1865.

Schulman, J. J., Cancro, R., Lowe, S., Lu, F., Walton, K. D., & Llinas, R. R. (2011). Imaging of thalamocortical dysrhythmia in neuropsychiatry. *Frontiers in Human Neuroscience, 5*, 69.

Sherman, S. M., & Guillery, R. W. (2011). Distinct functions for direct and transthalamic corticocortical connections. *Journal of Neurophysiology, 106*(3), 1068-1077.

Siegel, M., Donner, T. H., & Engel, A. K. (2012). Spectral fingerprints of large-scale neuronal interactions. *Nature Reviews Neuroscience, 13*(2), 121-134.

Siegel, M., Donner, T. H., Oostenveld, R., Fries, P., & Engel, A. K. (2008). Neuronal synchronization along the dorsal visual pathway reflects the focus of spatial attention. *Neuron, 60*(4), 709-719.

Sohal, V. S., Zhang, F., Yizhar, O., & Deisseroth, K. (2009). Parvalbumin neurons and gamma rhythms enhance cortical circuit performance. *Nature, 459*(7247), 698-702.

Song, S. K., Sun, S. W., Ramsbottom, M. J., Chang, C., Russell, J., & Cross, A. H. (2002). Dysmyelination revealed through MRI as increased radial (but unchanged axial) diffusion of water. *NeuroImage, 17*(3), 1429-1436.

Song, S. K., Yoshino, J., Le, T. Q., Lin, S. J., Sun, S. W., Cross, A. H., et al. (2005). Demyelination increases radial diffusivity in corpus callosum of mouse brain. *NeuroImage, 26* (1), 132-140.

Spear, L. P. (2000). Neurobehavioral changes in adolescence. *Current Directions in Psychological Science, 9*(4), 111-114.

Steinberg, L., Albert, D., Cauffman, E., Banich, M., Graham, S., & Woolard, J. (2008). Age differences in sensation seeking and impulsivity as indexed by behavior and self-report: evidence for a dual systems model. *Developmental Psychology, 44*(6), 1764-1778.

Steriade, M., Gloor, P., Llinas, R. R., Lopes de Silva, F. H., & Mesulam, M. M. (1990). Report of IFCN Committee on Basic Mechanisms. Basic mechanisms of cerebral rhythmic activities. *Electroencephalography and Clinical Neurophysiology, 76*(6), 481-508.

Stufflebeam, S., Witzel, T., Mikulski, S., Hamalainen, M., Temereanca, S., Barton, J., et al. (2008). A non-invasive method to relate the timing of neural activity to white matter microstructural integrity. *NeuroImage, 42*(2), 710-716.

Swann, N., Tandon, N., Canolty, R., Ellmore, T. M., McEvoy, L. K., Dreyer, S., et al. (2009). Intracranial EEG reveals a time- and frequency-specific role for the right inferior frontal gyrus and primary motor cortex in stopping initiated responses. *Journal of Neuroscience, 29*(40), 12675-12685.

Swann, N., Tandon, N., Pieters, T. A., & Aron, A. R. (2012). Intracranial electroencephalography reveals different temporal profiles for dorsal- and ventro-lateral prefrontal cortex in preparing to stop action. *Cerebral Cortex*.

Sweeney, J. A., Levy, D., & Harris, M. S. H. (2002). Commentary: eye movement research with clinical populations. *Progress in Brain Research, 140*, 507-522.

Sweeney, J. A., Takarae, Y., Macmillan, C., Luna, B., & Minshew, N. J. (2004). Eye movements in neurodevelopmental disorders. *Current Opinion in Neurology, 17*(37-42).

Tallon-Baudry, C., Bertrand, O., Delpuech, C., & Permier, J. (1997). Oscillatory gamma-band (30-70 Hz) activity induced by a visual search task in humans. *Journal of Neuroscience, 17*(2), 722-734.

Tamm, L., Menon, V., & Reiss, A. L. (2002). Maturation of brain function associated with response inhibition. *J Am Acad Child Adolesc Psychiatry, 41*(10), 1231-1238.

Tan, Z., Hu, H., Huang, Z. J., & Agmon, A. (2008). Robust but delayed thalamocortical activation of dendritic-targeting inhibitory interneurons. *Proceedings of the National Academy of the United States of America, 105*(6), 2187-2192.

Taulu, S., & Hari, R. (2009). Removal of magnetoencephalographic artifacts with temporal signal-space separation: demonstration with single-trial auditory-evoked responses. *Human Brain Mapping, 30*(5), 1524-1534.

Taulu, S., Kajola, M., & Simola, J. (2004). Suppression of interference and artifacts by the Signal Space Separation Method. *Brain Topography, 16*(4), 269-275.

Temereanca, S., Hamalainen, M. S., Kuperberg, G. R., Stufflebeam, S. M., Halgren, E., & Brown, E. N. (2012). Eye movements modulate the spatiotemporal dynamics of word processing. *Journal of Neuroscience, 32*(13), 4482-4494.

Thatcher, R. W., North, D. M., & Biver, C. J. (2008). Development of cortical connections as measured by EEG coherence and phase delays. *Human Brain Mapping, 29*(12), 1400-1415.

Thatcher, R. W., Walker, R. A., & Giudice, S. (1987). Human cerebral hemispheres develop at different rates and ages. *Science, 236*, 1110-1113.

Thut, G., Nietzel, A., Brandt, S. A., & Pascual-Leone, A. (2006). Alpha-band electroencephalographic activity over occipital cortex indexes visuospatial attention bias and predicts visual target detection. *Journal of Neuroscience, 26*(37), 9494-9502.

Uhlhaas, P. J., Roux, F., Singer, W., Haenschel, C., Sireteanu, R., & Rodriguez, E. (2009). The development of neural synchrony reflects late maturation and restructuring of functional networks in humans. *Proceedings of the National Academy of Sciences of the United States of America, 106*(24), 9866-9871.

Uhlhaas, P. J., & Singer, W. (2006). Neural synchrony in brain disorders: relevance for cognitive dysfunctions and pathophysiology. *Neuron, 52*(1), 155-168.

Uhlhaas, P. J., & Singer, W. (2012). Neuronal dynamics and neuropsychiatric disorders: toward a translational paradigm for dysfunctional large-scale networks. *Neuron, 75*(6), 963-980.

Van Der Werf, J., Jensen, O., Fries, P., & Medendorp, W. P. (2008). Gamma-band activity in human posterior parietal cortex encodes the motor goal during delayed prosaccades and antisaccades. *Journal of Neuroscience, 28*(34), 8397-8405.

van Dijk, H., Schoffelen, J.-M., Oostenveld, R., & Jensen, O. (2008). Prestimulus oscillatory activity in the alpha band predicts visual discrimination ability. *Journal of Neuroscience, 28*(8), 1816-1823.

Varela, F., Lachaux, J. P., Rodriguez, E., & Martinerie, J. (2001). The brainweb: phase synchronization and large-scale integration. *Nature Reviews Neuroscience, 2*(4), 229-239.

Velanova, K., Wheeler, M. E., & Luna, B. (2008). Maturational changes in anterior cingulate and frontoparietal recruitment support the development of error processing and inhibitory control. *Cerebral Cortex, 18*(11), 2505-2522.

Velanova, K., Wheeler, M. E., & Luna, B. (2009). The maturation of task set-related activation supports late developmental improvements in inhibitory control. *Journal of Neuroscience, 29*(40), 12558-12567.

Vierling-Claassen, D., Cardin, J. A., Moore, C. I., & Jones, S. R. (2010). Computational modeling of distinct neocortical oscillations driven by cell-type selective optogenetic drive: separable resonant circuits controlled by low-threshold spiking and fast-spiking interneurons. *Frontiers in Human Neuroscience, 4*, 198.

Vokoun, C. R., Mahamed, S., & Basso, M. A. (2011). Saccadic eye movements and the basal ganglia. In S. P. Liversedge, I. D. Gilchrist & S. Everling (Eds.), *The Oxford handbook of eye movements* (pp. 215-234). Oxford ; New York: Oxford University Press.

von Stein, A., & Sarnthein, J. (2000). Different frequencies for different scales of cortical integration: from local gamma to long range alpha/theta synchronization. *International Journal of Psychophysiology, 38*(3), 301-313.

Wang, X.-J. (2010). Neurophysiological and computational principles of cortical rhythms in cognition. *Physiological Reviews, 90*(3), 1195-1268.

Wehner, D., Hamalainen, M., Mody, M., & Ahlfors, S. (2008). Head movements of children in MEG: Quantification, effects on source estimation, and compensation. *NeuroImage, 40*(2), 541-550.

Whittington, M. A., Kopell, N., & Traub, R. D. (2010). What are the local circuit design features concerned with coordinating rhythms. In C. v. d. Malsburg, W. A. Phillips & W. Singer (Eds.), *Dynamic coordination in the brain : from neurons to mind* (pp. 115-132). Cambridge, Mass.: MIT Press.

Williams, B. R., Ponesse, J. S., Schachar, R. J., Logan, G. D., & Tannock, R. (1999). Development of inhibitory control across the life span. *Developmental Psychology, 35*(1), 205-213.

Winterer, G., Carver, F. W., Musso, F., Mattay, V., Weinberger, D. R., & Coppola, R. (2007). Complex relationship between BOLD signal and synchronization/desynchronization of human brain MEG oscillations. *Human Brain Mapping, 28*(9), 805-816.

Womelsdorf, T., & Fries, P. (2007). The role of neuronal synchronization in selective attention. *Current Opinion in Neurobiology, 17*(2), 154-160.

Worden, M. S., Foxe, J. J., Wang, N., & Simpson, G. V. (2000). Anticipatory biasing of visuospatial attention indexed by retinotopically specific alpha-band electroencephalography increases over occipital cortex. *Journal of Neuroscience, 20*, 1-6.

Yakovlev, P. I., Lecours, A. R., & Minkowski, A. (1967). The myelogenetic cycles of regional maturation of the brain *Regional Development of the Brain in Early Life* (pp. 3-70). Oxford: Blackwell Scientific.

Zhang, M., & Barash, S. (2000). Neuronal switching of sensorimotor transformations for antisaccades. *Nature, 408*(6815), 971-975.